Stony Brook University

Terrestrial and marine POC fluxes derived from ^{234}Th distributions and δ^{13}C measurements on the Mackenzie River Shelf

A Dissertation Presented

By

David Amiel

To

The Graduate School

In Partial Fulfillment of the

Requirements for the Degree of

Doctor of Philosophy

In

Coastal Oceanography

Stony Brook University

May 2007

Stony Brook University

The Graduate School

David Amiel

We, the dissertation committee for the above candidate for the

Doctor of Philosophy degree,

hereby recommend acceptance of this dissertation

J. Kirk Cochran, Dissertation Advisor
Professor, Marine Sciences Research Center

Mary I. Scranton, Chairperson of Defense
Professor, Marine Sciences Research Center

Robert C. Aller
Distinguished Professor, Marine Sciences Research Center

Steven L. Goodbred, Jr.
Adjunct Assistant Professor, Marine Sciences Research Center

S. Bradley Moran
Professor, Graduate School of Oceanography, University of Rhode Island

This dissertation is accepted by the Graduate School

Lawrence Martin
Dean of the Graduate School

Abstract of the Dissertation

Terrestrial and marine POC fluxes derived from ^{234}Th distributions and δ^{13}C measurements on the Mackenzie River Shelf

By

David Amiel

Doctor of Philosophy

In

Coastal Oceanography

Stony Brook University

2007

Water column deficits of ^{234}Th relative to ^{238}U in the Mackenzie shelf, Cape Bathurst Polynya and Amundsen Gulf were used to estimate sinking fluxes of POC in these areas. ^{234}Th fluxes were converted to marine and terrestrial POC fluxes using the POC/Th ratio on filterable particles > 70 μm and δ^{13}C measurements to determine the fraction of marine and terrestrial POC. In June/July 2004, the greatest ^{234}Th deficits (0-100 m: 56-95 dpm m^{-2}) were observed in the Mackenzie outer shelf. Deficits in the upper 100 m ranged from 3 – 59 dpm m^{-2} in the Cape Bathurst Polynya. δ^{13}C values of POC in the >70 μm particles filtered in situ pumps ranged from -25.1 ‰ to -28 ‰. Using a two-end member mixing model with marine POC = -21.4 ‰ and terrestrial POC = -28 ‰ shows that terrestrial POC is most evident at the Mackenzie shelf stations but is present throughout the region. The fraction of marine POC ranged from 0 to 59 % in the area in June/July 2004, with the highest values in

the Amundsen Gulf. Fluxes of marine POC in the polynya average ~5 mmol C m^{-2} d^{-1} at 50 m in June 2004 and increase to ~12 mmol C m^{-2} d^{-1} in July. Comparable fluxes are observed at 100 m in June, but values decrease to ~6 mmol C m^{-2} d^{-1} at 100 m in July. These fluxes are greater than estimates of organic carbon remineralization and burial in sediments of the polynya (~3 mmol m^{-2} d^{-1}), suggesting that POC may be exported out of the area, effectively remineralized by microbial activity in the twilight zone or incorporated into biomass.

Table of Contents

List of Figures.

List of Tables

Acknowledgments

I would like to thank the captains and crews of the Canadian Coast Guard Ships *Pierre Radisson* and *Amundsen* for their assistance. Thanks go to Louis Fortier for his leadership of the CASES program and to Martin Fortier and Josee Michaud for their help with logistics. I thank David Hirschberg for laboratory support and John Mak for his guidance in the stable carbon isotope analyses. I thank Mary Scranton, Bob Aller, Steve Goodbred, and Brad Moran for their patience and critical acumen in bringing this work to fruition. I also thank Dane Percy, Alex Kolker and Jenni Slozek for their help on the cruises. Last but certainly not least, I thank Kirk Cochran for his outstanding guidance and support. I was extremely fortunate to have him as my advisor. This research was supported by a US National Science Foundation, Office of Polar Programs grant to JKC.

Chapter 1: The Physical and Biological setting of the Mackenzie River Shelf.

INTRODUCTION

Arctic research has recently acquired a new mandate with the onset of fundamental alterations in the global heat balance that are primarily dictated by changes in the timing and magnitude of sea-ice retreat (Holland et al. 2006). Located within the Arctic Ocean and adjacent seas are sites where deep water formation occurs. The dense waters that sink at these sites trigger the flow of deep water around the globe known as global thermohaline circulation. This circulation is in large part responsible for regulating the Earth's climate system through a complex array of positive and negative feedback loops (Siedler et al. 2001). While the effects of alterations in the sea-ice budget upon deep–water formation are poorly understood, it is intuitively evident that sea-ice recession is coupled to a warming of surface water that could prevent its descent. The rate of sea-ice recession in the Arctic is such that by the year 2050 much of the North West passage will be open to commercial shipping lanes in the summer.

Concurrent with sea-ice recession is an increase in coastal, open water habitats known as polynyas. These regions are known to have higher rates of primary production compared to ice-covered ones due to open water, an ample supply of nutrients, and enough sunlight (Stirling and Cleator, 1981). Indeed, productivity maxima in polynyas can be similar in magnitude to highly productive coastal mid-latitude systems, although the growing season is shorter (Klein et al. 2002).

Continental shelves (< 200 m) occupy 36 % of the Arctic Ocean area, or ~ 20 % of the global ocean area (Macdonald and Thomas, 1991). Thus, a disproportionate amount of area is occupied by continental shelves in the Arctic. Furthermore, the Arctic Ocean receives a disproportionate amount of river inputs relative to its volume (10 % of global river discharge in 1 % of global water volume). As with any shelf system, shelf-mediated processes play a central role in nutrient regeneration, water composition, biological fluxes, the sorting and burial of terrestrial debris, and the overall cycling of particles and organic carbon (Macdonald and Thomas, 1991). Indeed, river-dominated shelves in the Arctic may have a large impact on the global carbon cycle, especially in the context of global change (Gõni et al. 2005). Specifically, the destabilization of Arctic permafrost will change both the composition and amount of material supplied to Arctic waters via rivers and this could significantly alter the rate of burial and preservation of terrestrial organic matter (Gõni et al. 2005). As another example, increases in the area of open water are linked to increases in primary production and thus have the potential to alter the direction and magnitude of exchange of CO_2 between the atmospheric and oceanic reservoirs (Yager et al. 1995). While there has been a lot of research on

carbon cycling in river-dominated shelf regions in lower latitudes, these, as well as most other Arctic areas, have been greatly under studied. The need for baseline measurements of parameters such as carbon fluxes and sedimentation rates is therefore urgent. (Macdonald et al. 1998).

Canadian Arctic Shelf Exchange Study (CASES)

CASES is a multi-national, multi-disciplinary, Canadian-led effort that continues the tradition of polynya research begun with the Northeast Water (NEW) and North Water (NOW) projects. The CASES region lies within a narrow band that encircles Arctic coastlines called the Marginal Ice Zone (Fig. 1-1).Unlike its predecessors, the CASES region is fed by the sediment-laden Mackenzie River, the only north American analog for the great Siberian rivers that also drain into the Arctic Ocean. The CASES region has dimensions of roughly 700 x 200 km, about half of which lies within the Beaufort Shelf (< 200 m). Although this shelf comprises < 2 % of the total Arctic shelf area, the shelf is the largest on the North American side of the Arctic Ocean. It is therefore, the most accessible site to compare with the vast continental shelves of the Eurasian basin (Macdonald and Thomas, 1991).

The central hypothesis of CASES is that sea-ice is the master variable controlling biogeochemical fluxes (Fig. 1-2). While seemingly reductionist and simplistic, the scope of this hypothesis has linkages with many fields that emphasize the aspiration of CASES to strengthen and understand the nature of these connections.

Annual Cycle of Physical Processes in CASES

In winter, the Mackenzie River has low flow, and the land-fast ice is dammed along with the river flow from the stamukhi (Fig. 1-3, panel a). The stamukhi arises from the collision of land-fast ice with first year pack ice before the flaw lead has developed. The flaw lead present in winter may convect with deeper waters of the outer shelf (Fig. 1-3, panel a). In spring, warmer temperatures melt the stamukhi and the Cape Bathurst Polynya is created from the expansion of the flaw lead (Fig. 1-3, panel b). Summer witnesses the melting of the land-fast ice and a maximum in open water (Fig. 1-3, panel c). In fall, the stamukhi begins to re-form signaling a return to winter. Ice cover has a 40 % interannual variability and in certain years the region undergoes several freeze-melt cycles that can limit the duration of maximum open water to only a month or so (Arrigo et al. 2004).

The Mackenzie River discharges about 3.3×10^{11} m^3a^{-1} of freshwater, the bulk of which is delivered between May-September (Fig. 1-4). The inter-annual variability of this discharge is ~ 25 % (Macdonald, et al. 1998). The spring freshet begins regularly around the first two weeks of May. The annual sediment load has been estimated by Carson (1994) to be 127 ± 6 Mt a^{-1}, the largest input of sediments to the Arctic Ocean. Due to the spring freshet and breakup of land fast ice, the maximum in sediment loading comes in mid-July, considerably after the maximum in freshwater discharge (Fig. 1-4). In winter, the organic carbon content of the sediment from the Mackenzie is $4.8 \pm 1.3\%$

while during freshet this percentage reduces to 1.4 ± 0.2 % (Yunker et al. 1993). The Mackenzie is the source of 95 % of terrigenous OM supplied to the shelf and the remaining 5 % comes from coastal erosion (Macdonald et al. 1998). Recent work by et al. (2005) using ^{14}C dating has shown that around ~ 60 % of this POC is ancient (>7000 old) and is likely derived from kerogen eroded from sedimentary rocks and from release of ice-bonded soils. The rest of the POC pool is a heterogenous mixture of C3 plants and angiosperms originating from tussock tundra in the Canadian Cordillera and boreal coniferous forest. There is no evidence for C4 plants in sediments of the Mackenzie shelf, consistent with inhibition of these types of plants at low temperatures (et al. 2005).

The advent of the spring freshet sets up an estuarine circulation in which a saline intrusion of water balances the Mackenzie River outflow (Fig.1-5a). Exactly how far up river the salt wedge travels is not known. Also unknown are the details of the seasonal cycle of the estuarine circulation, and the extent to which it operates underneath sea-ice. As with other estuarine flows, entrainment of dissolved components occurs and the outgoing "freshwater" can be expected to have salinities much higher than 0, even at close proximity to the river mouth (Fig. 1-5a). The cycling of solid material may exhibit much more vertical structure than dissolved constituents due to the density of the particulates that allows particle sinking to dominate over entrainment (Fig. 1-5b). The rate at which particulate material of marine origin is transported along with the estuarine flow is not known.

Figure 1-6 summarizes the range of physical, biological and chemical processes known to occur in the CASES region. In spring/summer, particulate material enters the inner shelf from the Mackenzie River and generates a turbid plume, some of which can flocculate and settle (Fig. 1-6a). This plume is clearly visible from space and may extend hundreds of kilometers offshore. The plume travels long enough distances so that the Coriolis force deflects it eastwards as it travels offshore. However, winds also influence the direction the plume takes as it disperses and may negate the Coriolis effect. For this reason, in some years the direction of the plume is predominantly northwards. Upon reaching the inner shelf, sediment carried by the plume is mixed with marine-derived biogenic material, and particles released from melting sea-ice (Fig. 1-6a). On the inner shelf, storms frequently occur, stirring and resuspending material from the bottom. Atmospheric deposition of particulate material may also occur during open water periods. In winter, communication between the atmosphere and water column is significantly reduced due to the sea-ice (Fig. 1-6b). Atmospheric deposition still occurs however, and much of this accumulates in sea-ice. Although sea-ice freezing will favor fresh versus salty water, significant quantities of salt are entrained during freeze-up such that in isolated pockets within the sea ice, salinities can reach 50 psu (Barber, personal communication). This brine can then gravitationally settle through the sea-ice and be released back into the water (Fig. 1-6b).

A surface (0-10 m) salinity contour plot across the entire CASES area for June, 2004 was constructed courtesy of Bob Wilson at the Marine Sciences Research Center (Fig. 1-7). This plot shows the northwards movement of the

Mackenzie River plume and suggests that the Cape Bathurst polynya was isolated from the influence of the Mackenzie river at the time of our June, 2004 cruise. Our sampling began on June 6th, 2004 just days after a flaw-lead opened in Cape Bathurst.

Annual cycle of primary production in CASES

Total annual primary production over the CASES region has been estimated to be 3.3 Mt a^{-1} of POC, of which ~ 40 % results from new production (Macdonald et al. 1998). The prevailing view is that most of this algal production is rapidly decomposed in the water column and at the sediment-water interface such that very little is preserved in sediments. On the other hand, about 50 % of the terrigenous OM supplied from the Mackenzie is unreactive and therefore has a greater likelihood of burial and preservation (Macdonald et al. 1998). The seasonal cycle in primary production for CASES was studied by Arrigo et al. (2004) using satellite imagery over a 5 year period (Fig. 1-8). Autochthonous carbon originating from primary production had a bimodal distribution over the 4 month (June-Sept) growing season. The first maximum was reached almost immediately after the flaw lead opened (early June). This bloom then crashed due to nutrient depletion. The second arose after mid season storms had reintroduced nutrients into the mixed layer, there was still enough light, and the polynya had reached maximum open water (Arrigo et al. 2004).

Maximum primary production rates from the Cape Bathurst Polynya were 2.7 g C m^{-2} d^{-1} reached in August (Arrigo et al. 2004). The unique feature of this distribution is that the second, late-season peak is usually larger than the first, an observation that was attributed to ice-coverage that decreases later in the season.

A Carbon Budget for CASES

Given the different labilities of different fractions of organic matter and hence their different preservation rates, any carbon budget for this system needs to discriminate between terrestrial and marine carbon. If, for example, all the terrestrial carbon from the Mackenzie River is buried and preserved on the shelf, one is simply transferring one inert carbon pool on land to nearshore. The key question then, regarding terrestrial carbon is what portion of this pool gets oxidized/metabolized prior to preservation. Regarding marine carbon, the key question is what fraction is preserved by burial on the shelf as compared to that which gets transferred into the deep sea (Macdonald et al. 1998, Hedges, 1992). The fraction of marine carbon transferred to the deep sea is critical since burial on the shallow shelf will only delay re-exchange of this carbon pool with the atmosphere on decadal time scales (Anderson et al. 1993). Sequestration in the deep sea however, can prevent re-exchange with the atmosphere on millennial time scales.

A budget constructed by Macdonald et al. (1998) for sediments, marine and terrestrial carbon is shown in Fig. 1-9. The Mackenzie Shelf is broken down into two boxes, the delta and the shelf. In the delta region, 88 % of

primary production is oxidized in the water column or in sediments. Apparently none of this carbon reaches the shelf and the remainder gets buried. Since primary production is relatively small within the delta, the amount of marine carbon buried is also small even though a higher proportion compared to the shelf escapes oxidation due to the shallow depths. On the shelf, due to its larger area, ~ 20-fold more carbon is fixed (3.0×10^6 compared to $.16 \times 10^6$ t yr^{-1}) and 98 % is decomposed in the water column or in surficial sediments. The fraction of the remaining 2 % exported from the shelf is unknown. There is little that is unusual in this budget in the sense that other shelf systems are also very efficient in trapping particles and recycling marine carbon (Bacon et al. 1988). The terrestrial carbon budget is considerably more uncertain than the marine one since many of the values in the budget were obtained by difference. The unusual result of the terrestrial carbon budget is that > 90 % of the carbon found in delta and shelf sediments appears to be of terrestrial origin. Most other shelf systems do not exhibit such large proportions of terrestrial carbon present in sediments (e.g. Keil et al. 1997). This dominance of terrestrial carbon may be pointing to a higher degree of recalcitrance of the Mackenzie river carbon; an idea supported by et al. (2005) who found that much of the carbon from the Mackenzie was old (> 7000 yr) and had therefore been extensively degraded before reaching the delta and shelf regions. The finding of ancient carbon on the Mackenzie shelf led et al. (2005) to refine the earlier budget of Macdonald (Fig. 1-10). This budget breaks up terrestrial carbon input from the Mackenzie into ancient and modern based on ^{14}C dating. Using the total terrestrial carbon input from the Macdonald et al. (1998) budget that had, and multiplying by mass fractionation factors for ancient and modern terrestrial carbon, et al. (2005) determined that 60-70 % of the carbon input from the Mackenzie is ancient (Fig. 1-10). Yet, despite its old age, apparently 66 % of this carbon is respired within the delta. Little new information within the et al. (2005) budget is revealed regarding the marine carbon pool except they estimate that 97 % (not 98 % like the Macdonald et al. [1998] budget) of the marine carbon is respired and 10-15 % of marine aquatic production is from ice algae.

Hypotheses to be tested

H1:

Sinking fluxes of particulate organic carbon in the water column and remineralization of POC in sediments depends on the direction the river plume expands. If the plume moves northwards *across* the shelf, primary production and POC export in the Cape Bathurst polynya (700 km away from the river) should be significant and comparable to other productive Arctic polynyas. In this case, the river plume would not generate much turbidity in Cape Bathurst allowing for a high flux POC.

H2:

Shelf systems from lower latitudes indicate a high degree of recycling with >20 % of carbon fixed on the shelf exported to the oceans interior. Given that high enzyme activities have been measured on sinking POC from the Northwater Polynya (Huston et al. 2002), and the fact that there is no

evidence from the literature indicating temperature inhibition of microbial activities, I hypothesize that sub-arctic shelf systems such as the Cape Bathurst polynya behave in a similiar manner as their lower latitude counterparts. Therefore, in the absence of large lateral effects, large amounts of autocthonously-derived sinking POC should be accounted for in sediments. Hence, the hypothesis I am testing is that there exists a carbon mass balance between water column POC fluxes descending from the sunlit layer and that which is found accumulating in sediments.

FIGURES

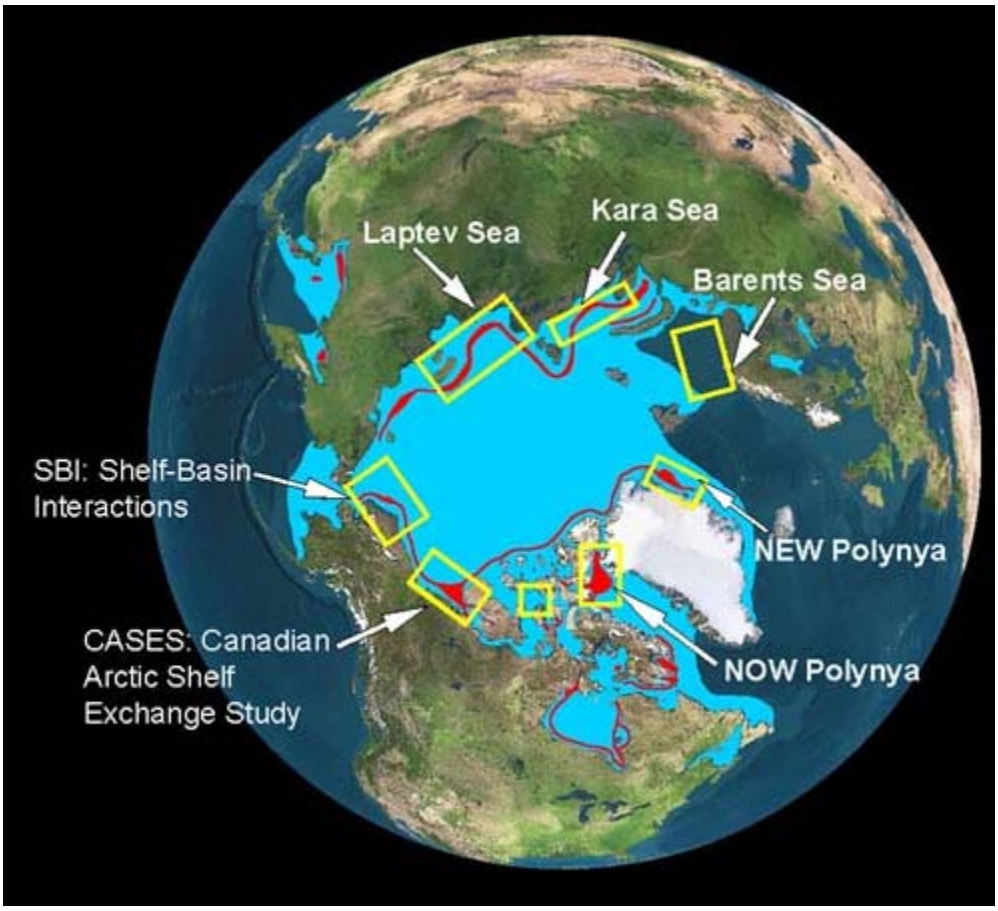

Figure 1-1. Marginal ice zones of the Arctic Ocean

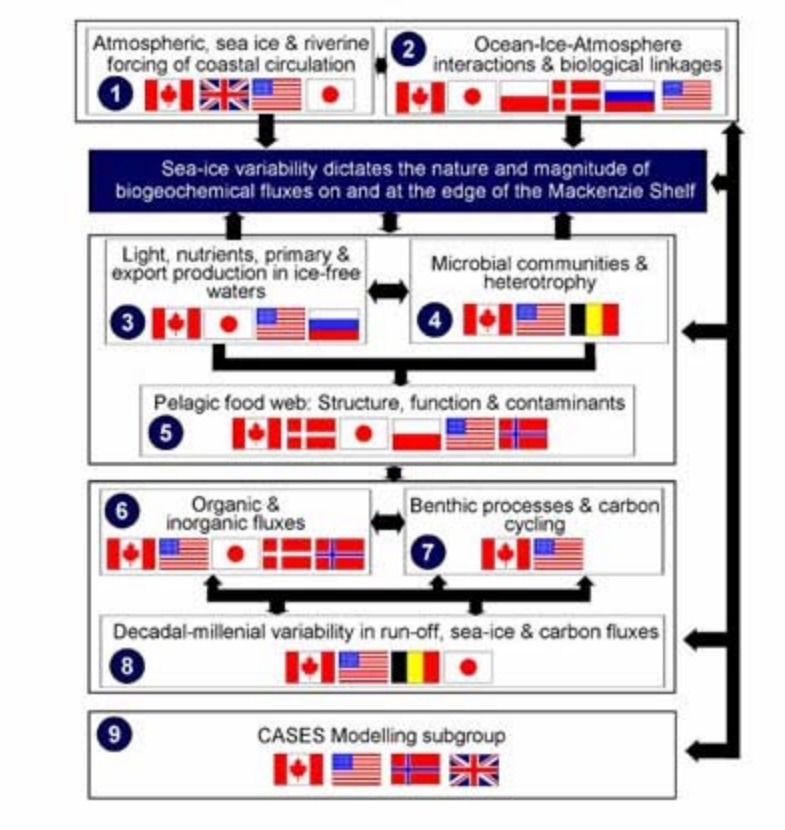

Figure 1-2. Schematic of different research groups within the CASES project and a unifying hypothesis.

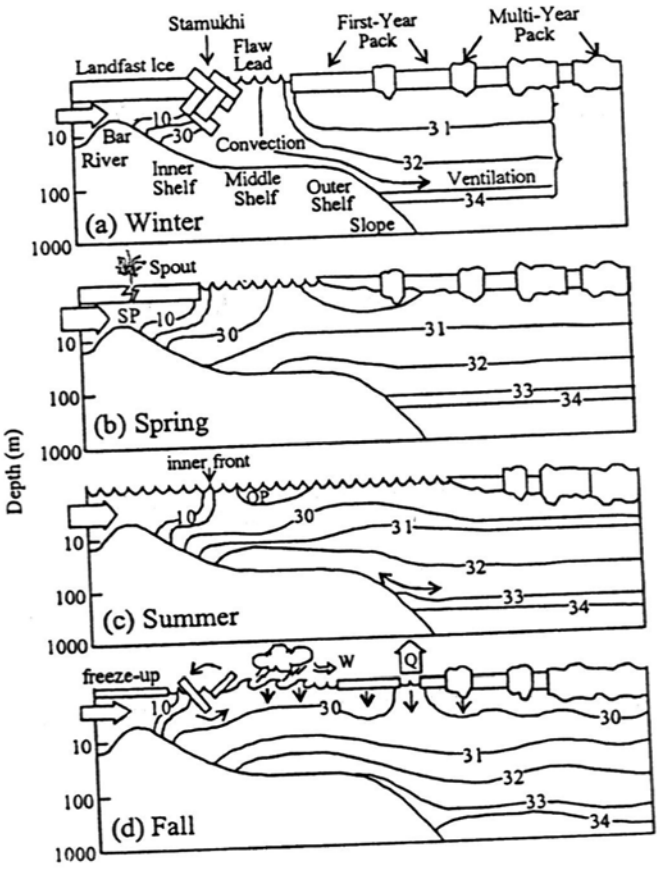

Figure 1-3. Annual cycle of physical processes for the Mackenzie Shelf.

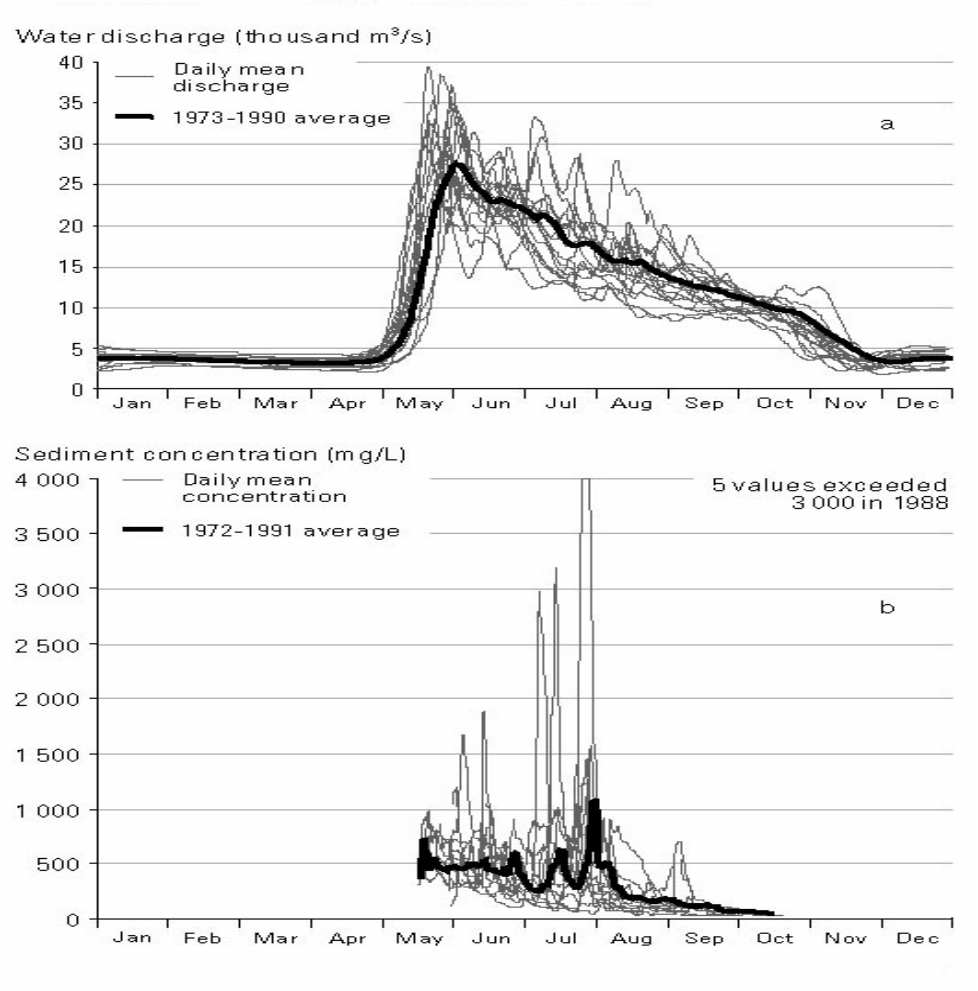

Figure 1-4. From Arctic monitoring and assessment program (AMAP). Monthly river flow and loading for the Mackenzie River.

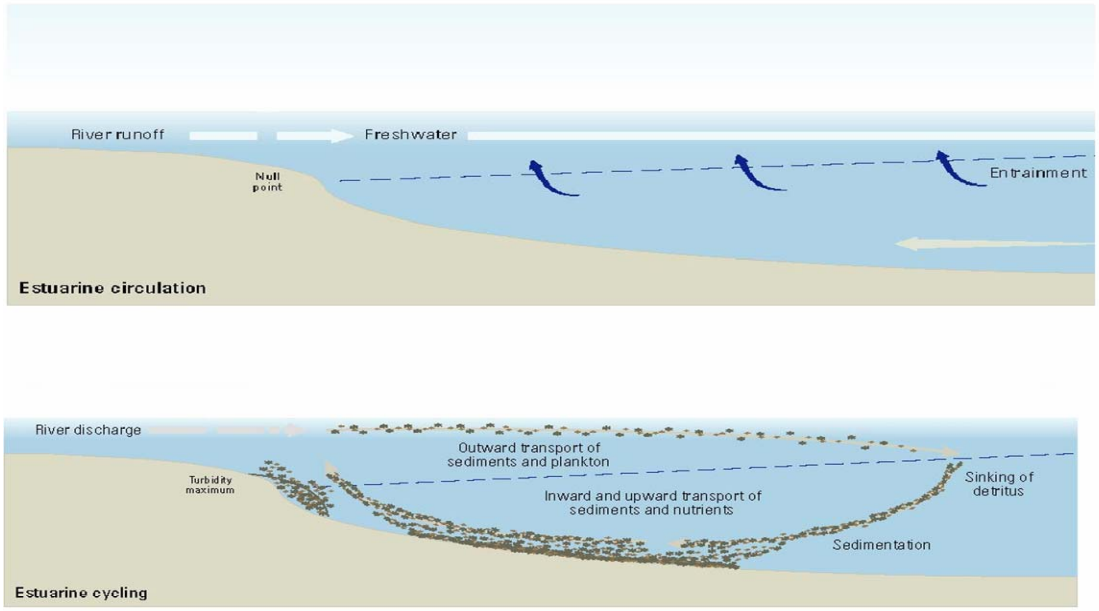

Figure 1-5. Estaurine flow of a) dissolved and b) particulate material within CASES.

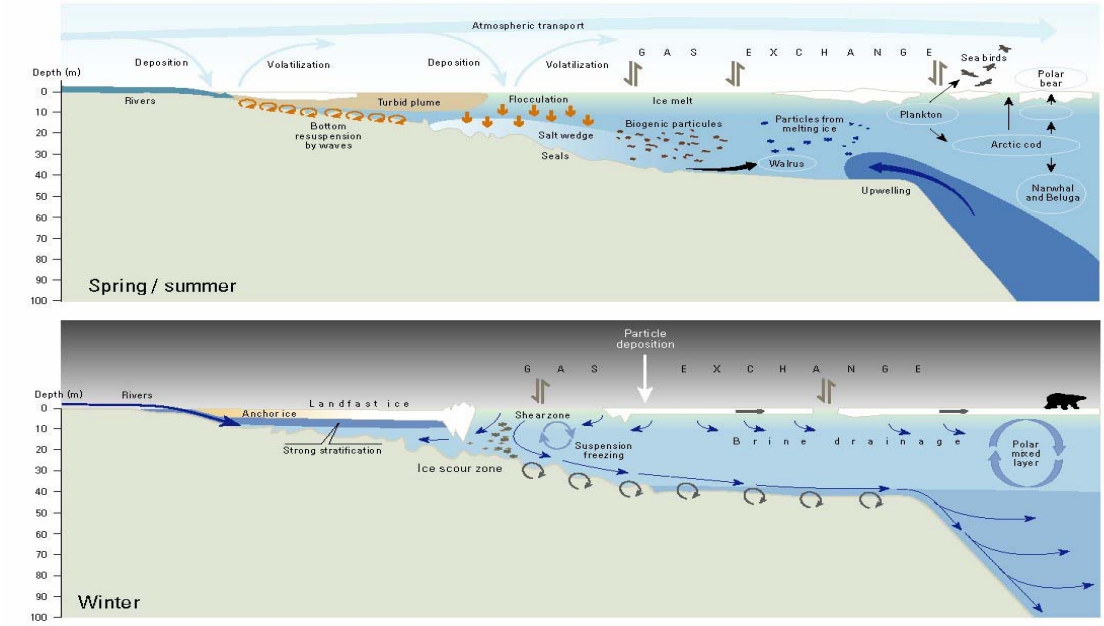

Figure 1-6. The range of physical processes at work on the Mackenzie Shelf during spring and winter.

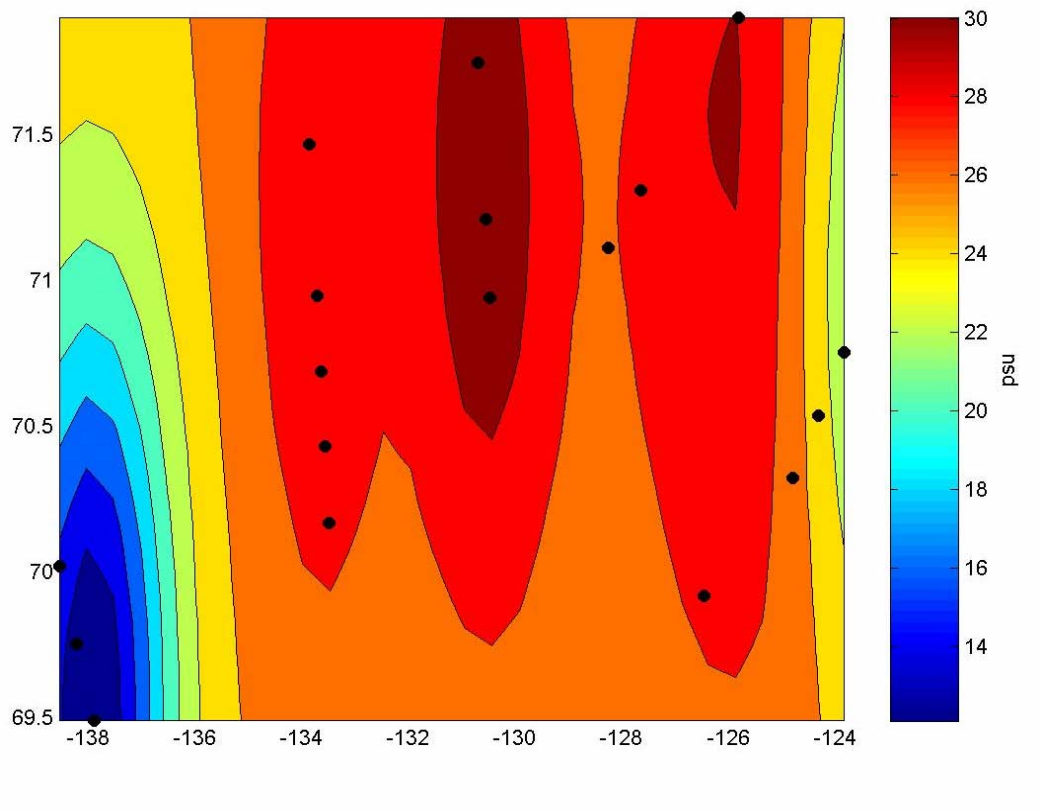

Figure 1-7. Courtesy of Bob Wilson. Salinity contour plot of CASES during June, 2004. Black dots are individual stations.

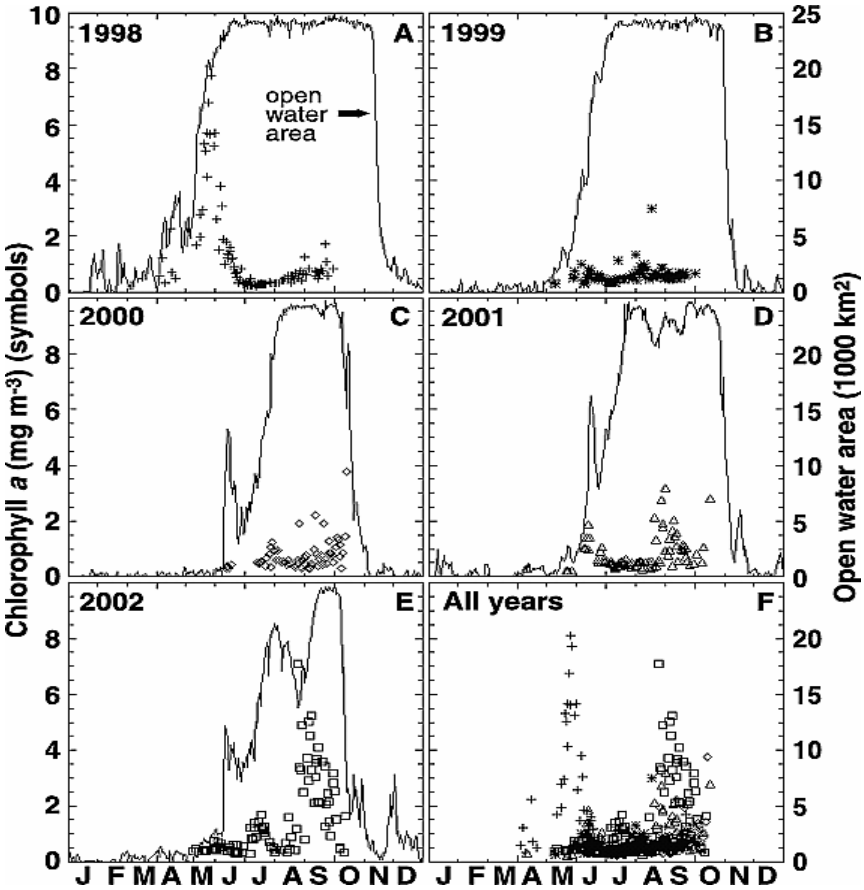

Figure 1-8. From Arrigo et al. 2004. Annual cycle of primary production (symbols) and extent of open water (lines) in Cape Bathurst between 1998-2002.

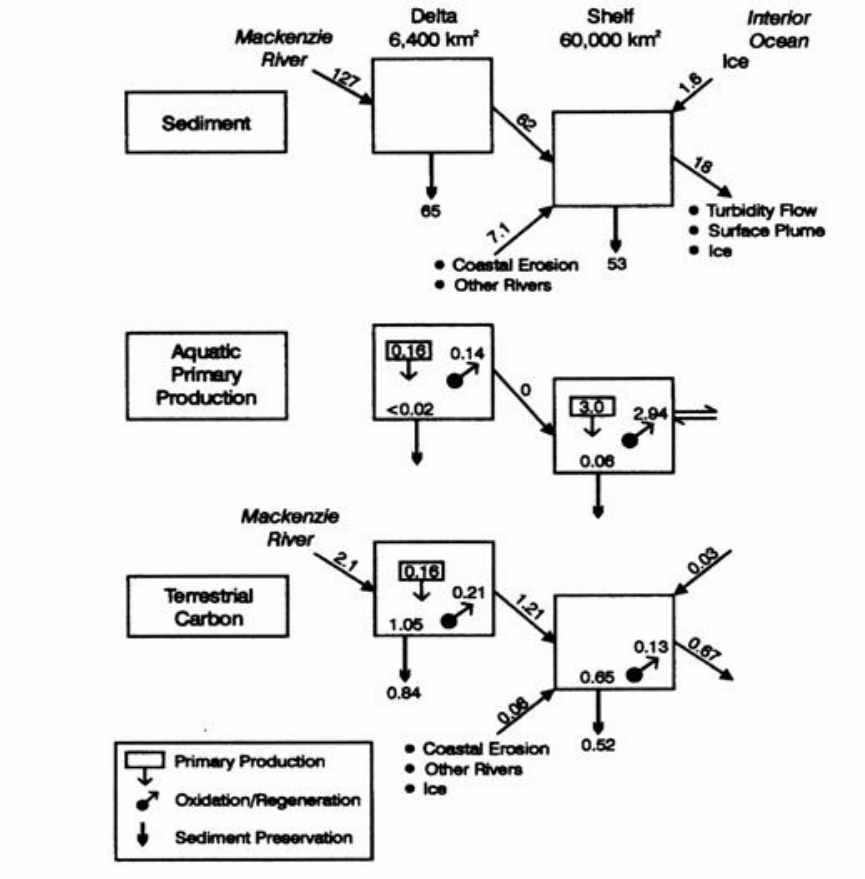

Figure 1-9. From Macdonald et al. 1998. Sedimentary, marine and terrestrial organic carbon budget for the Mackenzie shelf.

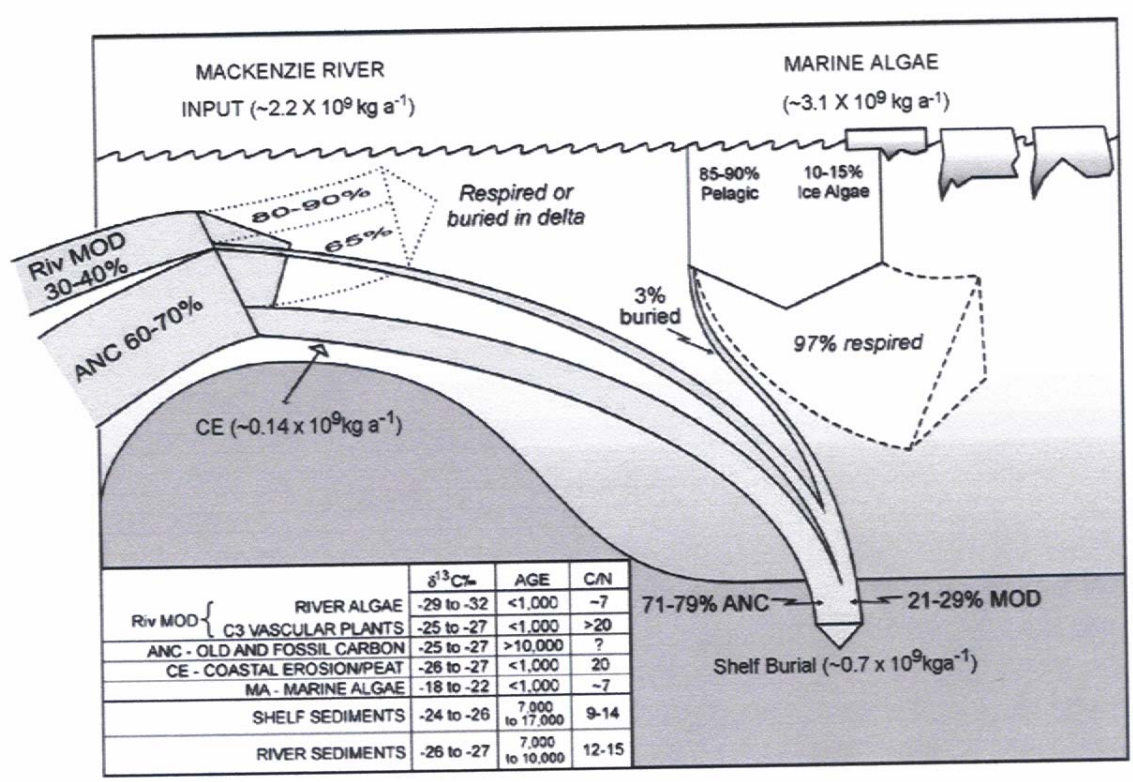

		$\delta^{13}C‰$	AGE	C/N
Riv MOD	RIVER ALGAE	-29 to -32	<1,000	~7
	C3 VASCULAR PLANTS	-25 to -27	<1,000	>20
ANC - OLD AND FOSSIL CARBON		-25 to -27	>10,000	?
CE - COASTAL EROSION/PEAT		-26 to -27	<1,000	20
MA - MARINE ALGAE		-18 to -22	<1,000	~7
SHELF SEDIMENTS		-24 to -26	7,000 to 17,000	9-14
RIVER SEDIMENTS		-26 to -27	7,000 to 10,000	12-15

Figure 1-10. From Gõni et al. 2005. Carbon budget for the Mackenzie Shelf.

REFERENCES

Arrigo, K.R., Dijken, G., 2004. Annual cycles of sea ice and phytoplankton in Cape Bathurst Polynya, southeastern Beaufort Sea, Canadian Arctic. *Geophysical Research Letters*. 31, LO8304.

Bacon, M.P., Belastock, R., Tecotzky, M., Turekian, K., Spencer, D., 1988. Lead-210 and polonium-210 in ocean water profiles of the continental shelf and slope south of New England. *Continental Shelf Research.* 8:841-853.

Carson, M.A. 1994. Mackenzie Delta sediment regime. Unpublished manuscript. Inland Water Directorate. Yellow-knife, NWT.

Gõni, M., Yunker, M., Macdonald, R., Eglington, T. 2005. The supply and preservation of organic carbon in the Canadian Beaufort Shelf of the Arctic Ocean. *Marine Chemistry*. 93:53-73.

Hedges, J.I., 1992. Global biogeochemical cycles: progress and problems. *Marine Chemistry*. 39: 67-93.

Holland, M. M., Bitz, C.M., Tremblay, B (2006). Future abrupt reductions in the summer Arctic sea ice. *Geophysical Research Letters* 33: L23503.

Keil, R.G., Mayer, L.M., Quay, P.D., Richey, J.E., Hedges, J.I., 1997. Loss of organic matter from river particles in deltas. *Geochim. Cosmochim. Acta*. 61: 1507-1511.

Klein, B., LeBlanc, B., Mei, Z-P., Beret, R., Michaud, J., Mundy, C-J., Quillfeldt, C., Garneau, M-E., Roy, S., Gratton, Y., Cochran, J.K., Belanger, S., Larouche, P., Pakulski, J., Rivkin, r., Legendre, L. Phytoplankton biomass, production and potential export in the North Water Polynya. 2002. *Deep-Sea Research II*, 49: 4983-5002.

Macdonald, R., Solomon, S.M., Cranston, R.E., Welch, H.E., Yunker, M.B., Gobeil, C., 1998. A sediment and organic carbon budget for the Canadian Beaufort Shelf. *Marine Geology*. 144: 255-273.

Macdonald, R., Thomas, D.J. 1991. Chemical interactions and sediments of the Western Canadian Arctic Shelf. *Continental Shelf Research*. 11:843-863.

Stirling, I., Cleator, H., 1981. Polynyas in the Canadian Arctic. Canadian Wildlife Service, Occasional Paper 45, 70 pp.

Wasniewski, J. 2001. Ocean Circulation and Climate. In: Siedler, G., Church, J., Gould, J (Eds.), Ocean circulation and climate. Academic Press, London, pp. 8-12.

Yager, P.L., Wallace, D.W.R., Johnson, K.M., Smith Jr., W.O., Minnett, P.J., Deming, J.W., 1995. The Northeast Water Polynya as an atmospheric CO_2 sink: a seasonal rectification hypothesis. *Journal of Geophysical Research*. 100: 4389-4398.

Yunker, M.B., Macdonald, R.B., Cretney, W., Fowler, B.R., McLaughlin, F.A., 1993. Alkane, terpene, and polycyclic aromatic hydrocarbon geochemistry of the Mackenzie River and Mackenzie Shelf: Riverine contribution to Beaufort Sea coastal sediment. *Geochim. Cosmochim. Acta*. 57: 3041-3061.

Chapter 2: ^{234}Th distributions and fluxes and suspended particle concentrations on the Mackenzie River Shelf as part of the Canadian Arctic Shelf Exchange Study (CASES)

INTRODUCTION

The naturally occurring radionuclide ^{234}Th has been used in many oceanic environments as a tool to understand the phenomena of scavenging and particle sinking in the water column (e.g.Cochran et al. 2003, 2000, 1995; Buesseler et al. 1992, 1998, 2003; Cochran and Másque 2005; Amiel et al. 2002). Where particles inputs are dominated by phytoplankton, ^{234}Th distributions in combination with particulate organic carbon measurements have allowed the calculation of POC export rates (see above references). However, the linkage between Th scavenging and carbon cycling in coastal areas that have both terrestrial and marine carbon sources has been much less studied.

With the intent to obtain marine carbon fluxes, many recent applications of ^{234}Th have occurred in regions where particle inputs are dominated by in situ production by phytoplankton. Conversely, earlier studies have documented that in coastal waters, there are large increases in the scavenging rates of both dissolved ^{234}Th onto particles and the rates at which those particle sink (Santschi et al. 1979, Mckee et al. 1984). Hence, it is by no means evident that ^{234}Th can be used to obtain POC fluxes in an Arctic shelf located near a large allochthonous carbon source (the Mackenzie river).

Before applying Th data to obtain carbon fluxes, this chapter examines along and across shelf Th distributions collected at increasing distances from the Mackenzie River mouth. To further understand links between Th and carbon, suspended particle concentrations and Chl a profiles are presented in an effort to discover any patterns that may exist between the various particle reservoirs. A secondary objective was to determine what physical processes were responsible for Th removal and to identify distinct provinces in which specific processes dominate.

Besides the assumption of in situ particle production via phytoplankton, Th derived POC fluxes also assume steady state and that particle sinking is predominantly in the vertical direction. In this chapter, these assumptions will be tested.

In Chapter 4 of this thesis, the ^{234}Th flux data will be applied to the determination of POC fluxes in the Mackenzie Shelf.

Methods

Sampling

Water samples were collected on four expeditions of the C.C.G.S Pierre Radisson and Amundsen (October 2002, October 2003, and June and July,

2004) as part of the Canadian Arctic Shelf Exchange Study (CASES). Figure 2-1a,b shows the regions sampled, as well as station locations and sampling times. Several stations were occupied multiple times (718, 406, CA-12) and one station (406) was sampled in June, 2004 and again five weeks later, in July, 2004.

Samples from the water column were collected in two ways. The first used battery and ship-powered *in situ* pumps with flow rates between 1-9 L/min to filter a total volume of ~100-1000L. Water was passed through two prefilters (142 mm diameter) followed by two manganese or iron hydroxide-impregnated polypropylene cartridges to collect dissolved thorium (Livingston and Cochran, 1987). The prefilters, made of Teflon and microquartz (Whatman QM/A, here designated as MQZ), collected particles from two size-classes: >70 and 1-70 μm respectively. These size-classes were chosen based on previous results that show > 90% of the mass flux into sediment traps is from the >53 μm size fraction (Bishop et al. 1977, Clegg and Whitfield, 1990). Thus, the choice of filter sizes was designed to separate particles into operationally-defined suspended and sinking fractions.

A second approach involved small volume water samples (Van der Loeff et al. 1999). In this method, 2L of water were collected from Niskin bottles, and reagents were added to precipitate MnO_2 that scavenged thorium (see below).

Particulate ^{234}Th analyses

Analysis of particulate and dissolved ^{234}Th from in situ pumps was detailed in Amiel et al. (2002) and was similar to methods that can be found in Buesseler et al. (1998) and references therein. Briefly, the Teflon filters from the pumps that contain the >70 μm particle fraction were rinsed with filtered seawater and re-filtered onto 25 mm MQZ filters and dried overnight. The filters were then mounted onto a counting ring, covered with plastic film and aluminum foil, and counted on a RISØ, low background beta counter. The detector efficiency for a single 25 mm MQZ filter was determined by spiking three separate filters with a known amount of ^{238}U in equilibrium with ^{234}Th. The beta counting efficiency determined for the triplicates was 43.7 ± 3.2 %, in agreement with the range in efficiencies (41-43%) obtained from steel ^{99}Tc planchets that have a similar geometry as the samples.

The 142 mm MQZ filters that contained the 1-70 μm particulate fraction were also dried overnight. Twenty punches (21 mm in diameter, comprising 50 % of the filter) were then taken, and these were mounted into counting rings for beta counting (Buesseler, et al. 1998). This mounting step consists of stacking the 20 punches in counting rings and wrapping this ring in a layer of plastic film and aluminum foil. This is designed to block low energy beta particles that might emanate from other radionuclides such as ^{210}Pb and ^{226}Ra daughters.

Samples were then counted multiple times on a RISØ beta counter and the count rate was regressed against $e^{-\lambda t}$ where λ is the ^{234}Th decay constant (.0288 d^{-1}). Such regressions confirmed that ^{234}Th was being measured (see Aller and Cochran, 1976). After all the ^{234}Th excess had decayed (about 5

months), count rates were determined by subtraction of the initial from the final counts. Thus, any contributions from longer-lived radionuclides was taken into account in determining ^{234}Th count rates. As well, any U-supported ^{234}Th present in the sample is subtracted from the total ^{234}Th by this method.

Determination of precipitation efficiency for 2L samples

Following the adaptation by Buesseler et al. (2001) to Van der Loeff and Moore's original 20 L procedure, 10 % of the stock solutions of NH_3 (1 drop 25 % w/w), $KMnO_4$ (25 µl of a 60 g/l solution), and $MnCl_2$ (10 µl of a 400 g $MnCl_2 \cdot 4H_2O$/l solution) were added to 2 liter samples collected from Niskin bottles. A MnO_2 suspension formed and this was allowed to sit for 8h, after which it was filtered onto 25 mm MQZ filters, and mounted for beta counting. As the samples were unfiltered, this method yields total ^{234}Th (particulate + dissolved). No yield tracer was added to the samples and consequently, experiments were done in the lab to evaluate the precipitation efficiency.

The precipitation efficiency for the small volume procedure was determined using 2 L of filtered (1µm) DI water spiked with 7.595 dpm ^{238}U in equilibrium with ^{234}Th. The reagents were added, and the MnO_2 suspension was allowed to stand for 6 h. The extraction efficiency of the suspension was obtained from the equation:

$$Eff = \frac{CPM \text{ recovered}}{7.595\, DPM * DE}$$

where DE is the detector efficiency (.437 ± .032), CPM recovered is the count rate obtained after 6h, DPM is the absolute count rate, and Eff is the efficiency of precipitation of ^{234}Th. The precipitation efficiency was 101 % ± 6.2 %, and I concluded that the procedure quantitatively scavenged all the ^{234}Th present in the samples.

For the 2 L samples collected in 2002, the concentrations of stock solutions were the same as above. It was found however, that it required five 25 mm MQZ filters to filter completely the MnO_2 suspension. We could have used a larger diameter filter (Rutgers van der Loeff et al. 2005) but this would have altered the geometry for beta counting (and thereby change the counting efficiency), if indeed a consistent geometry could be maintained for larger sized filters. In order to reduce the amount of precipitate, we evaluated whether less manganese chloride and potassium permanganate could be used to quantitatively scavenge Th. The reaction for the formation of the MnO_2 precipitate is:

$$MnCl_2 + 2KMnO_4 \rightarrow 3MnO_2 + 2KCl + O_2$$

Based on the concentrations of potassium permanganate (60 g/l) and manganese chloride (400 g $\cdot$ 4 H_2O/l) calculations suggest that permanganate and manganese chloride were in excess.

Concentrations of $MnCl_2$ were reduced to ¼ of the original amounts, added to DI water spiked with ^{238}U, and MnO_2 was precipitated as described above. This dilution showed complete removal of ^{234}Th with the precipitate readily filterable onto a single MQZ filter. New stock solutions were made up that were 100 g/l $MnCl_2$, and 15 g/l $KMnO_4$, and these concentrations were used

on all subsequent samples. Results from using these new reagent concentrations in the field often showed ^{234}Th to be present in equilibrium or even in excess (see Fig. 2-5e). If incomplete precipitation of ^{234}Th had occurred, this would have resulted in large ^{234}Th depletions relative to ^{238}U, the opposite of what was found. Hence, the field results using the reduced concentration of reagents were consistent with laboratory ones in showing complete removal of ^{234}Th.

Dissolved ^{234}Th

Although we follow methods that have been used many times before, we did use different types of cartridges, manganese or iron hydroxide at some stations sampled in 2004 (Amiel et al. 2002, Cochran et al. 2000, and references therein). Iron hydroxide impregnated cartridges were used in an attempt to capture dissolved ^{7}Be and ^{210}Pb, as well as ^{234}Th (Benitez-Nelson et al. 2000).

However ^{7}Be and ^{210}Pb were below the detection limit on these cartridges, if they were scavenged at all and further data are not presented.

The two cartridges from each pump depth were dried, compressed, wrapped in plastic wrap and non-destructively gamma counted by 1, 2, 3, or 3.8 K planar intrinsic germanium detectors (Buesseler et al. 1998).

The extraction efficiency for each pair of cartridges is given by:

$$E = 1 - (MnB/MnA),$$

where MnA and MnB are the count rates on the first and second cartridge, respectively (Livingston and Cochran, 1987). The mean value of E for the manganese oxide cartridges was .72 ± .10 (n = 75) and for the iron hydroxide cartridges was .79 ± .06 (n=15). Due to detector problems on one leg, not all pairs of cartridges were counted. In these cases, only the A's were counted and the average efficiency for either the iron hydroxide or manganese oxide cartridges was applied.

Absolute errors in total ^{234}Th (particulate + dissolved) were propagated from the relative errors obtained from 1σ counting statistics of the two fractions. In addition, dissolved phase errors were propagated with errors calculated from the extraction efficiency (E) given by:

$$\sigma_E = E * \sqrt{\left(\frac{\sigma_a}{A}\right)^2 + \left(\frac{\sigma_b}{B}\right)^2}$$

where A and B are count rates on cartridges, and $\sigma_{A,B}$ are proportional to $(n/n)^{1/2}$, where n is the number of counts registering on the gamma detector. Generally, errors derived from the cartridge extraction efficiency are smaller than those obtained from counting statistics; however for cases where the count rates on B cartridges were high, extraction efficiency errors can be significant (> 10%). ^{234}Th dissolved phase errors range from 5-15 %. In all cases, > 95 % of the error in total ^{234}Th comes from the dissolved fraction.

Floating traps

Floating trap (FST's) samples were obtained at 15, 50, and 100 m depths in June and July 2004 through the generosity of Dr. Christine Michel (University of Winnipeg). FST's were deployed using surface tethered buoys

for durations between .97 and 1.58 days (Table 1).The traps had diameters of 10 cm with 70 cm lengths (aspect ratio = 7.0). Our samples consisted of collections of whole floating traps. After recovery, the unpoisioned traps were allowed to stand for 8h to permit settling of all material. Visible swimmers were removed. The supernatant was partially decanted, and the remaining 2 L solution was transferred to a thoroughly rinsed plastic bottle. Shortly thereafter, the 2 L solution was filtered onto a 25 mm MQZ filter and mounted for beta counting. Sediment trap samples from both the inner Mackenzie Shelf, as well as the relatively deep Amundsen Gulf were measured. ^{234}Th fluxes in floating traps were calculated by dividing the count rate on the filtered trap samples by the area of the trap (.0075 m^2) and the trap deployment times (Table 1). Count rates were decay-corrected to the midpoint of the collection time.

Ice cores

At station 200, in May, 2004, before the Cape Bathurst Polynya opened, 2 m ice cores were collected using an ice auger (courtesy of Jens Ens, University of Winnipeg). Two of these cores were divided into three sections, 0-30 cm, 90-120 cm, and 170-200 cm respectively. Cores were allowed to sit at room temperature until they melted. Sections of the same interval were combined from the two cores to obtain 2 L for each depth horizon. The first two sections (0-30, 90-120 cm), were treated identically to the 2 L samples collected from Niskin bottles (see above), i.e. reagents were added to precipitate Th, and the precipitate was then filtered and beta counted. In the deepest section of the core, the particulate material was so concentrated it was reasoned that any ^{234}Th present would absorb onto the solid phase; hence no further MnO_2 precipitation was carried out in this sample. The filtered samples were mounted onto counting rings, and the beta activity measured.

Suspended Particle Concentrations

Stations were selected during the June and July, 2004 cruises to capture the full range in particle concentrations. A measured aliquot (1-2 L) of seawater from Niskin bottles was passed through pre-weighed 0.4 μm Nuclepore filters. The filters were rinsed with deionized water to remove sea salt and stored at room temperature in petri dishes. In the lab, the filters were dried overnight at 50° C, re-weighed and particle concentrations were calculated in units of mg/l.

^{238}U-salinity relationship

In order to validate the assumption that ^{238}U concentrations can be estimated from salinity, several samples of 0.4 μm-filtered Niskin water were analyzed for ^{238}U courtesy of A.M Rodriguez (IAEA Marine Environmental Laboratory, Fig. 2- 2). The total salinity range from these samples was ~ 25.0-33.0 PSU, with lower salinities collected from sites closer to the river (station 718). Of the 11 data points, 6 were from the surface 0-25 m, and the rest were from 50-100 m. The ^{238}U vs. salinity relationship (Fig. 2-2) in the CASES area has a slightly different slope from open ocean data (Chen et al. 1986). We interpret this to reflect the fact that the relationship in the CASES area reflects

the influence of the Mackenzie River as the dominant fresh water source. The U vs. Salinity relationship was applied to obtain ^{238}U concentrations from CTD salinity data at all stations where ^{234}Th was measured.

Transmissometry and Fluorometry

During June and July, 2004, CTD and fluorometry data (used to obtain Chl-a profiles in figures below) were collected using a Sea-Bird CTD that was also fitted with a Sea-Point fluorometer. Particle concentrations (C_p in units of mg/l) from the samples we collected were correlated with opacity (1-transmissometer values) readings taken from the CTD and yielded a good correlation ($r^2 = .91$, Fig. 2-3). Using the relationship from Fig. 2-3, C_p values were calculated from transmissometer values at all stations where water column ^{234}Th samples were collected (Fig. 2-4a-d).

Since the correlation between Cp and transmissivity was determined using 0.4 μm filtered material, particles smaller than 0.4 μm are not included. However, the good correlation suggests that these particles are not major contributors to the transmissometry readings. This result is similar to that of Gardner et al. (1993), who found that the particles responsible for attenuation of the beam coefficient are removed using 0.4 μm filters. Moreover, as pointed out by Gardner et al. (1993), the beam coefficient (from which transmissometer reading are directly obtained) can be affected by particle type, size distribution, index of refraction and shape, with the first two factors being the most important. However, the correlation we obtained was from locations that ranged from the river mouth to the far eastern portion of the CASES study area. The latter may have been only marginally affected by the Mackenzie plume (during June), and thus, might have different particle sources. That a good correlation was obtained suggests that particle properties were largely uniform and did not affect the relationship between opacity and particle concentrations despite the different environmental regimes.

RESULTS

^{234}Th scavenging

Mackenzie inner shelf

A complete list of all Thorium data is in Appendix A.

Two stations were sampled on the inner shelf (Fig. 2-1b) corresponding to Reindeer Channel to the west (stn 912) and Kugmallit Channel in the east (stn 718). Station 718 was occupied three times, twice at times of low river flow (October, 2002 and 2003), and once after the spring freshet (July, 2004). At stn 718, fluorometer readings reached a maximum of 4μg/l at 10 m in July, and were <1μg/l during October 2002 and 2003 (Fig. 2- 4a). Particle concentrations at stn 718 were roughly constant (~ 2.5 mg/l) in October 2002-2003, and showed maxima where fluorometer readings were highest (10 m). Particle concentrations at stn 912 reached 5 mg/l (highest of any station sampled) in the 0-10 m range, and were constant and low at ~ 1 mg/l until the bottom (Fig. 2-4b).

Salinities at stn 718 clearly show the influence of the Mackenzie River on ^{238}U, with U values that are ~1.5 dpm/l, at a salinity of ~ 22.0 ppt (Fig. 2-5a). Below 10 m, calculated ^{238}U values approach 2.0 dpm/l as salinities increased to 30 ppt. This stratification is especially evident at stn 912. In contrast, the October, 2002 profile suggests a less well defined boundary and a more highly mixed water column.

Total ^{234}Th activities at these stations were the lowest of any sampled in the CASES area, with $^{234}Th/^{238}U$ activity ratios ~ 0.3 dpm/l in October 2002 and 2003 (Fig. 2-5a). Particulate ^{234}Th activities were low and invariant in these channel areas and did not show any significant trend with time.

Mackenzie outer shelf

Stations 906 and 803 lie along a 300 m isobath while stn 709 was located in a water depth of 80 m. All these sites lie directly in the path of the Mackenzie river plume. Fluorometer readings were all < 2 μg/l; however, stations 803 and 906 had particle concentration maxima (2.0 and 2.5 mg/l respectively) at 5-10 m (Fig. 2-4a). Station 709 had particle concentrations that were constant until near the bottom where a slight increase was observed.

Disequilibrium between ^{234}Th and ^{238}U persists on the outer shelf, but calculated ^{238}U concentrations in the surface water were higher than at the inner shelf region (Fig. 2-5b). Greater-than-equilibrium values of total ^{234}Th with respect to ^{238}U were found at two depths at stations 906 and 709 (Fig. 2-5b). Particulate ^{234}Th in the 1-70 μm fraction was high in these samples, and the excess ^{234}Th probably resulted from suspended bottom sediments at these stations. Indeed, particulate ^{234}Th in this size-fraction increased towards bottom, a feature found in all areas sampled except the inner shelf.

Shelf/Slope

This area included stations 49 and CA-12, both taken in deep water (1000-2000 m). Particle concentrations in the deeper waters of the shelf/slope region were ~ 0.2 mg/l, roughly 10-fold lower than inner shelf sites (data not shown). Fluorometer readings also were low (data not shown). ^{234}Th depletion was much less compared to shelf areas, however particulate (1-70 μm) ^{234}Th activities were very high (Fig. 2-5c).

Banks Island

These stations (CA-13, CA-14, CA-5, 124) were taken in the northernmost region of the Cape Bathurst polynya, where ice-melting throughout spring and summer is an important physical process. In October 2003, ^{234}Th was present in excess of ^{238}U in the upper 25-50 m at stations CA-13 and CA-5. Station CA-14 had a small subsurface maximum in particle concentrations (~1.5 mg/l) and had a small fluorometer maximum (~ 2 μg/l, data not shown). At station CA-13, a small particle maximum is seen (~ 0.7 mg/l) in the 50-100 m range along with a small fluorometer maximum. At station CA-5, particle concentrations were quite high and approached 2.0 mg/l while the fluorometer maximum registered only ~ 0.5 μg/l (data not shown). In

June, 2004, this area was the most recently ice covered. Indeed, all sampling in June occurred within a few days to 2 weeks after the polynya opened. These are the only stations where excesses in total ^{234}Th activities were consistently found.

Franklin Bay

Station 200 was the over-wintering site of the RV Amundsen in Franklin Bay. In October, 2002, particle concentrations were low (< 0.2 mg/l) and invariant at this station. In July, 2004, particle concentrations increased to 1.0 mg/l at the surface and decreased to constant values thereafter (Fig. 2-4b). A small fluorometer maximum (~ 1 μg/l) was observed centered around 50 m.

In October 2002, ^{234}Th was in equilibrium with ^{238}U down to 100 m at this station (Fig. 2-5d). In July, total ^{234}Th activities displayed a minimum at ~ 50 m but were close to equilibrium at all other depths. Particulate ^{234}Th activities in the > 70 μm fraction had a maximum at 20 m while 1-70 μm activities showed ~ factor of two increases with depth (Fig. 2-5d).

Cape Bathurst Polynya

On 1 June 2004, a wind-driven lead in the sea-ice developed in this region that included stns CA-06, 117, 303, 309, and 406. The ships' moving vessel profiler (MVP) found a phytoplankton bloom with an areal extent of around 20 km centered at stn 303 but extending to 406. At stn 303, the fluorometer registered 20 μg/l at the subsurface, the highest of any station occupied (Fig.2- 4b). Particle concentrations at this maximum were ~ 1.4 mg/l (Fig. 2-4b). This station showed significant ^{234}Th depletion centered around the chlorophyll maximum (Fig. 2-5f). Similar depletions were evident at stn 406 which was occupied twice about five weeks apart. At stn 117, a full-length water column (0-300 m) profile was obtained that reached equilibrium at 200 m, although disquilibrium was evident near the bottom (Fig. 2-5f).

Particulate (1-70 μm ^{234}Th) activities show a range of patterns. Values generally increased with depth, although the July sampling at stns 309 and 406 showed high values in surface waters.

Amundsen Gulf

These stations (101, 108, 206) are located in the eastern-most sector of the CASES study area (Fig. 2-1a). Two stations were collected from deep water (~ 500 m). In October, 2002, Th profiles showed equilibrium between ^{234}Th and ^{238}U at depths > 50 m.

^{234}Th in a sea-ice core

Supported Th values (^{238}U) were calculated from salinities measured in the core (salinity values were measured by Ryan Galley at the University of Winnipeg). Supported values were low in the top meter of the core (< 1 dpm/l) and high towards bottom as the ice approached contact with sea water (Fig. 2-6). Total ^{234}Th values were also low in the top of the core but were a factor of 3 higher than the supported value at the core bottom.

DISCUSSION

Water column ^{234}Th deficits

The box-model derived equation used to describe changes in ^{234}Th activities with time is:

$$\frac{\partial A_{Th}}{\partial t} = \lambda A_U - \lambda A_{Th} - P + V \qquad (1)$$

where A_U and A_{Th} are the total activities in units of dpm m^{-2}, λ is the ^{234}Th decay constant (0.0288 d^{-1}), P is the ^{234}Th flux (dpm $m^{-2}d^{-1}$), and V is the sum of advection and diffusion terms (Savoye et al. 2005).

The simplest expression of eqn (1) is to assume steady state ($\partial A_{Th}/\partial t$ = 0), and to neglect advective and diffusive terms. In this case, one obtains:

$$P = \lambda(A_U - A_{Th}) \qquad (2)$$

The term in parentheses is the ^{234}Th deficit, that upon multiplication by λ, yields the ^{234}Th flux (P) in units of dpm $m^{-2}d^{-1}$. Thus, the activity flux of ^{234}Th (P), is equal to the integrated ^{234}Th deficit over some depth range, multiplied by the ^{234}Th decay constant. Depth integrations were done trapezoidally.

Frequently, the depth of integration of the ^{234}Th deficit is chosen to be the bottom of the euphotic zone to facilitate comparisons with carbon and nutrient cycling. In much of the study area, euphotic zones are ~ 30 m. Trap fluxes are available at 50 and 100 m, and we have chosen these depths to permit best comparison with other data sets.

One expects that ^{234}Th deficits will be high where particulate fluxes are high. Such areas include those where there are significant inputs from the Mackenzie River, in situ particle production (in the Cape Bathurst Polynya), and release from ice melting (around Banks Island), or some combination of these factors. Indeed, ^{234}Th deficits are highest near the Mackenzie River and lowest in the Banks Island region (Fig. 2-7). During June and July, when spatial coverage was best, deficits in the 0-50 m layer displayed low values at Banks Island (< 5 x 10^3 dpm/m^2), and 7-16 fold higher values near the river (35-80 x 10^3 dpm/m^2). Deficits in 0-100 m generally show similar regional patterns as shown by those in the 0-50 m depth range (Fig. 2-7). While area-to-area differences are evident, seasonal patterns are not so apparent due to the large interannual variability in this system, the fact that different stations were samples (October) sampled in two different years (2002-2003), and coverage in June, 2004 was restricted to Cape Bathurst while July, 2004 sampling occurred mostly near the Mackenzie River. Cape Bathurst had the best temporal coverage with three different cruises yielding data. This region had lower ^{234}Th deficits (0-50 m) by a factor of 2 in July compared to October, 2003, although only a single station was sampled in October, 2003 (Fig.2-7).

Juxtaposing a satellite photo taken from mid-June 2004 (Fig. 2-8) with the deficits shown in Figure 2-7, the two patterns overlay quite well: newly ice-free regions (Franklin Bay, Cape Bathurst, Amundsen Gulf, Banks Island) have low deficits while those locations within the river plume have comparatively large ones. Thus, the tabulation of ^{234}Th deficits correlates with physical features and potentially quantifies processes within them.

At the shallow (30 m) inner shelf station 718, 0-30 m deficits were $Oct_{2002} \sim Oct_{2003} >$July (Values = 27, 30, 24 x 10^3 dpm/m^2, respectively) and seasonality is less apparent since values were not significantly different. The relative stability in ^{234}Th deficits between sampling times at this site is likely related to the fact that there are always substantial particle inputs from the Mackenzie River, even during late-season periods of low-flow. Furthermore, the relative invariance of Th deficits at this site indicates that the supply of Th from offshore is not a large factor. In other words, the seasonal movement of the salt wedge does not appear to affect the degree to which Th is scavenged.

Moran et al. (2000) sampled the Beaufort Shelf in August-September, 1995 and measured a 0-50 m ^{234}Th deficit of 22 ± 2 x 10^3 dpm/m^2 at stations close to 906 and 803. This deficit can be compared with our value of 38 ± 7 x 10^3 dpm/m^2 for those two stations in July, 2004. In the shelf/slope region, Moran et al. (2000) obtained a ^{234}Th deficit of 2.6 ± .2 x 10^3 dpm/m^2 while we obtained 6.0 ± 2 x 10^3 dpm/m^2. Given the high current speeds of the inner shelf (up to 1 m/s, Hill, 1991), the proximity to the Mackenzie (~ 50 km), the different sampling dates and the substantial inter-annual variability in ice-cover, such offsets are not surprising. The fact that both sets of values show large gradients between the inner shelf and shelf/slope is consistent with greater Th removal closer to the Mackenzie River. In the Northeast Water Polynya, Cochran et al. (1995) obtained ^{234}Th deficits (0-50 m) in July, 1992 of 20 ± 3 x 10^3 dpm/m^2. Our values from the Cape Bathurst Polynya were 17 ± 4 x 10^3 dpm/m^2 (0-50 m). The agreement between these two estimates is likely attributed to both areas being sampled in July, and the fact that both are high-latitude polynyas.

Scavenging of ^{234}Th near the Mackenzie River outflow

Stations 718 (Kugmallit channel) and 912 (Reindeer Channel) are located ~ 50 and 35 km from the river mouth respectively. This distance is far enough away that the very high particle concentrations expected closer to the river have attenuated to a maximum of ~ 5 mg/l. This value is in agreement with Hill et al. (1991), who also obtained particle concentrations of 5 mg/l using Landsat multispectral scanner data at a site close to stn 718. In July, in the surface 20 m, particle concentrations were higher by a factor of 5 at stn 912 compared with stn 718 (Fig. 2-4c-d). Coupled with the fact that the salinity at stn 912 reached a minimum of 11 ppt at the surface (compared to ~25 ppt at 718), it seems reasonable to conclude that Reindeer Channel was the more active of the two channels sampled. Both channel stations from July registered fluorometer maxima in the 3-4 μg/l range. Although hardly constituting a "bloom", these values are higher than most other stations except stn 303 and hence, it is likely that suspended particles at these near-river stations were not just river-derived detrital material (although river algae may have been responsible for the fluorometer readings).

Although total ^{234}Th activities < 1 dpm/l have only rarely been reported from open ocean settings, they have been found in similar coastal setting at sites close to river mouths (e.g. see Mckee et al. 1986). As stated above, ^{234}Th/^{238}U

activity ratios near the Mackenzie River were the lowest measured in the CASES area. Total ^{234}Th activities in surface waters of the North Water Polynya were in the range 1.0-2.0 dpm/l, even during a phytoplankton bloom (Amiel et al. 2002). In a transect across the central Arctic Ocean, Moran et al. (1997) found only one station situated on the Chukchi shelf that had total ^{234}Th activities < 0.5 dpm/l. Similarly, in a transect across the Canada Basin, Trimble and Baskaran (2005) measured total ^{234}Th activities < 1 dpm/l at only the most coastal location.

Despite the intense scavenging observed at these sites, the difference in particle concentrations between stns 718 and 912 was not reflected in the ^{234}Th profiles. One might have expected greater ^{234}Th removal at 912 compared with 718, but this was not the case. One factor contributing to disagreement between particle concentrations and ^{234}Th depletions at these two sites could be temporal offsets between information obtained with the CTD and in situ pump casts. Pump casts were generally positioned last during occupation of a station, while hydrocasts, from which CTD information was obtained, were usually first. Current speeds within the highly energetic inner shelf may reach 1.0 m s^{-1} (Hill, 1991), sufficiently rapid for a particle front detected in the hydrocast to have moved away from the area and be missed by the pump cast. Furthermore, as pointed out by Hill et al. (1991), as one moves closer to shore on the Beaufort shelf, the directional variance in currents increases as bottom topography and the influence of wave motions becomes more important. In view of these considerations, differences between measurements taken from the hydrocast and those from pump casts are not surprising.

Scavenging of ^{234}Th onto biogenic material

Of the three particle types (terrestrial, marine, material released via sea-ice melting) present in unknown ratios throughout the study area, marine-derived material is perhaps the most difficult to characterize. This is because the ubiquitous presence of the Mackenzie River plume makes it difficult to obtain marine end member values for a parameter like POC. In later sections of this thesis, marine POC is distinguished from terrestrial POC using δ^{13}C measurements. The samples most likely to reflect inputs of marine particles were stns 303 and 406 in the Cape Bathurst Polynya sampled in June, 2004. At these sites, the influence of the river plume was minimized due to the heavy ice conditions that obstructed plume dispersal. In concert with the recent onset of river flow, this allowed for inputs from phytoplankton to dominate particle loading. Indeed, the CTD data from stn 303 show that the Chl a maximum (~ 20 μg/l) is coincident in depth (30 m) with the particle maximum (~1.3 mg/l, see Fig. 2-4b). Below 50 m however, particle concentrations were not constant, whereas fluorometer readings were very low (<.01 μg/l) and invariant indicating that control of particle concentrations by phytoplankton was limited to the top 50 m.

Total ^{234}Th activities at stn 303 showed a minimum centered at 25 m in agreement with the fluorometer and particle measurements. The small depletions between 50-100 m may have been due to the small variations seen in

particle concentrations. The case for ^{234}Th scavenging onto marine debris between 0-50 m is supported by the > 70 μm activities that increase five-fold at 25 m (not apparent in Fig. 2-5f, however, due to the scaling). This is consistent with ^{234}Th scavenging onto nascent, marine particles (see Buesseler et al. 1992).

Excess ^{234}Th supplied to surface waters from ice melt

As stated previously, a lead developed in the ice around Cape Bathurst in early June, 2004. Although the principal agent that formed the polynya at this point in the season was southerly winds that advected the ice northwards and not ice melting, the latter process did occur as well. The relative contributions of ice melt and wind to formation of the Cape Bathurst polynya are not known; however early in the season it is likely that advection, not ice melt, will be more important. Later in the season, when temperatures are higher, ice melt is expected to have greater importance.

The underside of the ice cores we collected were coated with a particle rich mat of ice algae that provided an ample supply of surfaces onto which ^{234}Th could scavenge. Indeed, significant excess ^{234}Th was present in the ice core (Fig.2-6). In contrast, the top section of the core had very few particles in it (pers.comm. S. Belanger, S, Unversity of Quebec). In the top 1.5 m, ^{234}Th concentrations are, within errors, in equilibrium with ^{238}U, and no excess is present. This changes abruptly at 1.7 m where ^{234}Th is ~ 3-fold higher than the predicted equilibrium value. The interpretation of this excess is that ^{234}Th is scavenged from the surrounding sea-water onto the ice algae.

If excess ^{234}Th is injected into surface waters in association with sea-ice melting, we should see a freshening of the surface waters at the same time we see ^{234}Th concentrations above equilibrium with U. Such ^{234}Th excesses in concert with a surface freshening were observed at stations CA-13, CA-14, and CA-5 in October, 2003 (Fig. 2- 5e-f). Our conclusion is that ice melt is the agent responsible for the Th excesses that were measured at these sites (as opposed to a biological mechanism such as remineralization of POC and release of previously scavenged ^{234}Th).

^{234}Th distributions near the sea floor

Although the sampling strategy we employed focused on determining ^{234}Th deficits and fluxes in the upper water column, stn 406, which was sampled in both June and July, 2004 allowed the serendipitous sampling of a mid-water particle maximum (See Fig. 2- 4b). This particle layer does not seem to be the result of resuspension of material as is evident at many of the stations where the 1-70 μm fraction shows increasing ^{234}Th activities towards the sea-floor. Mid-water particle layers were also present at the 100-200 m depth horizons at stations 803 and 303, but were much less pronounced (Fig. 2-4c). Such mid-water particle maxima were absent from stations in the Amundsen Gulf and Banks Island region. If the particle layer at stn 406 in July originated from the Mackenzie River (as opposed to local resuspension of material), one might expect more intense layers closer to the river at similar isobaths. This however was not observed and indicates that other processes were at work in forming the

particle layer at stn 406. Such processes could be turbulence at the shelf-break and detachment of nepheloid layers from the shelf to station 406. Or perhaps the source of the layer was locally derived material coming from the top or bottom of the water column. Still another possibility is that the layer originated from the Mackenzie River plume but had branched off and was no longer clearly connected to its origin.

Suspended particle concentrations within the particle layer increased from 0.66 to 0.78 mg/l between June and July at station 406 (Fig. 2- 4c). During both cruises, the constant, "background" particle concentration (measured between 110 and 160 m where particle concentrations were low and constant) was 0.55 mg/l and so concentrations were enhanced in the particle layer ~ 20 to 30 % between June and July compared to background.

Two pieces of evidence suggest that ^{234}Th was scavenged by particles in the layer at stn 406. First, there was clear ^{234}Th depletion at the depths of the particle layer in both June and July (Fig.2-5f). These depletions were responsible for ~ 20 % of the total water column ^{234}Th deficit in June and July, and were thus similar to the relative increases in particle concentrations (also 20-30 %). Also at the depth of the particle layer maxima, there were decreases in dissolved ^{234}Th activities that were coupled with high suspended particle ^{234}Th activities. This is consistent with the interpretation that dissolved ^{234}Th had been scavenged onto surfaces within the particle layer.

Bacon and Rutgers van der Loeff (1989) examined ^{234}Th scavenging from nepheloid layers of the Western Boundary Undercurrent of the North Atlantic and found that a concentration of total suspended material of 0.2 mg/l produced a 19 % depletion in ^{234}Th. In the Arctic, on the western flank of the Yermak Plateau, ^{234}Th depletions were linearly related to suspended matter concentrations within the nepheloid layer (Rutgers van der Loeff, et al. 2002). It was also found that sediments in the western Yermak Plateau supported higher concentrations of benthic organisms compared with the eastern areas where there was no nepheloid layer. This situation is similar to that described by Renaud and collegues (pers. comm. P. Renaud, University of Connecticut) who found greater infaunal abundances at station 406 compared to other stations, suggesting that the particle layer might be a potential food source for bottom dwelling animals.

Th deficits and particle concentrations

While ^{234}Th has been widely used as a proxy for POC fluxes, there have been few attempts to explicitly link thorium distributions with another independent variable such ambient particle concentrations.

Figure 2-9 shows the relationship between Th deficits and particle concentrations in the CASES area. If particle concentrations determine the extent of Th scavenging, one would expect a positive correlation. A non-linear relationship points to the combined influences of particle composition, the inherent problems in relating fluxes to concentrations, and temporal offsets between the acquisition of particle concentration (C_p) and ^{234}Th data. The results of this exercise are not statistically convincing with the implication that

these other factors complicate any relationship between particle concentrations and Th scavenging in the study region. There was equally no relationship between Chla and Th deficits (Fig.2-9). Other correlations, that regressed 1-70 and > 70 μm concentrations versus C_p also yielded poor correlations (data not shown).

Trimble and Baskaran (2005) undertook a similar exercise along a transect from the Canada Basin. They plotted log J_{Th} (J is the rate of conversion of $^{234}Th_{diss} \rightarrow {}^{234}Th_{part}$, see below) versus log SPM, and found significant scatter with the interpretation that particle composition plays an important role in Th scavenging. On the other hand, Rutgers Van der Loeff (2002) found a convincing relationship between the extent of Th depletion ($1-{}^{234}Th/{}^{238}U$) and particle concentrations in bottom nepheloid layers of Fram Strait.

Figure 2-10 shows averages of 1-70 μm and > 70 μm ^{234}Th activities, as well as particle concentrations from 0-50 m, lying roughly along a 100 m isobath from west to east. The ~ 25 % decrease in particle concentrations compares with a 3-fold decrease in the > 70 μm ^{234}Th activities, and a 3-fold increase in 1-70 μm activities. Decreases in the concentrations of large particles with increasing distance from the river source may be expected due to the geostrophic flow set up from the Mackenzie River and the preferential settling of larger particles away from a point source (Robert Wilson, personal comm.). The force balance (pressure gradient versus Coriolis) that determines the direction of geostrophic flow indicates that offshore motion of the river plume ought to be parallel to the shoreline, in an eastward direction, and will closely follow bottom contouring. Large particles (and their sorbed ^{234}Th) entrained within the plume will settle out along the path of this flow, leading to the observed trend in the > 70 μm ^{234}Th.

The increase in 1-70 μm activities does not, however, fit into this interpretation. Most of the 1-70 μm ^{234}Th profiles show increases with depth beginning at 50 m (too shallow at many sites to be explained by bottom resuspension) whereas > 70 μm ^{234}Th activities do not. This suggests that cycling of the two size classes is distinct in this system. The consistent pattern in the increases in the 1-70 μm ^{234}Th activities, both eastward and with depth, is an increasing marine signature to the water moving eastwards and with depth. Indeed, $\delta^{13}C$ measurements show the 1-70 μm size-fraction becoming isotopically heavier (~0.4 per mil) with depth, unlike the > 70 μm size fraction (See Chapter 4). This marine character suggests enhanced sorption of ^{234}Th onto particles of marine origin compared to terrestrial dominated particle inputs near the Mackenzie River (and in 0-50 m of the water column). Thus, the two size classes may derive from different sources, and as such, may be diagnostic for distinct water masses: > 70 μm particles have an origin related to the Mackenzie River and 1-70 μm ones comprise a mixture of offshore-marine, Mackenzie, and coastal provenance. The coastal provenance is significant since coastal erosion rates along the study area are some of the highest in the world (up to 20 m/yr. Macdonald et al. 1998). Furthermore, the composition of the eroding material may be quite different in western versus to eastern areas. Thus, a combination of physical (geostrophic flow) and chemical (particle

composition) factors are important in altering the partitioning of ^{234}Th onto large and small particles as one moves away from the Mackenzie River. The consequences of this observation to carbon cycling are examined in Chapter 4.

Evidence of lateral and non steady-state effects on ^{234}Th fluxes

Previous studies have evaluated the advection-diffusion terms and the assumption of steady state in the conservation equation (Buesseler et al.1993, Murray et al.1996, Gustafsson et al. 2000, Savoye et al. 2006). These studies have shown that, depending on the physical environment, (e.g. upwelling near the equator, large tidal prisms such as Casco Bay, ME, proximity to rivers and coasts, the progression of a phytoplankton bloom) the advection and diffusion terms from eqn (1) may contribute significantly to measured ^{234}Th distributions. However, in "blue water" regions, and even some coastal systems, the assumptions of this model can be surprisingly good first approximations at explaining ^{234}Th deficits (Savoye et al. 2006). For example, Savoye et al. (2006) tested the steady state assumption in settings that included open ocean, coastal, and high latitude sites, and found no statistical differences between steady state and non steady state estimates of ^{234}Th fluxes 60 % of the data (Savoye et al. 2006). On the other hand, the range in the ratio $P_{\text{Non Steady State}}$:$P_{\text{Steady State}}$ (P = ^{234}Th export flux) from these environments was between 2-6. Offsets, when they occur, can be substantial. While the steady state assumption can not be rigorously tested in the present study since most sites were only occupied once, station 406 was occupied twice, 5 weeks apart between June and July, 2004. Buesseler et al. (1998) solved eqn 3 for the non-steady state case and, using that approach at stn 406, one obtains a value of 0.85 dpm m^{-2} d^{-1} for the nss ^{234}Th flux, which compares with 0.56 and 0.36 dpm m^{-2} d^{-1} (average 0.46 dpm m^{-2} d^{-1}) for steady state values for June and July, respectively. Thus, steady and non steady state estimates are within a factor of two.

Sorption equilibrium between dissolved and particulate ^{234}Th

Another approach to evaluating non-steady state effects on Th distributions is through consideration of whether partitioning of Th between dissolved and particulate fractions is in sorption equilibrium. For example, Mckee et al. (1984) examined changes of particulate and dissolved ^{234}Th over a 38 hour period from surface and near-bottom waters of the inner Amazon Shelf (~15 m depth) and found 4 and 13-fold differences between dissolved and particulate Th over the sampling period. Since many other parameters such as SPM and salinity also varied significantly, the master variable invoked to explain the changes in ^{234}Th was tidal forcing. Mckee et al. (1984) also studied whether ^{234}Th in the dissolved and particulate fractions were in equilibrium over the 38 hour period. The result was that they were not, and Mckee at al. (1984) developed a term quantifying the extent of disequilibrium ($1-e^{-kt}$) that was always < 1 during the sampling period. They concluded that the amount of time to reach sorption equilibrium between particulate and dissolved Th is a critical parameter. Although the sampling interval was not sufficient time to reach equilibrium, 2-3 days was enough time to "average out" all the tidal

fluctuations, and a steady state model was deemed appropriate for use on these (and longer) time scales (Mckee et al. 1984).

In our system, tidal fluctuations were small (< 50 cm), sampling was not conducted close to the river mouth where disequilibrium may be expected, and calculated residence times of particulate and dissolved Th were significantly longer than the minimum 1-2 d required to reach equilibrium (Table 2). Conversely, as noted earlier, increases in dissolved and 1-70 μm ^{234}Th activities, coupled with decreases in > 70 μm ^{234}Th activities along an eastward transect in the CASES area indicate a shift in the partitioning of Th between dissolved and particulate pools.

Although such changes may be attributed to changes in particle type, the possibility exists that such shifts also may be related to disequilibrium phenomenon. In this interpretation, the increasing marine composition of entrained material moving away from the river (as we observed) facilitates desorption of Th from large particles and scavenging onto small ones that could possess different surface areas compared with their terrestrial analogs of the same size. If, furthermore, the transit time from the river-to marine-dominated regions is less than 1d, then the snapshot of Th distributions we have measured may be one in which equilibrium was not attained. While the transit time from river to marine environments is not precisely known, as an exercise one can assume a current speed and estimate the transit time. Given a distance of ~ 250 km from Reindeer Channel to Cape Bathurst, the assumption that mixing between river and marine material is linear (i.e. the midpoint at 125 km is 50 % river, 50 % marine) and an assumed current speed of 10 cm/s (9 km/d), an estimate of ~ 14 days is obtained. However, current speeds within the plume may be much larger, especially early in the season (when sampling occurred in 2004) during peak river flows when current speeds may be closer to 1 m/s (Hill et al. 1991). In this case, the expanding plume would reach half way to Cape Bathurst in only 1.5 d. This is close enough to the estimate of Mckee, et al. (1984) to question whether sorption equilibrium has been reached.

Floating trap ^{234}Th fluxes

A third approach to evaluating the relative importance of non-steady state and advective influences in eqn 1 is to compare ^{234}Th fluxes from the water column profiles with those from floating sediment traps and with sediment inventories of excess ^{234}Th (Murray et al. 1996, Amiel et al. 2002, Aller and Cochran, 1976).

Average ^{234}Th fluxes determined from water column deficits at all stations increase with depth by two-fold from 316 ± 96 to 614 ± 173 dpm m^{-2} d^{-1} between 15 and 50 m (Table 1), while floating traps increased from 280 ± 133 to 708 ± 393 dpm m^{-2} d^{-1} over the same depth interval. Water column ^{234}Th fluxes increase to 1606 ± 810 dpm m^{-2} d^{-1} at 100 m and those in floating traps increased to 792 ± 539 dpm m^{-2} d^{-1}.

Temporally, water column ^{234}Th fluxes did not show increases at 15 m between June and July, 2004 (308 ± 72, 327 ± 120 dpm m^{-2} d^{-1}, respectively) but at 50 m, fluxes increased from 530 ± 48 to 836 ± 264 dpm m^{-2} d^{-1} between

the two sampling periods. At 100 m, water column fluxes increased to 2367 ± 652 dpm m^{-2} d^{-1} (a value that is largely driven by the high flux from station 803. Similarly, in June and July 2004, floating trap fluxes increased from 227 ± 127 to 352 ± 104 dpm m^{-2} d^{-1} at 15 m, 250 ± 100 to 883 ± 249 dpm m^{-2} d^{-1} at 50 m and 476 ± 452 to 1214 ± 310 dpm m^{-2} d^{-1} at 100 m. The range in percent standard deviations of FST ^{234}Th fluxes between June and July is much higher (26-95 %) than from water column deficits (9-37 %).

In the simple case in which vertical fluxes dominate, trap collection efficiencies are 100 %, and the flux of particles collected in the traps produces the ^{234}Th deficit in the overlying water column, ^{234}Th fluxes calculated from water column profiles and recorded in traps should be identical. Indeed, water column-derived ^{234}Th (or ^{230}Th) fluxes have frequently been used to calibrate sediment trapping efficiency (Murray et al. 1996, Scholten et al. 2001). Thus, in a correlation of water column and trap ^{234}Th fluxes, values which deviate below the 1:1 line indicate trapping efficiency ≠ 100% or advective influences (Table 1). In the CASES area, ^{234}Th fluxes measured by traps compared with pumps are constrained within a factor of ~ 2 at 15 and 50 m, including the high energy stations near the Mackenzie River (stns 803, 906; Fig. 2-11b). On the other hand, trap fluxes in 75-100 m are consistently lower than pump-derived fluxes by ~ 3-fold with the exception of station 906 (Fig. 2-11a). It seems the case that at a given station offsets in the 15 and 50 m traps are over or under the 1:1 line in a consistent pattern i.e. traps over or under-collect consistently at all depths (see stns 200, 406, 803 in Fig 2-11a-b). The fact that offsets between pump and trap ^{234}Th fluxes were found east and west indicates that proximity-to-the-river was not responsible for the offsets. Furthermore, under-collection by traps is not explained by distance drifted during collection (Table 1). In fact, if anything, Table 1 shows that lower distances traveled resulted in greater offsets. More likely, increases with water depth in offsets between trap and pump Th fluxes arise from a combination of factors, including different temporal scales related to each method, trapping efficiency, and lateral effects. Our intention here is not to provide a detailed explanation of why such offsets occur. Instead, we view the agreement between trap and pump thorium fluxes as being one indication of lateral effects, albeit a crude one. To the extent the two measurements of ^{234}Th fluxes agree, lateral effects are less likely to dominate water column Th scavenging. The relatively good agreement between the two methods at 15 and 50 m suggests that vertical fluxes dominate the ^{234}Th profiles at most of our stations at the time of sampling. This seems reasonable in that the comparison is made in summer when biogenic particle fluxes are greatest.

Comparison of water column ^{234}Th deficits and sediment excess ^{234}Th inventories

Sediments measure net effects since they are the “last stop” for settling particles. The first measurements of excess ^{234}Th in sediments were made by Aller and Cochran (1976) who calculated the expected standing crop of $^{234}Th_{xs}$ in sediments from Long Island Sound based on complete removal of ^{234}Th

produced from ^{238}U in the overlying water. They found a general balance, but local variability existed that they attributed to lateral transport of ^{234}Th into the sediments. In general, ^{234}Th sediment inventories greater than can be supplied from the overlying water column require lateral transport of the radionuclide into the sediments. The reverse case indicates transport of material away from the site.

Figure 2-12 shows ratios of sediment excess ^{234}Th inventories to water column deficits in the CASES area. Propagated errors are between 20-70 %. A better comparison would measure the complete water column, not just the upper 100 m as we have done. This was accomplished at station 117, where water column ^{234}Th measurements extended to 300 m i.e. the full water column depth. Since most stations were only sampled to 100 m, the water column deficits from Fig. 2-12 are minima. However, if additional scavenging that takes place at depths greater than 100 m contributes similar amounts to the total deficit as at station 117 (where < 10 % of the deficit came from depths > 100 m at station 117), then the underestimation caused lack of integrating throughout the full water column is not significant. The sediment profiles from which the inventories are calculated are discussed in Chapter 3.

Apart from a high sediment:water column ratio at stn 108 (ratio = 7.4), values were ~ 0.5 to 2.0 and hence water column and sediment ^{234}Th inventories were roughly in balance within propogated errors. Surprisingly, this range is found at sites near the Mackenzie River as well as the Cape Bathurst Polynya (Fig. 2-12).

On the inner Amazon Shelf, Smoak et al. (1996) measured excess ^{234}Th inventories in sediments and compared them with the calculated production of ^{234}Th from ^{238}U the overlying water column. The ratios of sediment ^{234}Th inventory to production were generally < 1, and Smoak et al. (1996) concluded that most of the excess Th (> 90 %) was found in surficial mobile mud layers (as opposed to the region acting as giant Th source) that can traverse the bottom for considerable distances. Since no such mobile mud layers are known to exist in our study region, the general agreement of $^{234}Th\ sediment_{xs}$ with water column deficits (within a factor of 2) gives some indication that lateral transport of particulate material does not dominate their distribution in the water column.

The above results are broadly consistent with the comparison of ^{234}Th fluxes estimated from the water column and sediment traps that are also within a factor of two in the upper 50 m.

^{234}Th scavenging rates, particle sinking rates, and residence times

The rates for Th uptake from the dissolved phase onto particles, and the rates at which those particles sink can be estimated using a one dimensional box model (lateral effects assumed to be small) with two boxes; one for dissolved ^{234}Th and one for particulate Th (Bruland and Coale, 1986). The equations that balance ^{234}Th activity sources and sinks between the dissolved and particulate pools are:

$$\frac{\partial A_{Th}^{d}}{\partial t} = A_U \lambda - A_{Th}^{d} \lambda - J_{Th} \quad (3)$$

$$\frac{\partial A_{th}^{p}}{\partial t} = J_{Th} - A_{Th}^{p} \lambda - P_{Th} \quad (4)$$

where A_U, A^d_{Th} and A^p_{Th} are the activities of ^{238}U, dissolved and particulate ^{234}Th respectively. λ is the decay constant for ^{234}Th (.0288 d^{-1}). J is the rate of adsorption of dissolved ^{234}Th onto particles, and P is the loss of particulate ^{234}Th via settling (J, P = dpm m^{-2} d^{-1}). Equations (3) and (4) are solved assuming steady state ($\partial A_{Th}/\partial t = 0$). With these constraints, the steady state solutions to equations (3) and (4) are:

$$J_{Th} = \lambda(A_u - A_{Th}^{d}) \quad (5)$$

$$P_{Th} = J_{Th} - A_{Th}^{P} \lambda \quad (6)$$

for dissolved and particulate ^{234}Th. Following Bruland and Coale (1986), residence times ($\tau_{d,p}$) are defined as:

$$\tau_d = \frac{A_d}{J_{Th}} \quad (7)$$

$$\tau_P = \frac{A_P}{P_{Th}} \quad (8)$$

To emphasize geographic differences, we compared eastern stations (206,108,117,124,406) from June to western stations (709, 803, 906) from July. In addition, three eastern stations (309, 200,406) were sampled in July permitting comparison to June. Errors from these comparisons are calculated from the standard deviations of samples from within these regions.

Average values of $J_{Th\ @50\ m}$ were higher by a factor of ~ 2 (1.14 ± .6 vs 2.42 ± .8 · 10^3 dpm/m^2/d for east and west, respectively; Table 2) in western areas while $P_{Th\ @50m}$ was five-fold higher, also in the west (0.3 ± 0.2 east,1.4 ± 0.4 x 10^3 dpm/m^2/d west). $J_{Th\ @100m}$ was only slightly higher in the west (2.4 ± 0.4, 3.0 ± 0.3 x 10^3 dpm/m^2/d respectively) while $P_{Th@100m}$ was higher by a factor of 3 (0.8 ± 0.6, 2.2 ± 0.5 x 10^3 dpm/m^2/d east to west). No statistical difference was observed between eastern stations from June to July (July east $J_{Th\ @50\ m}$ = 1.4 ± 0.3, $J_{Th\ @100\ m}$ = 2.8 ± 0.7, $P_{Th@\ 50\ m}$ = 0.6 ± 0.1, $P_{Th@\ 100\ m}$ = 0.6 ± 0.2 x 10^3 dpm/m^2/d).

Gradients east and west were also apparent with respect to residence times (Table 2). Averages residence times of $\tau_{diss\ @50\ m}$ and $\tau_{diss@\ 100\ m}$ were both a factor of two higher in the east ($\tau_{d\ @50\ m}$ = 61 ± 21, 29 ±16, $\tau_{d\ @\ 100\ m}$ = 52 ±13, 25 ± 9 d, east and west respectively). The extremely high values for τ_p at stations 206 and 124 arise from high activities of ^{234}Th 1-70 μm fraction and low P_{Th}. Although the standard deviation at eastern stations for $\tau_{p\ @100\ m}$ was higher than the measurement (295 ± 305 d) it is nonetheless apparent that τ_p

$_{@100m}$ is significantly higher here than in the west (17±7 d). Similarly, $\tau_{p\ @50\ m}$ in the east also had a very large range (42-315 d, avg_{east} = 184 ± 139 d) but was narrowly constrained and significantly lower in western regions (13 ± 4).

Most interpretations of J_{Th}, P_{Th}, and τ are done in the context of the carbon cycle. For example, the original work by Bruland and Coale (1986) hypothesized that J_{Th} was proportional to primary production while τ_p was controlled by zooplankton grazing pressure. Other work has explicitly related P_{Th} to POC fluxes using POC: Th ratios on sinking particles (Cochran et al. 1995, Buesseler et al. 1997, Amiel et al. 2002). Moran et al. (2000) made measurements in the Beaufort Sea (stations 803, 906) but only compared J, P and τ to literature values and did not discuss their importance to particle cycling within the study area except to say that τ generally increased with distance offshore. The east-west gradients in J, P and τ that are estimated to be a factor of two from this study are likely caused by particle concentrations that are a factor of two higher in western regions relative to eastern ones. If particle concentrations are the controlling factor determining differences in J and P, the observation that J is always higher than P implies that there are fewer sinking particles than suspended ones. This interpretation is consistent with the much smaller discrepancy between J and P found in western regions compared to eastern ones, because western areas lie closer to particles input from the Mackenzie River.

The CASES area became ice-free only after June 1, 2004 and this might suggest that the flow of the Mackenzie River was obstructed by sea ice until this time. Thus, sampling done in eastern regions during early June was relatively free from the influence of the river. Stations sampled in the Cape Bathurst Polynya in late July, 2004 depending on the speed and direction of the river plume, may have been more affected by the river. However, J, P and τ do not show statistical differences in eastern locations between June and July, and this could suggest that the presence of sea ice does not affect the plumes mode of dispersal. Instead, values of J, P and τ are similar in the east between June and July imply a ubiquitous river influence that can travel underneath the sea-ice.

SUMMARY

Calculations of ^{234}Th deficits (0-100 m) obtained from measurements of ^{234}Th disequilibria in surface waters varied from ~ 0-100 x 10^3 dpm/m^2. The highest values of the Th deficit were found in close proximity to the Mackenzie River while the lowest deficits were from areas only recently ice-free. Temporal patterns in ^{234}Th deficits were not readily evident.

1- 70 μm ^{234}Th activities increased (0.3 to 0.9 dpm/l) moving eastwards away from the Mackenzie River, >70 μm ^{234}Th activities decreased (~ .05 to .008 dpm/l) while total particle concentrations also decreased (1 to .5 mg/l). Since 1-70 μm ^{234}Th activities also generally increased with depth that was not attributed to particle rebound, we suggest that distributions of sorbed Th to small particles may reflect increasing marine composition while sorbed Th to large particles is diagnostic of Mackenzie River-derived material.

Average ^{234}Th fluxes determined from water column deficits at all stations increased by two-fold from 316 ± 96 to 614 ± 173 dpm m^{-2} d^{-1} between 15 and 50 m while floating traps increased from 280 ± 133 to 708 ± 393 dpm m^{-2} d^{-1} over the same depth interval. Offsets between floating traps and water column ^{234}Th fluxes increased substantially between 50 and 100 m. A comparison between surficial sediment inventories of ^{234}Th and water column inventories was also within a factor of 2. Based on these comparisons, we conclude that ^{234}Th distributions can be interpreted using a vertical, one dimensional model in which lateral effects are constrained to within a factor of 2.

Residence times of dissolved and particulate ^{234}Th at 100 m were much longer in eastern compared to western areas with ranges between 25 and 52 d for dissolved Th and 17-295 d for particulate Th. No difference in Th residence times between recently ice-covered (June) and ice-free (July) sampling times was observed suggesting that distance from the Mackenzie River is a controlling factor in determining the extent of Th scavenging on the Beaufort Shelf.

TABLES

Table 2-1

^{234}Th fluxes in floating traps

Stn	Depth (m)	Pump dpm m^{-2} d^{-1}		Trap dpm m^{-2} d^{-1}		days	Distance Traveled (km)
108	15	264	±53	106	±11	1.58	15
	50	449	±90	121	±12	1.58	15
	80	789	±158	245	±25	1.58	15
117	15	259	±52	96	±10	1.51	3
	50	547	±109	175	±18	1.51	3
	75	850	±170	239	±24	1.51	3
406	15	275	±55	323	±32	1.16	9
	50	552	±110	647	±65	1.16	9
	75	1469	±294	660	±70	1.16	9
303	15	432	±86	163	±38	1.27	16
	50	573	±115	1192	±119	1.27	16
	75	1036	±207	1257	±126	1.27	16
803	15	490	±98	460	±46	0.97	6
	50	922	±184	868	±87	0.97	6
	100	3283	±657	1174	±117	0.97	6
906	50	1165	±233	1294	±129	1.51	57
	100	1817	±363	1612	±129	1.51	57
200	15	202	±40	385	±39	0.99	50

	50	432	±86	654	±65	0.99	50
	100	2000	±400	857	±86	0.99	50
309	15	288	±58	211	±21	1.11	23
	50	826	±165	718	±72	1.11	23

Table 2-2. Residence times of particulate and dissolved ^{234}Th in June and July, 2004

STN	Depth (m)	Date	J_{Th} x 10^3 dpm/m^2/d		P_{Th} x 10^3 dpm/m^2/d		τ_{diss} days		τ_{Part} days	
206	50	6/3/2004	2.24	±.11	0.11	±.10	27	±3	428	±42
	100	6/3/2004	2.20	±.11	0.11	±.10	42	±4	700	±80
108	50	6/7/2004	1.01	±.10	0.21	±.14	79	±4	132	±13
	100	6/7/2004	2.60	±.20	1.04	±.20	49	±5	74	±8
117	50	6/9/2004	1.17	±.10	0.34	±.11	72	±3	90	±9
	100	6/9/2004	2.32	±.25	1.63	±.25	54	±5	40	±5
124	50	6/11/2004	0.86	±.10	0.10	±.02	87	±4	315	±32
	100	6/11/2004	1.81	±.25	0.10	±.02	78	±7	750	±80
406	50	6/15/2004	1.24	±.10	0.56	±.10	47	±3	42	±5
	100	6/15/2004	2.35	±.4	1.05	±.20	51	±5	62	±7
303	50	6/18/2004	1.31	±.10	0.33	±.12	53	±4	102	±10
	100	6/18/2004	3.04	±.8	0.60	±.22	36	±4	145	±16
709	50	6/30/2004	2.18	±.30	1.89	±.10	12	±3	8	±2
	100	6/30/2004	2.81	±.5	2.35	±.35	16	±3	16	±3
906	50	7/3/2004	1.61	±.10	1.18	±.20	25	±3	13	±3
	100	7/3/2004	2.72	±.4	1.61	±.26	37	±4	26	±3
803	50	7/8/2004	1.16	±.10	0.98	±.10	50	±2	17	±4
	100	7/8/2004	3.47	±.5	2.70	±.29	22	±3	9	±3
200	50	7/17/2004	1.33	±.24	0.67	±.12	43	±3	37	±6
	100	7/17/2004	2.34	±.3	0.80	±.30	52	±6	80	±8
309	50	7/19/2004	1.77	±.10	0.61	±.11	24	±3	75	±8
	100	7/19/2004	3.74	±.35	0.40	±.10	20	±4	45	±4
406	50	7/24/2004	0.99	±.10	0.36	±.12	68	±3	61	±7
	100	7/24/2004	2.29	±.26	0.50	±.15	53	±4	136	±14

FIGURES

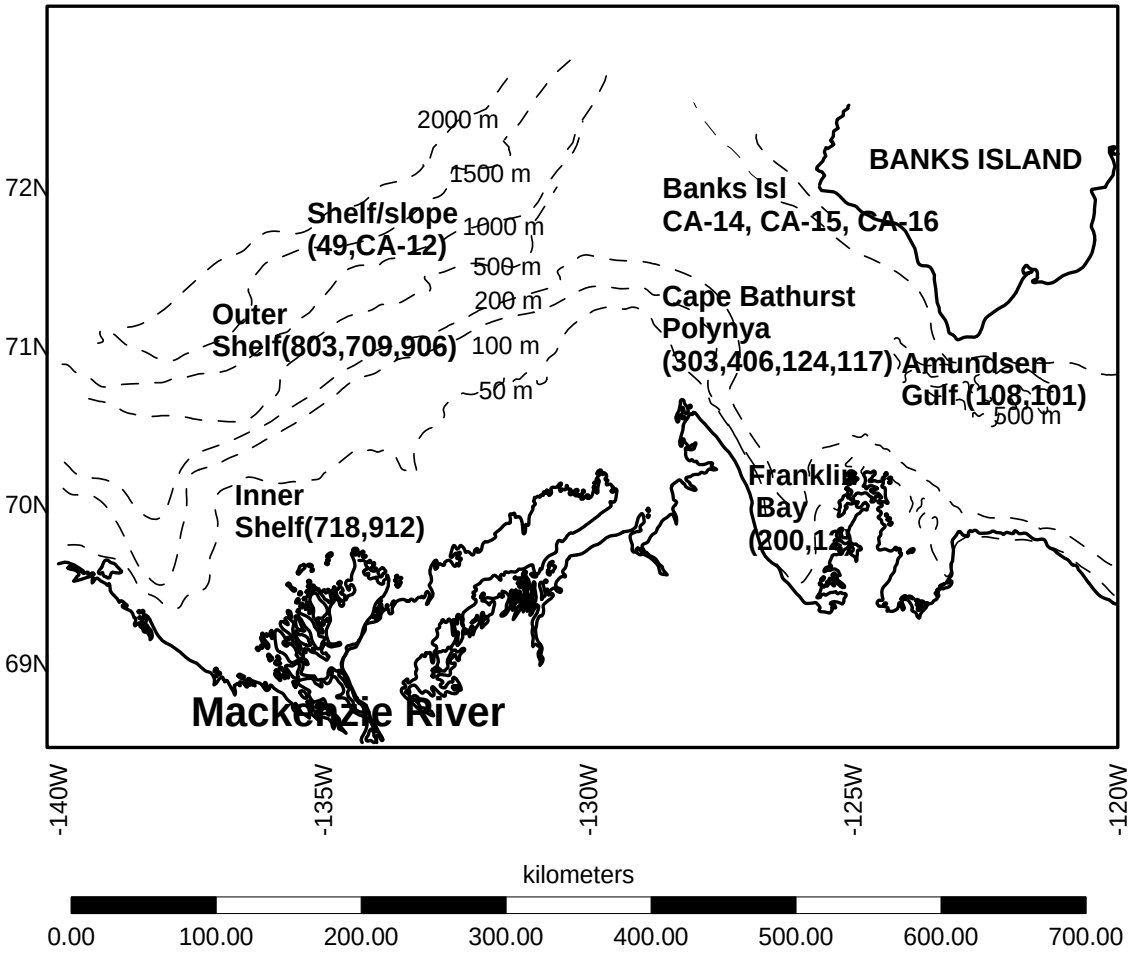

Figure 2-1a. Regions in CASES including stations assigned to each region.

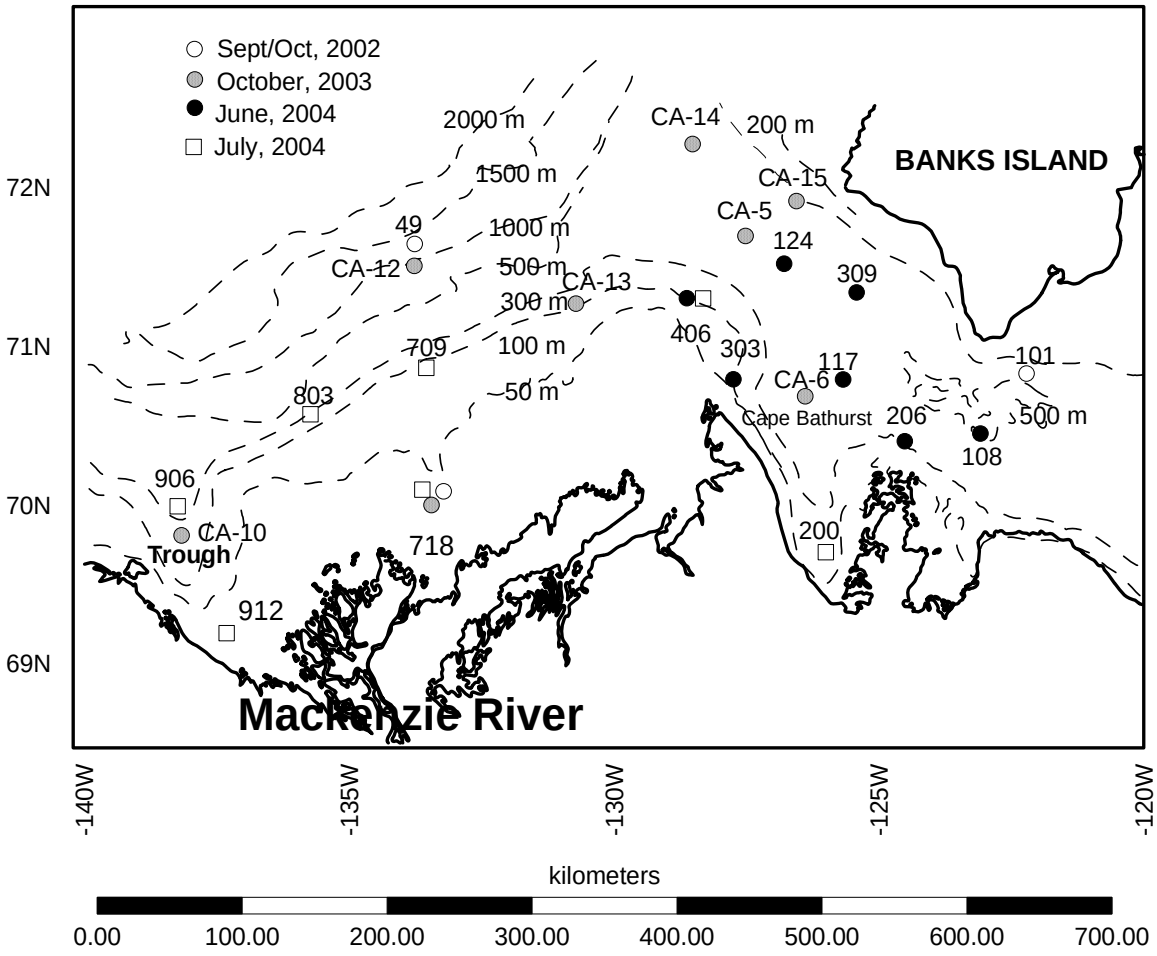

Figure 2-1b. Station locations and times where sampling for ^{234}Th occurred.

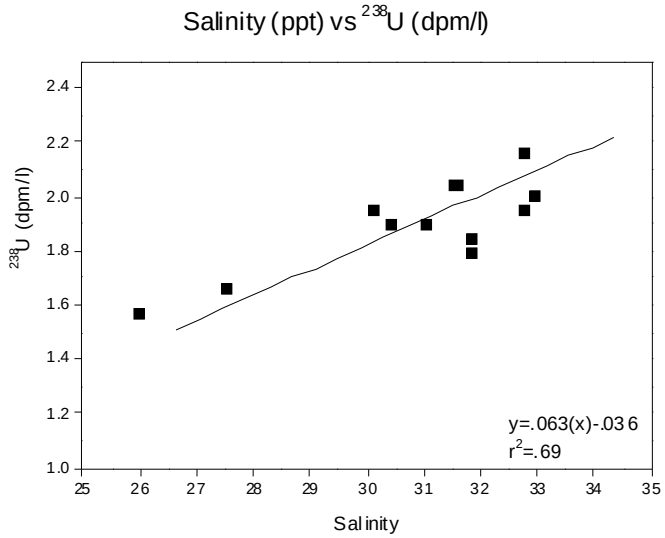

Figure 2-2. Plot of ^{238}U (dpm/l) vs. Salinity (ppt)

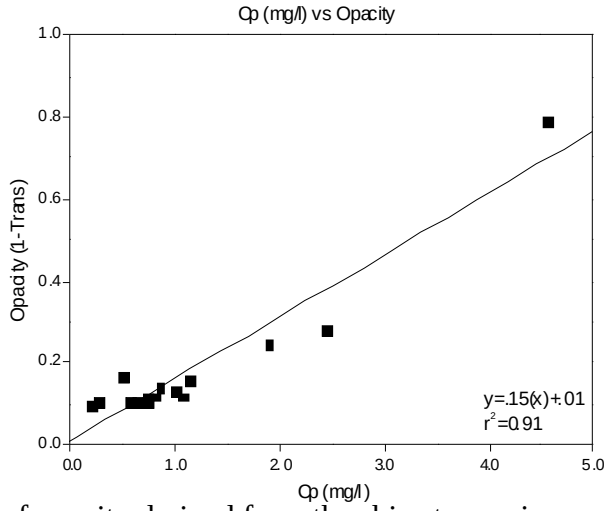

Figure 2-3. Plot of opacity derived from the ships transmissometer vs. particle concentrations measured on individual samples.

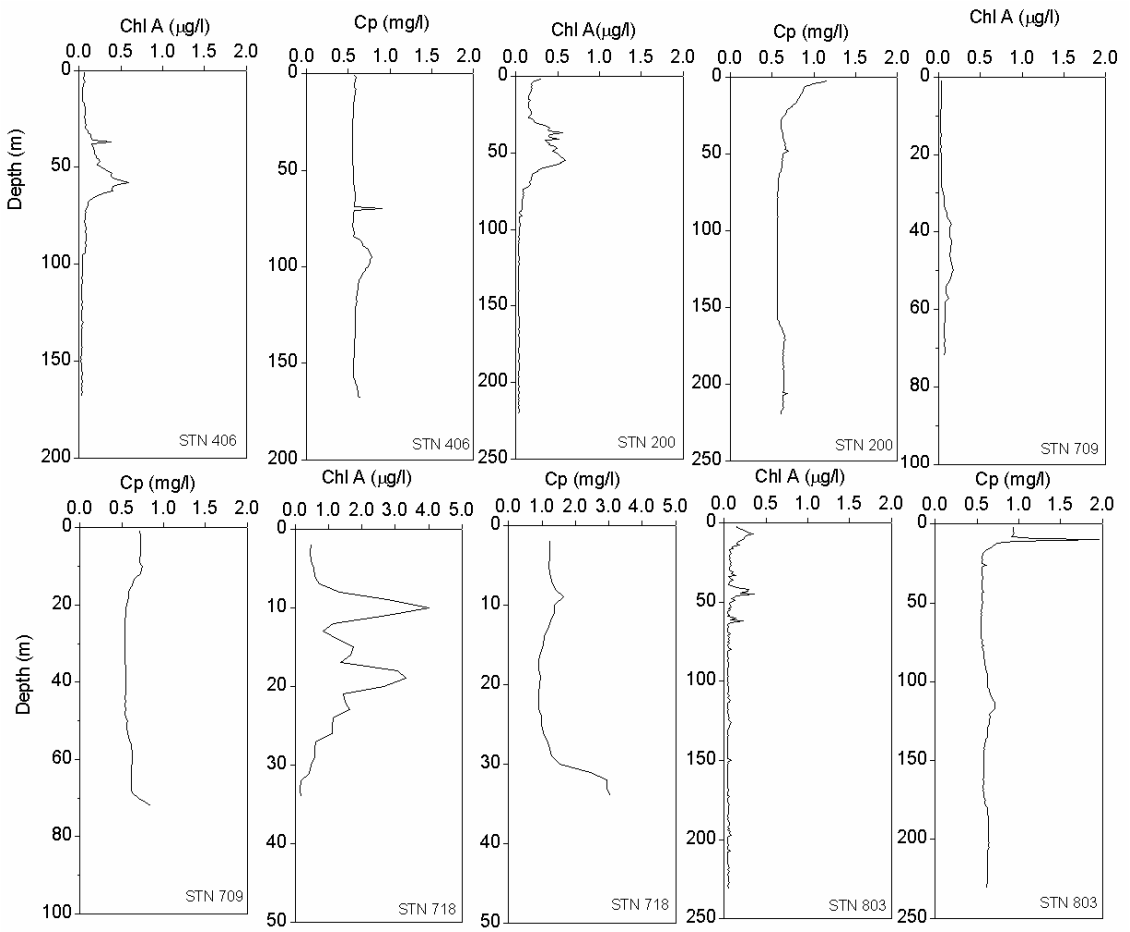

Figure 2-4a. Depths profiles of Cp and Chl-a at selected sites during June and July, 2004.

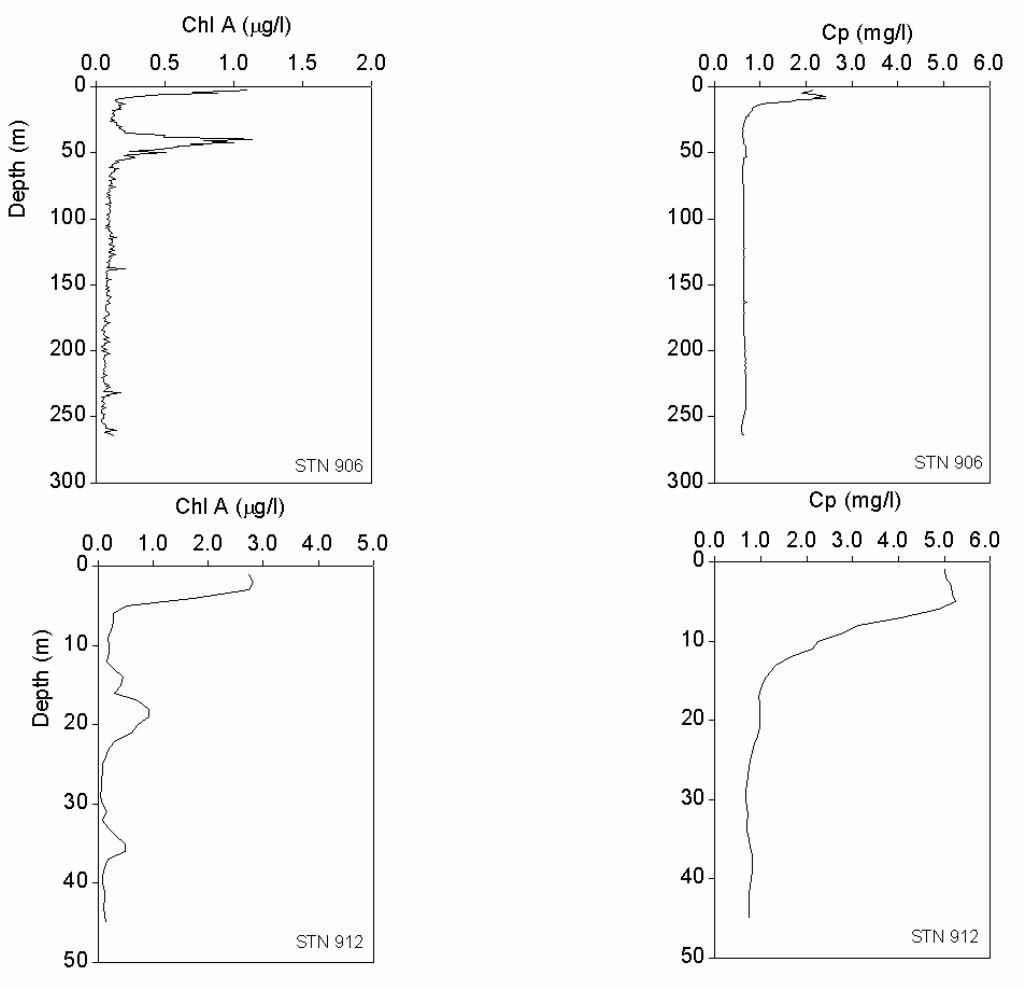

Figure 2-4b. Depth profiles of Chl-a and Cp for selected sites.

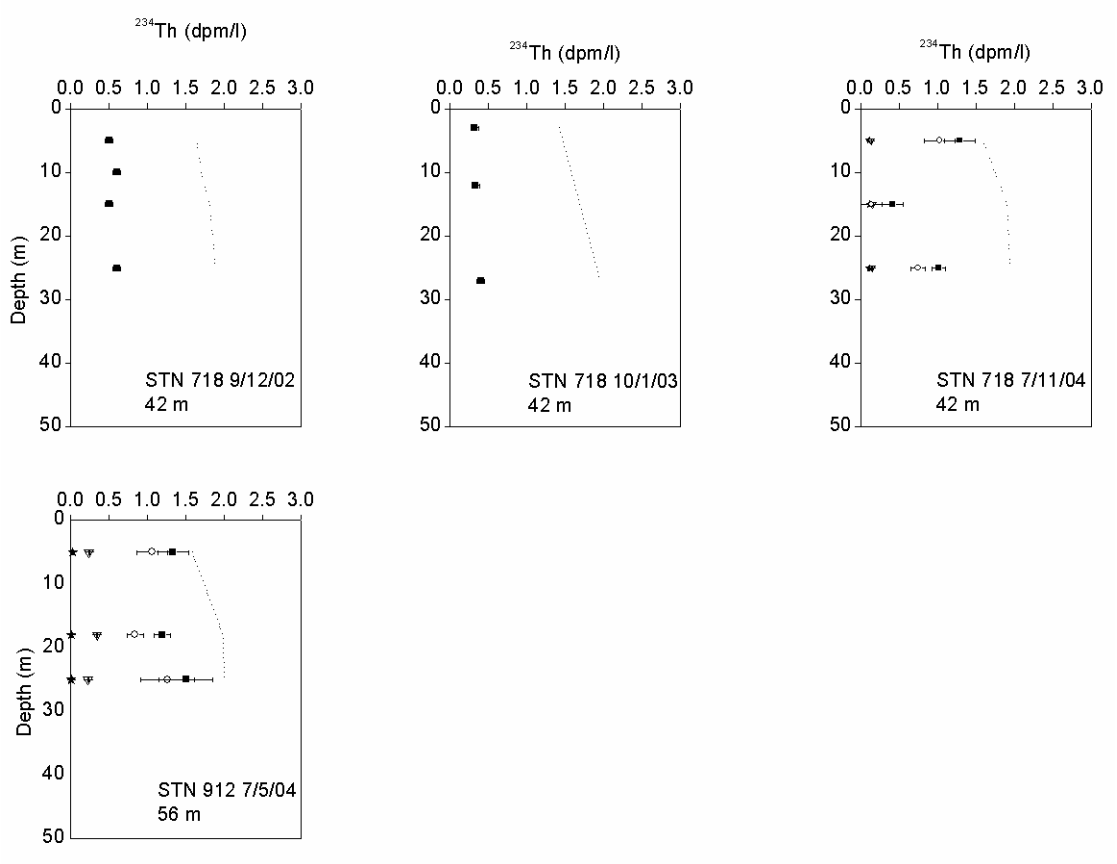

Figure 2-5a. Profiles of ^{234}Th (dpm/l) from the Mackenzie Inner Shelf. Square box = total, circle = dissolved, upside down triangle = 1-70 μm, star = > 70 μm, dotted line = ^{238}U.

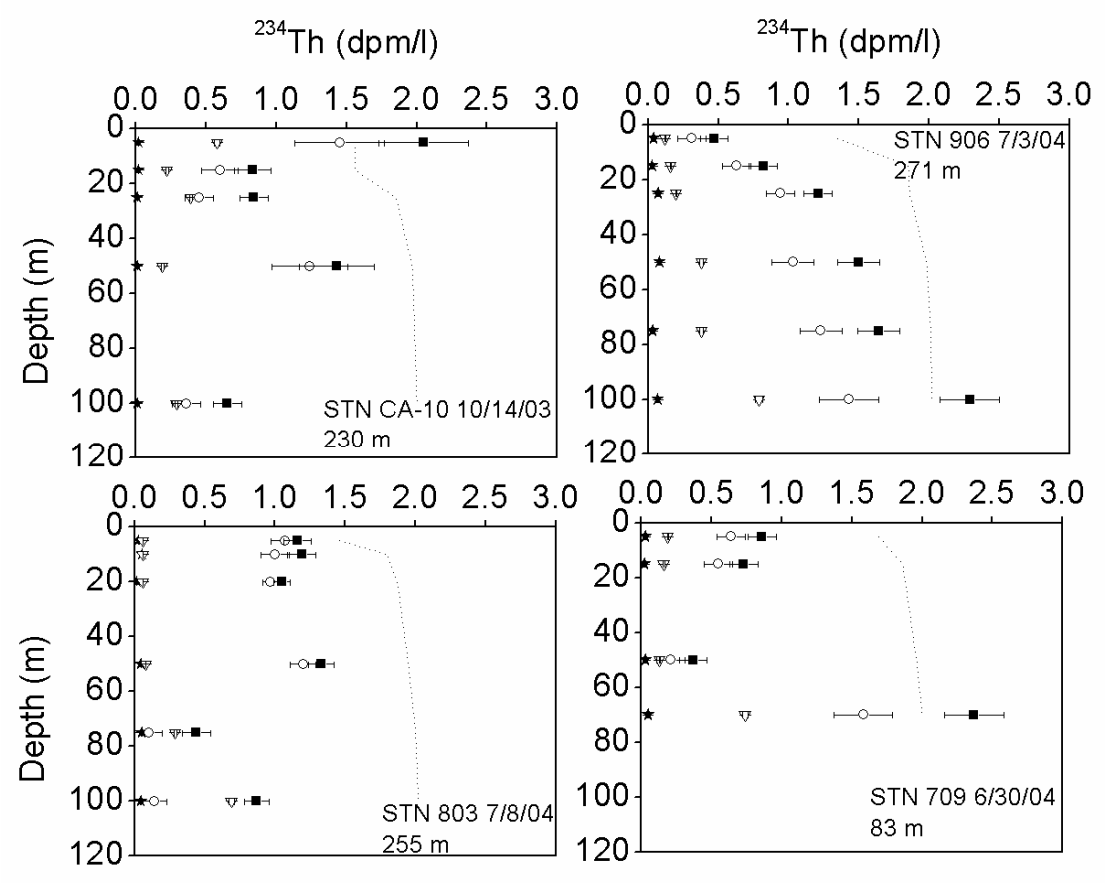

Figure 2-5b. Profiles of ^{234}Th from the Mackenzie Outer Shelf. Square box = total, circle = dissolved, upside down triangle = 1-70 μm, star = > 70 μm, dotted line = ^{238}U.

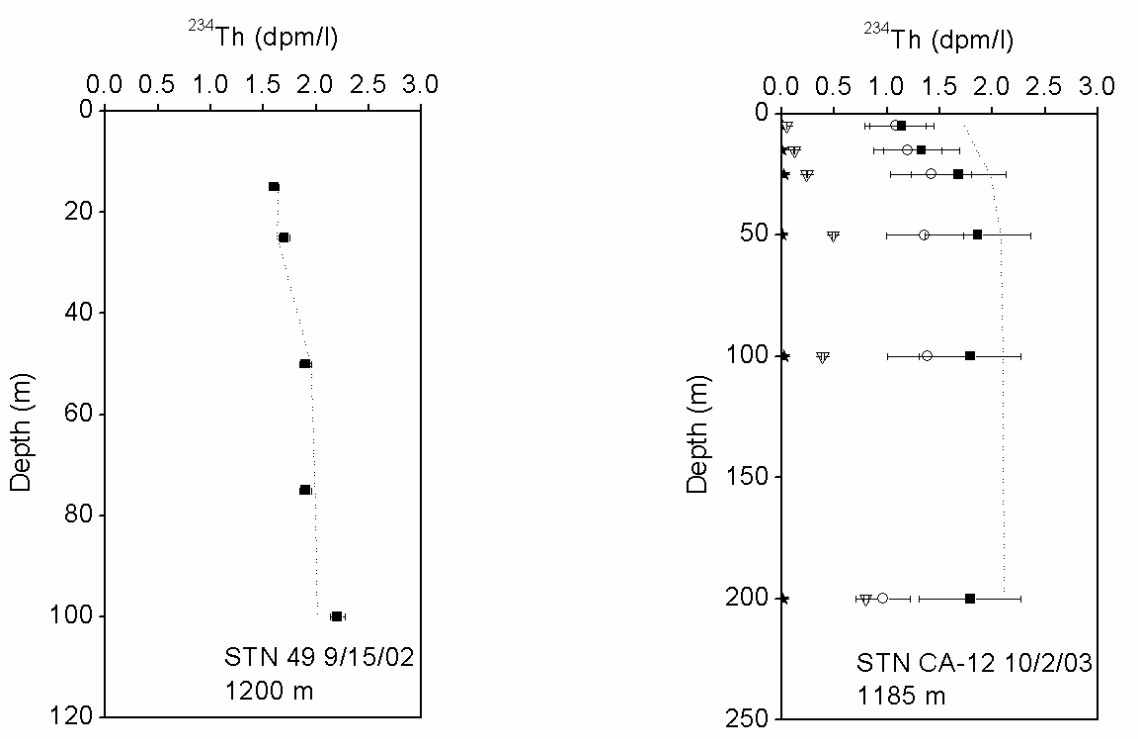

Figure 2-5c. Profiles of ^{234}Th from the Shelf/Slope. Square box = total, circle = dissolved, upside down triangle = 1-70 μm, star = >70 μm, dotted line = ^{238}U.

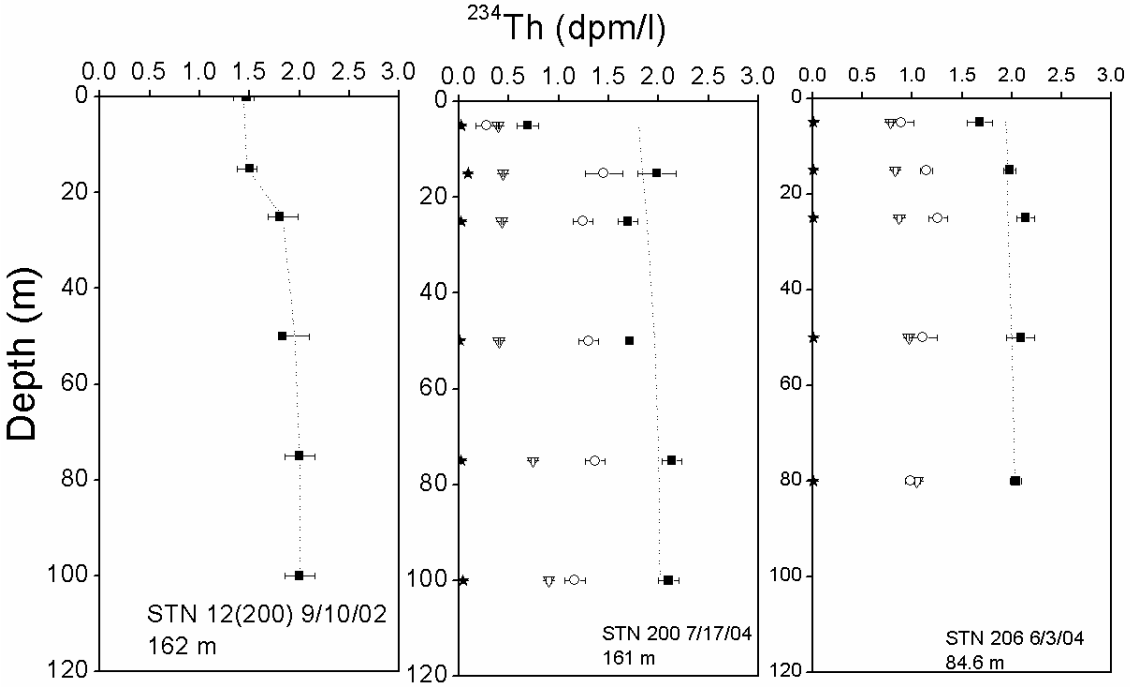

Figure 2-5d. Profiles of ^{234}Th from Franklin Bay. Square box = total, circle = dissolved, upside down triangle = 1-70 μm, star = > 70 μm, dotted line = ^{238}U.

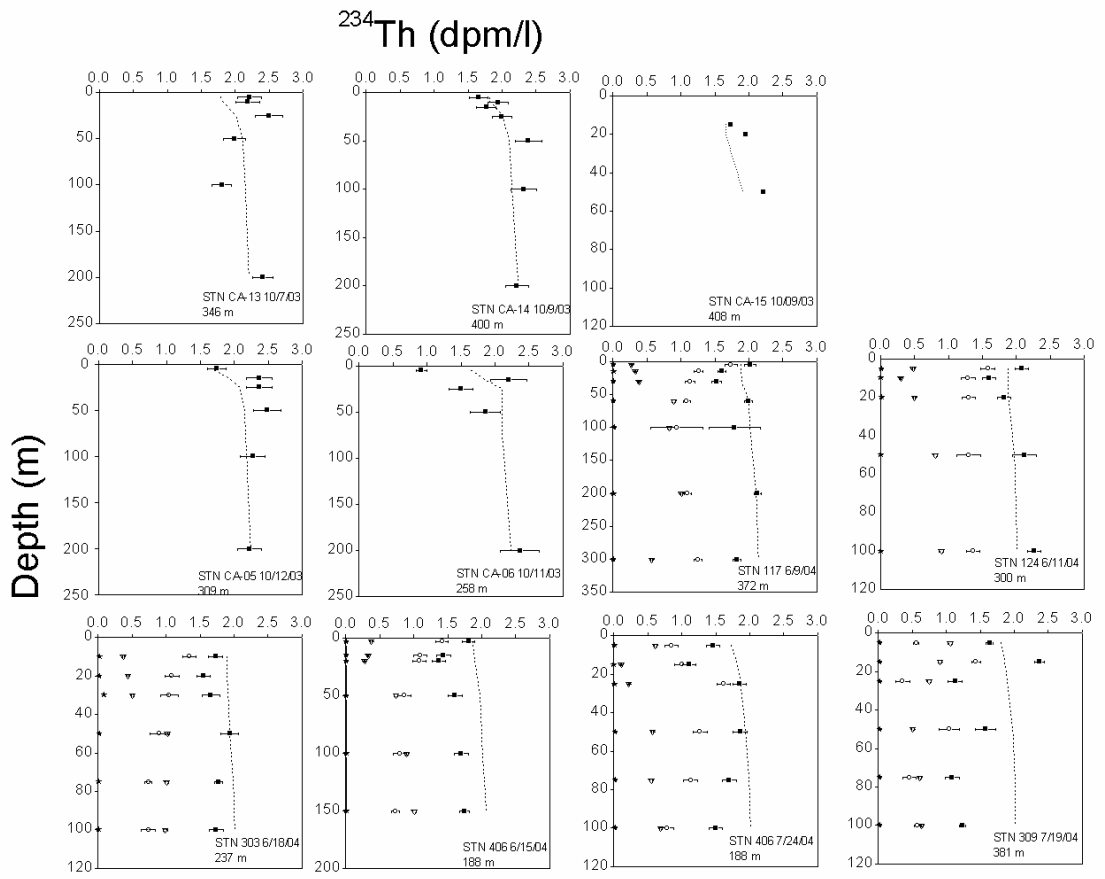

Figure 2-5e. Profiles of ^{234}Th from Cape Bathurst. Square box = total, circle = dissolved, upside down triangle = 1-70 μm, star = > 70 μm, dotted line = ^{238}U.

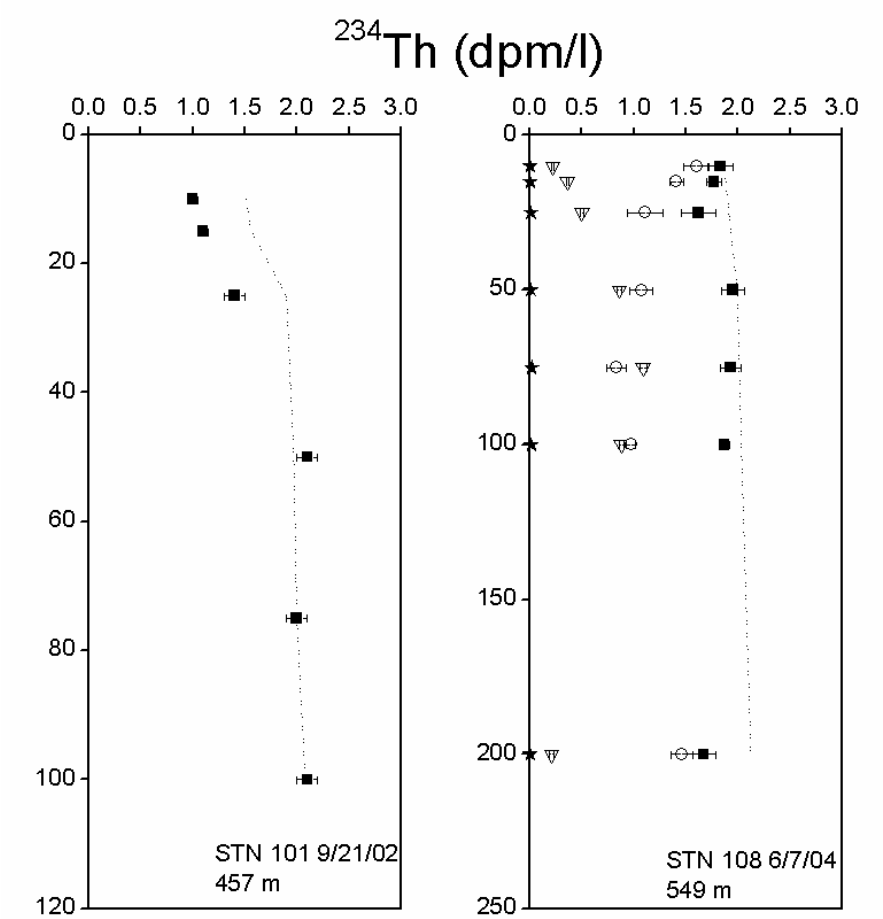

Figure 2-5f. Profiles of ^{234}Th from the Amundsen Gulf. Square box = total, circle = dissolved, upside down triangle = 1-70 μm, star = > 70 μm, dotted line = ^{238}U.

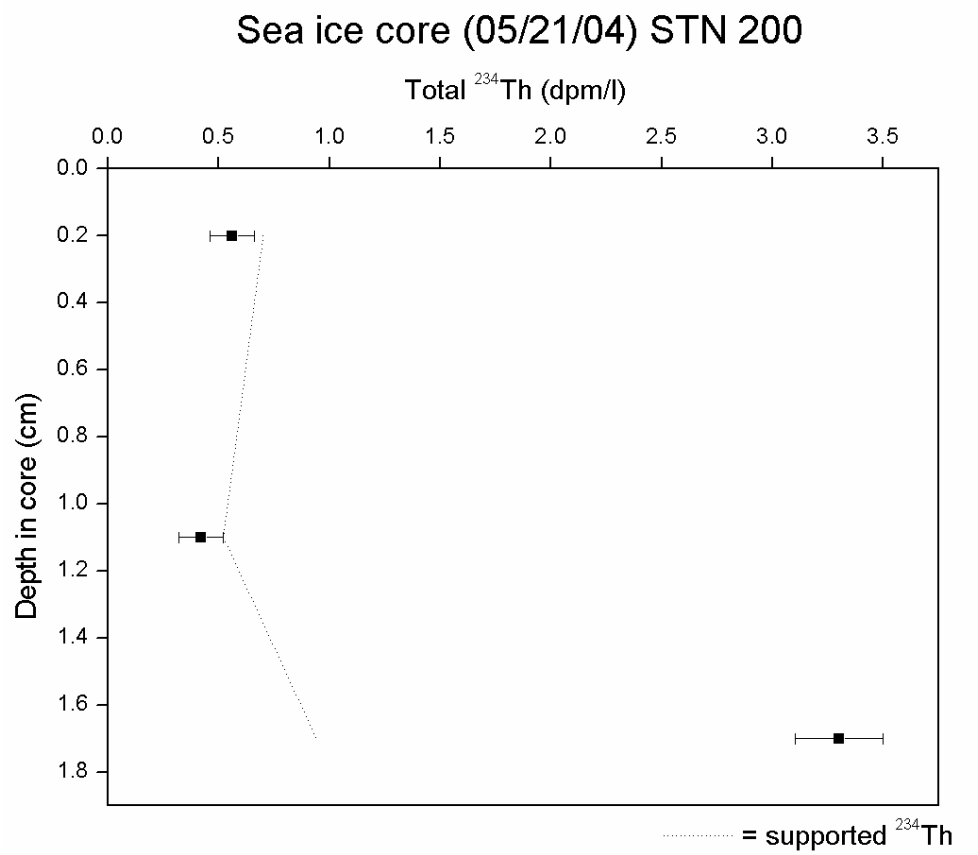

Figure 2-6. ^{234}Th profile in an ice core.

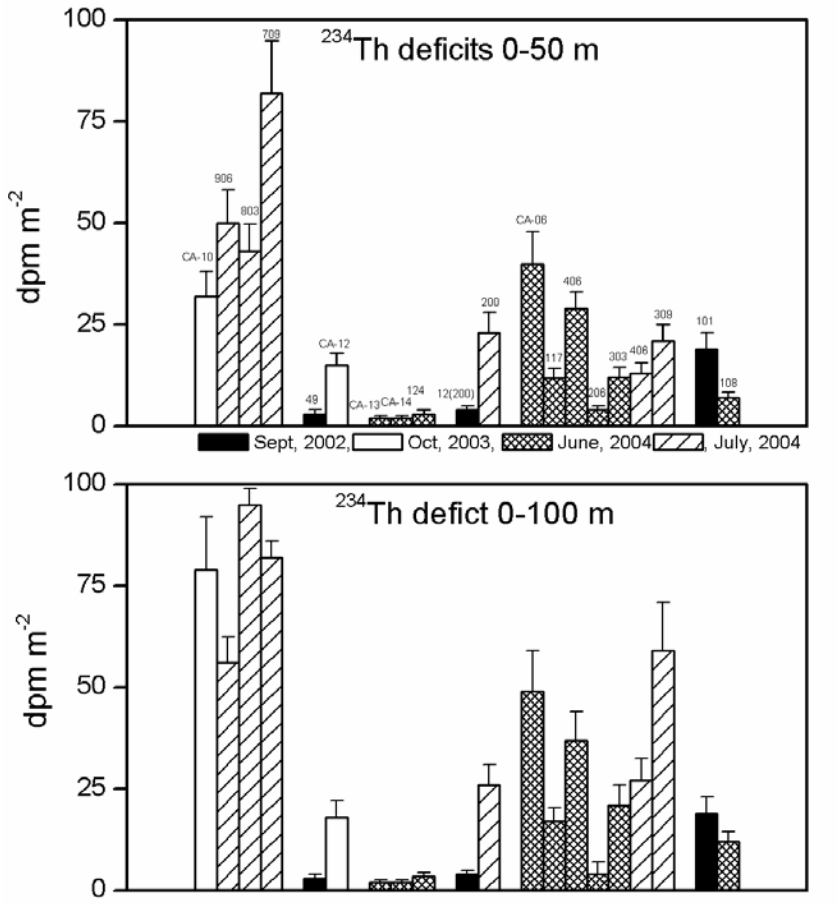

Figure 2-7. ^{234}Th deficits 0-50 and 0-100 m.

Figure 2-8. Image of the Mackenzie Shelf taken from the MERIS satellite on June 29th, 2004.

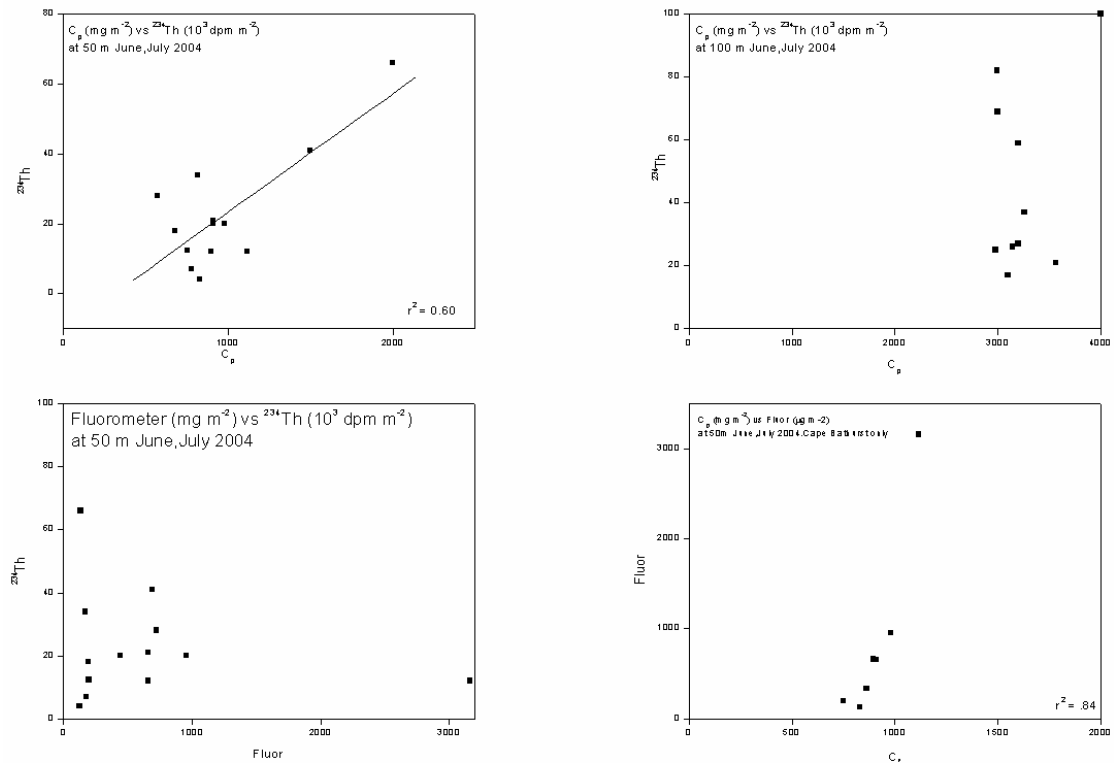

Figure 2-9. Regressions of ^{234}Th vs particle concentrations (Cp)

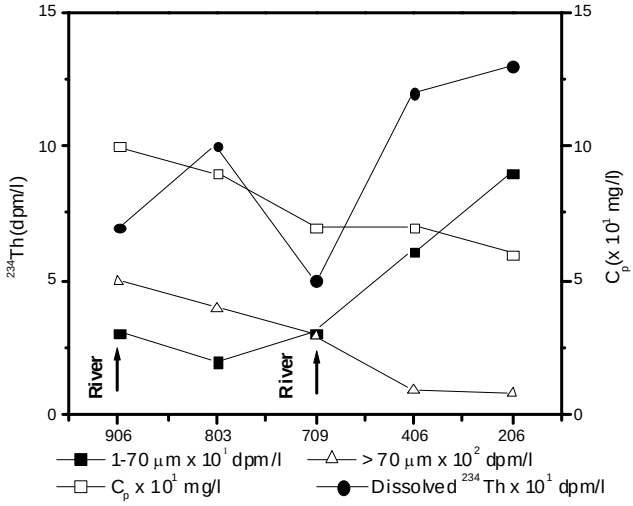

Figure 2-10. Spatial gradients in Th and particle concentration (Cp)

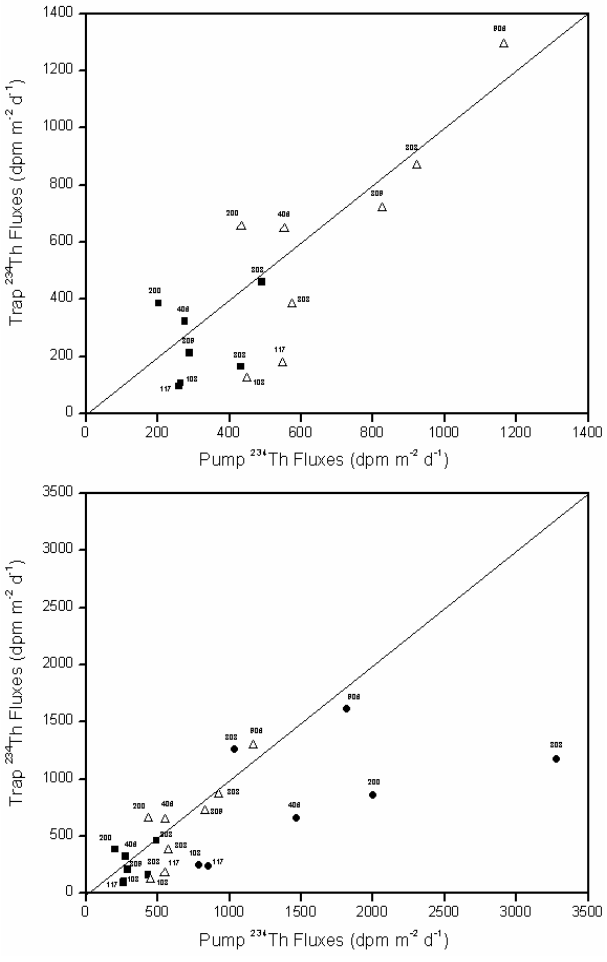

Figure 2-11. 1:1 correlation between floating and water column ^{234}Th fluxes.

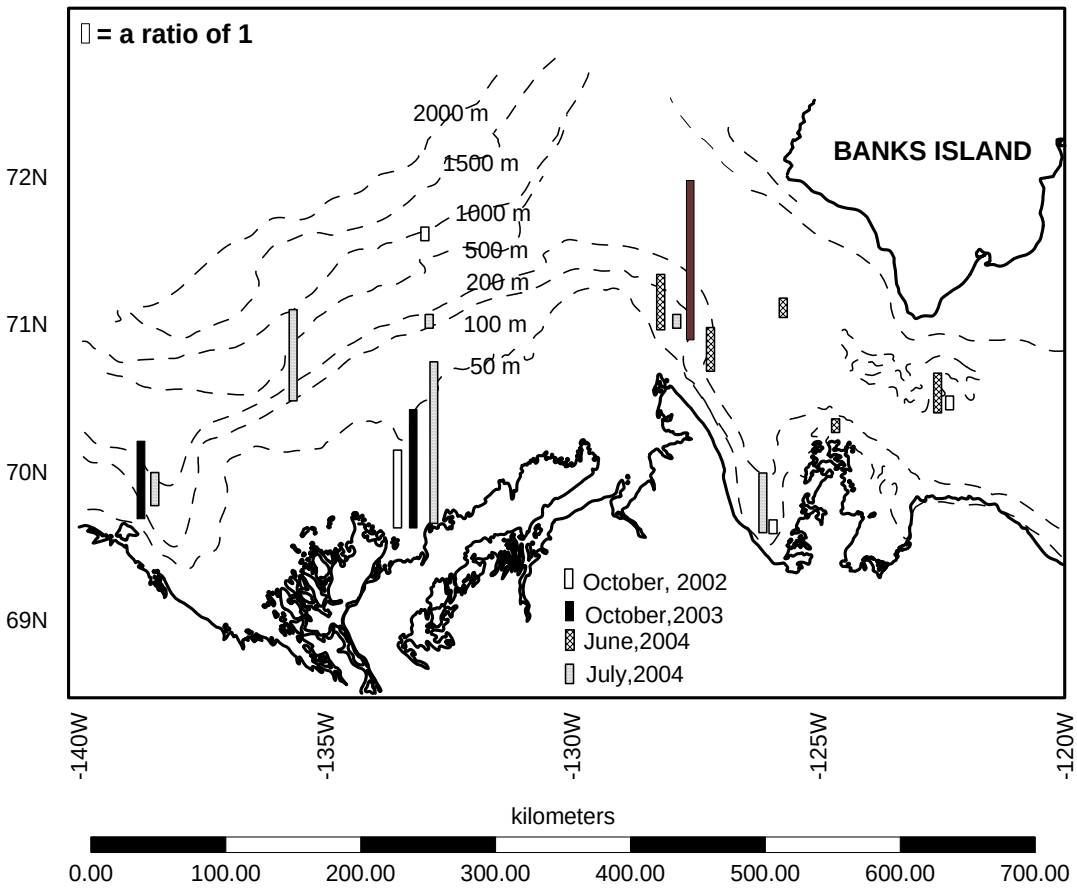

Figure 2-12. Sediment/water column inventories of ^{234}Th.

REFERENCES

Aller, R. C., and J. K. Cochran. 1976. 234Th/238U disequilibrium in near-shore sediment: particle reworking and diagenetic timescales. *Earth and Planetary Science Letter* 29: 37-50.

Amiel, D., J. K. Cochran, and D. J. Hirschberg. 2002. 234Th/238U disequilibrium as an indicator of the seasonal export flux of particulate organic carbon in the North Water. *Deep Sea Research II* 49: 5191-5209.

Bacon, M. P., and M. M. Rutgers Van Der Loeff. 1989. Removal of Th-234 by Scavenging in the Bottom Nepheloid Layer of the Ocean. *Earth and Planetary Science Letters* 92: 157-164.

Benitez-Nelson, C. R., Buesseler, K.O., Crossin, G. 2000. Upper ocean carbon export, horizontal transport, and vertical eddy diffusivity in the southwestern Gulf of Maine. *Continental Shelf Research* 20: 707-736.

Bishop J.K., Edmond J.M., Ketten D.R., Bacon M.B., Silker W.B. 1977. The chemistry, Biology and vertical flux of particulate matter from the upper 400 m of the equatorial Atlantic Ocean. *Deep-Sea Research.* 24: 511-548.

Buesseler, K., Bacon, M.P., Cochran, J.K., Livingston, H.D. 1992. Carbon and nitrogen export during the JGOFS North Atlantic Bloom Experiment estimated from 234Th:238U disequilibria. *Deep-Sea Research I* 39: 1115-1137.

Buesseler, K., L. Ball, J. Andrews, C. Benitez-Nelson, R. Belastock, F. Chai, and Y. Chao. 1998. Upper ocean export of particulate organic carbon in the Arabian Sea derived from thorium-234. *Deep-Sea Research Part II*-Topical Studies in Oceanography 45: 2461-2487.

Buesseler, K. O., Benitez-Nelson, C., Rutgers Van Der Loeff, M., Andrews, J., Ball, L., Crossin, G., Charette, M. 2001. An intercomparison of small- and large-volume techniques for thorium-234 in seawater. *Marine Chemistry* 74: 15-28.

Buesseler, K. O., R. T. Barber, M. L. Dickson, M. R. Hiscock, J. K. Moore, and R. Sambrotto. 2003. The effect of marginal ice-edge dynamics on production and export in the Southern Ocean along 170 degrees W. *Deep-Sea Research Part II*-Topical Studies in Oceanography 50: 579-603.

Bruland, K. W., and K. H. Coale. 1986. Surface water 234Th/238U disequilibria: spatial and temporal variations of scavenging rates within the Pacific Ocean. In: Burton, J.D., Bewer, P.G., Chesselet, R. (Eds), Dynamic Processes in the Chemistry of the Upper Ocean. Plenum Publishing Co., New York: 159-172.

Chase, Z., R. F. Anderson, M. Q. Fleisher, and P. W. Kubik. 2002. The influence of particle composition and particle flux on scavenging of Th, Pa and Be in the ocean. *Earth and Planetary Science Letters* 204: 215-229.

Clegg, S. L., and M. Whitfield. 1990. A generalized model for the scavenging of trace metals in the open ocean - I: Particle cycling. *Deep Sea Research* 37: 809-832.

Cochran, J. K., Buesseler, K.O., Bacon, M.P., Livingston, H.D. 1993. Thorium isotopes as indicators of particle dynamics in the upper ocean: Results from the JGOFS North Atlantic Bloom Experiment. *Deep-Sea Research, Part 1* 40: 1569-1595.

Cochran, J. K., Barnes, C., Achman, D., Hirschberg, D.J. 1995. Thorium-234/Uranium-238 disequilibrium as an indicator of scavenging rates and particulate organic carbon fluxes in the Northeast Water Polynya, Greenland. *Journal of Geophysical Research 100*: 4399-4410.

Cochran, J. K., Buesseler, K.O., Bacon, M.P., Wang, H.W., Hirschberg, D.J., Ball, L., Andrews, J., Crossin, G., Fleer, A. 2000. Short-lived thorium isotopes (super(234)Th, super(228)Th) as indicators of POC export and particle cycling in the Ross Sea, Southern Ocean. *Deep-Sea Research, Part II* 47: 3451-3490.

Cochran, J. K., and P. Másque. 2003. Short-lived U/Th series radionuclides in the ocean: Tracers for scavenging rates, export fluxes and particle dynamics, p. 461-492, Uranium-Series Geochemistry. Reviews in Mineralogy & Geochemistry.

Gardner, W.D., Walsh, I.D., Richardson, M.J. 1993. Biophysical forcing of particle production and distribution during a spring bloom in the North Atlantic. Deep-Sea *Research II* 40:171-195

Gustafsson, O., Buesseler, K.O., Geyer, W. Rockwell, Moran, S. Bradley, Gschwend, P.M. 1998. On the relative significance of horizontal and vertical transport of chemicals in the coastal ocean: application of a two-dimensional Th-234 cycling model. *Continental Shelf Research* 18: 805-829.

Hill, P.R., Blasco, S.M., Harper, J.R., Fissel, D.B. 1991. Sedimentation on the Canadian Beaufort Shelf. *Continental Shelf Research* 11:821-842.

Livingston, H. D., and J. K. Cochran. 1987. Determination of Transuranic and Thorium Isotopes in Ocean Water - in Solution and in Filterable Particles. *Journal of Radioanalytical and Nuclear Chemistry*-Articles 115: 299-308.

Macdonald, R.W., Pedersen, T.F. Geochemistry of sediments of the western Canadian continental shelf. *Continental Shelf Research* 11:843-863

Mckee, B. A., D. J. Demaster, and C. A. Nittrouer. 1984. The use of 234Th/U238 disequilibrium to examine the fate of particle-reactive species on the Yangtze continental shelf. *Earth and Planetary Science Letters* 68: 431-442.

Mckee, B.A. 1986. The fate of particle reactive radionuclides on the Amzon and Yangtze continental shelves. Ph.D. thesis, North Carolina State Univ.

Moran, S. B., K. M. Ellis, and J. N. Smith. 1997. Th-234/U-238 disequilibrium in the central Arctic Ocean: implications for particulate organic carbon export. *Deep-Sea Research Part II*-Topical Studies in Oceanography 44: 1593-1606.

Moran, S. B., Smith, J.N. 2000. 234Th as a tracer of scavenging and particle export in the Beaufort Sea. *Continental Shelf Research* 20: 153-167.

Murray, J. W., J. Young, J. Newton, T. Dunne, and B. P. Chapin. 1996. Export flux of particulate organic carbon from the central equatorial Pacific determined using combined drifting trap 234Th approach. *Deep Sea Research II 43*: 1095-1132.

Pickard, G.L., Emery, W.J. 1990. Estuarine circulation. In: Descriptive Physical Oceanography. Pergammon Press.

Santschi, P. H., Y.-H. Li, and J. Bell. 1979. Natural radionuclides in the water of Narragansett Bay. *Earth and Planetary Science Letters* 45: 201-213.

Scholten, J.C., Fietzke, J., Vogler, S., Van der Loeff, M.M., Mangini, A., Koeve, Waniek, J., Stoffers, P., Antia, A., Kuss, J. 2001. Trapping efficiencies of sediment traps from the deep Eastern North Atlantic: the ^{230}Th calibration. *Deep-Sea Research II* 48: 2383-2408.

Smoak, J. M., D. J. Demaster, S. A. Kuehl, R. H. Pope, and B. A. Mckee. 1996. The behavior of particle-reactive tracers in a high turbidity environment: 234Th and 210Pb on the Amazon continental shelf. *Geochim. Cosmochim. Acta* 60: 2123-2137.

Savoye, N., Benitez-Nelson, Claudia., Burd, A. B., Cochran, J. K., Charette, M., Buesseler, K. O., Jackson G. A., Roy-Barman, Matthieu., Schmidt, Sabine and Elskens, Marc (2006) ^{234}Th sorption and export models in the water column: A review. *Marine Chemistry* 100: 234-249.

Trimble, S.M., Baskaran, M. The role of suspended matter in ^{234}Th scavenging and ^{234}Th-derived export fluxes of POC in the Canada Basin of the Arctic Ocean. 2005. *Marine Chemistry* 96: 1-19.

Van Der Loeff, M. M. R., and W. S. Moore. 1999. The analysis of natural radionuclides in seawater. in: methods of seawater analyses.

Van Der Loeff, M. M. R., Buesseler, K., Bathmann, U., Hense, I., Andrews, J. 2002. Comparison of carbon and opal export rates between summer and spring bloom periods in the region of the Antarctic Polar Front, SE Atlantic. Deep-Sea Research II 49:3849-3869.

Van Der Loeff, M. M. R., Meyer, R., Rudels, B., Rachor, E. 2002. Resuspension and particle transport in the benthic nepheloid layer in and near Fram Strait in relation to faunal abundances and ^{234}Th depletion. *Deep-Sea Research I* 49:1941-1958

Chapter 3: Sediment and carbon accumulation rates on the Mackenzie River Shelf

INTRODUCTION

Sediment accumulation rates, coupled with sediment organic carbon measurements, allow for estimation of organic carbon fluxes into sediments and thus can provide critical information on carbon cycling. Sedimentation rates have been commonly obtained using ^{210}Pb distributions in surficial sediments (Koide et al. 1972, Turekian and Cochran, 1978, Benninger et al. 1979, Krishnaswami et al. 1980, DeMaster and Cochran, 1982, Carpenter et al. 1981, Cochran et al. 1992, Baskaran and Naidu, 1995, Roberts et al. 1996). In this approach, "excess" ^{210}Pb (calculated as the total ^{210}Pb activity above supported activity of ^{226}Ra) are incorporated into a vertical, one dimensional mixing model whose solution gives an estimation of the sedimentation rate. Although the method has been successfully used in a wide variety of marine systems, its application is particularly challenging in a seasonally ice-covered, river-dominated shelf. In such a setting, the complex interactions between winds, ice cover and scour, the tidal prism, timing of river debouchement, benthic storms, and the coriolis force, present significant analytical and modeling obstructions toward reliable estimation of sedimentation rates. The approach taken here was to use radionuclides such as ^{137}Cs and ^{234}Th in addition to ^{210}Pb to help illuminate the physical processes that control ^{210}Pb distributions (and therefore sedimentation rates).

The objectives of this chapter were to:

- Obtain sediment accumulation rates using measured ^{210}Pb distributions in surficial sediments
- Compare sediment and carbon accumulation rates with an independent measurement of carbon respiration rate to construct a mass balance for carbon on the Mackenzie Shelf.
- Explain patterns of inventories obtained from ^{234}Th, ^{210}Pb and ^{137}Cs

METHODS

Sediment Cores

Box cores (1.0 m^2) were collected from the C.C.G.S Pierre Radisson and Amundsen as part of the Canadian Arctic Shelf Exchange Study (CASES). Four different periods were sampled; October 2002, October 2003, and June and July 2004 (Fig.3-1). During October, 2003 sampling was opportunistic and occurred whenever ice conditions permitted. In June 2004, sampling was restricted to eastern regions centered around Cape Bathurst (Fig. 3-1). July 2004 was the only period during which both eastern and western areas were sampled during the 6-week period of a single leg. Although locations were chosen primarily to overlap with sampling in the water column (Chapter 2), two

additional cores from the shelf/slope region (stations 850 and 750) also were collected (Fig.3-1).

A 50 x 40 x 60 cm Plexiglas sub-corer was used to sample the box core. The sub- cores were carefully transported to the ship-board lab to be sectioned. After transport to the lab, overlying water was siphoned off. Sectioning was done at 1 and 2 cm intervals down to 15-20 cm in most cases. However at some stations in July, cores were sectioned only to 10 cm. Samples were stored in zip-lock bags at -15° C. At Stony Brook, samples were allowed to thaw, wet weights taken, and were dried in an oven overnight. Following drying, samples were re-weighed, and were powdered using a mortar and pestle, and 50-120 g of dry sediment was transferred to an aluminum can and sealed. If there was insufficient sample to fill the can, table salt was added so that sample heights in cans were identical. This insured a constant geometry for gamma spectrometry. Samples were gamma counted on planar intrinsic germanium detectors for ^{137}Cs, ^{210}Pb, ^{226}Ra and ^{234}Th. The gamma energies measured were 661 KeV for ^{137}Cs, 46.5 KeV for ^{210}Pb, 63.3 KeV for ^{234}Th and 352 KeV (^{214}Pb) for ^{226}Ra.

Correction for self absorption

Since low energy (< ~150 Kev) γ emissions do not have the same penetrating power as high energy γ rays, nuclides such as ^{234}Th and ^{210}Pb must be corrected for absorption by the sample itself. Furthermore, sediments exhibit variations in grain size (and therefore density) that can affect γ absorption, and consequently the use of a single standard composed of a single sediment type is insufficient to make this correction. The approach in our lab was to prepare two sets (one each for ^{234}Th and ^{210}Pb) of silica gel standards. Each set was spiked with known amounts of ^{234}Th and ^{210}Pb. Solutions of varying concentrations of $Pb(NO_3)_2$ were used to adjust the density of the gel to cover the range of densities observed in the samples. Quantification of gamma self-absorption was accomplished by counting an ^{241}Am gamma source (59.5 Kev) on each gel standard, and on an empty can. The ^{241}Am counts recorded though a given standard (T) were divided by those recorded through an empty can (T_0), and values of T/T_0 were plotted vs the cpm/dpm ratio for the ^{234}Th or ^{210}Pb in each standard. The ^{241}Am standard was counted on every canned sediment sample to obtain individual sample values of T/T_0, and the appropriate cpm/dpm value was obtained from the straight-line regression of the standard T/T_0 vs cpm/dpm. Counting efficiencies for the high energy emitters ^{137}Cs and ^{214}Pb were obtained by counting sediment standards obtained from NIST.

Carbon, Nitrogen and Carbon Isotopes

A few milligrams of dried sediment were acid treated with fuming HCL to remove any calcium carbonate, weighed and run on a Carlos Erba CHN analyzer to determine organic carbon and total nitrogen. Following methods described in Chapter 2, CO_2 gas from the combustion of carbon on the CHN analyzer was trapped and run on a Finnegan Delta Plus mass spectrometer to obtain δ^{13}C values (Table 2).

RESULTS

Water, porosity and dry bulk density

The percentage water from each depth horizon was calculated from:

$$\%H_2O = 1 - (dry\,mass / wet\,mass) * 100 \quad (1)$$

Porosity was calculated from:

$$\Phi = V_w / V_s + V_w \quad (2)$$

where V_w is the volume of water per gram of sediment obtained from $V_w = f_w/\rho_{water}$ and f_w = % H_2O/100, V_s = 1-f_w/ρ_{solid}

ρ_{water} = 1.02 g/cm^3. ρ_{solid} = 2.65 g/cm^3

The *in situ* dry bulk density was calculated from:

$$\rho_{dry} = \rho_{solid} * (1 - \Phi) \quad (3)$$

Values for % water, ϕ and ρ_{dry} are given in Table 1. Water content in the 0-5 cm interval from all sampling times ranged from 31-66 % and generally decreased with depth. Station 709 had the lowest water contents of any station sampled. Porosities from surficial sediments were generally in the range of 0.78 - 0.82; however stations 709-July,108-June, and 718-October, 2003 were notable exceptions that had significantly lower porosities (range 0.60-0.64). Dry bulk densities of surficial sediments were in the range 0.42 – 1.2 g/cm^3 with values generally increasing with depth in the core.

Determination of radionuclide inventories

Inventories of $^{234}Th_{xs}$, $^{210}Pb_{xs}$ and ^{137}Cs were calculated following equation (4).

$$I_{^{234}Th_{xs},\,^{210}Pb_{xs},\,^{137}Cs} = \Sigma\ [\rho^i{}_{dry}\,\Delta x\ \ A^{i}{}_{^{234}Th_{xs},\,^{210}Pb_{xs},\,^{137}Cs}] \quad (4)$$

where I is the inventory of the radionuclide of interest (dpm/cm^2), Δx is the sampling interval, ρ^i_{dry} is the dry bulk density (g sed/cm^3 wet sediment), and A^i is the activity of excess ^{234}Th, excess ^{210}Pb or ^{137}Cs in the ith interval (dpm/g).

^{234}Th activities in sediments

One factor that affected the quality of the excess ^{234}Th data was the time elapsed before samples were counted. With 4 % of the excess ^{234}Th activity lost per day due to decay, it is a race against time to get samples counted. In some samples, the excess ^{234}Th activities were subject to large decay corrections. For Oct 2002, Oct 2003, June 2004 and July2004, losses due to radioactive decay ($e^{-\lambda t}$) averaged .14, .45, .35 and .20, respectively. Thus, in all legs, more than half the ^{234}Th signal was gone by the time samples were counted. Errors on total ^{234}Th activities averaged ±10 % and were derived from 1σ counting statistics.

Activities of total ^{234}Th in the 0-5 cm horizon from all sampling periods were in the range 2.0 - 7.5 dpm/g (Table 1, Fig. 3-2a-b). Most of the cores from October, 2002 showed constant profiles due to the large decay errors and are not included in Fig. 3- 2a-b. Profiles obtained from subsequent periods generally displayed relatively high values in the surface 0-5 cm but were constant below this depth.

Calculation of ^{234}Th excesses

^{234}Th excesses are calculated from the equation:

$$^{234}Th_{xs} = [\text{total } ^{234}Th \text{ total} - \text{total } ^{238}U]/e^{-\lambda t} \quad (5)$$

where t = time between sample collection and counting and $\lambda = .693/^{234}Th$ half-life (24 d).

Perhaps the best way to obtain supported ^{234}Th (^{238}U) values is to recount samples after ~ 5 half-lives of Th have elapsed. This method has the advantage that supported values are obtained directly from the same depth horizons as the total activity. The method also avoids having to apply an average supported value to all depth horizons. Fifteen samples were recounted from October, 2003 and June-July 2004, and these had an average value of 2.46 ± 0.2 dpm/g. However, not all samples were recounted and despite the low standard deviation, this approach was deemed not inclusive enough to apply to all the data.

Another method for obtaining supported ^{234}Th activities (used in this study) is to assume that ^{234}Th excess activities are restricted to the upper 5 cm and that activities below this in a given core indicate supported levels. A tabulation from all sampling times of ^{234}Th concentrations deeper than 5 cm (excluding obvious outliers based on % H_2O, dry bulk density and porosity values) yielded 2.9 ± 0.5 dpm/g as the mean supported value (Table 1). To account for station to station differences in mineralogy, ^{234}Th supported activities were ultimately calculated by obtaining an average supported value for each core (Table 1). The large decay corrections and the use of averaged supported ^{234}Th activities required a criterion for decay correction of excess ^{234}Th activities. We established such a criterion by plotting the difference between individual ^{234}Th activities and the average ^{234}Th activity for depths > 5 cm in each core (Fig. 3-3). This distribution is approximately Gaussian with an approximate mean of 0.0 dpm/g and 1σ of 0.4 dpm/g. We conclude that we are unable to determine the presence of excess ^{234}Th with confidence for apparent excess ^{234}Th activities < 0.4 dpm/g. Accordingly, excess activities less that 0.4 dpm/g have not been decay corrected to the time of collection and these data were not included in subsequent calculations. In addition, no excess ^{234}Th was calculated for samples counted after a decay of > 85 % (designated as "*" in Table 1). For most stations, excess ^{234}Th is confined to the upper 1-2 cm of the sediment column (Table 1).

^{234}Th excess inventories

Equation (5) was applied to the ^{234}Th profiles in the upper 5 cm to obtain excesses and from the decay corrected dpm/g values, inventories were obtained (Table 1) The range in $^{234}Th_{xs}$ inventories from all stations was 0.1- 4.0 dpm/cm^2 and were lowest in June, 2004 (0.80 ± 0.8) when the region had been most recently ice-covered. $^{234}Th_{xs}$ inventories from the Cape Bathurst Polynya region were relatively high at stations 303 and 117 but low to undetectable at stations 406 and 206. In general however, (for stations of similar depths) western stations were not significantly different than eastern ones.

^{210}Pb activities in sediments

The range in specific activities of ^{210}Pb in the 0-10 cm horizon for all the data was 3.0 to 18.0 dpm/g (Fig. 3-4a-b). Most of the profiles showed decreases with depth although profiles at two stations (718, 200) from October, 2002 showed constant activities with depth. Three stations were sampled multiple times (718, 200, and 406) and these profiles showed clear differences between sampling times. Another frequent feature of the ^{210}Pb profiles was a maximum centered at 2-3 cm (101,108, 406, 803, 200-July, 206). As was the case for ^{234}Th, values at depth in the cores were largely constant below ~ 10 cm but had station to station differences in the range of 2.0 to 4.0 dpm/g.

Calculation of ^{210}Pb excesses

^{210}Pb excesses were calculated from:

$^{210}Pb_{xs}$ = total ^{210}Pb – ^{226}Ra (^{214}Bi) activity. (6)

No decay corrections were made to the excess ^{210}Pb activities because the time between sample collection and counting was short compared with the ^{210}Pb half-life (22.3 y). Although ^{226}Ra data were not collected from 2002, samples were measured to greater depths in these cores (usually four points > 10 cm) compared with other legs. It was apparent from examining the profiles of total ^{210}Pb of the entire data set, that at the overwhelming majority of sites, activities were constant and low at depths > 10 cm. Therefore, during 2002, supported values of ^{210}Pb were obtained by subtraction of average ^{210}Pb activities > 15 cm from each site. For all other legs, supported ^{210}Pb values were obtained by point-by-point subtraction of ^{226}Ra at each depth (Table 1).

In an effort to understand some of the factors that may be determining how much $^{210}Pb_{xs}$ is present at a given location, regressions were done of $^{210}Pb_{xs}$ versus % water content. Of 22 stations sampled, 10 had regression coefficients of 0.5 or greater (Fig. 3- 5. r^2 was 0.2 for the entire data set). From the 10 stations that displayed a correlation, 8 of these were confined to western areas that included near-shore and shelf/slope sites. No such relationships with % water were found for ^{234}Th.

^{210}Pb excess inventories

$^{210}Pb_{xs}$ inventories had a range of 1-65 dpm/cm^2 (Fig. 3-6). The two stations with depths > 100 m (CA-10, CA-6) sampled in October, 2003 registered the highest $^{210}Pb_{xs}$ inventories of any period sampled while October, 2002 had the lowest (64 ± 3, 9 ± 5 dpm/cm^2, respectively; Fig. 3-6). Station 718, sampled the same month (Oct) but different years, had a large range in $^{210}Pb_{xs}$ inventories (1-31 dpm/cm^2). Gradients in $^{210}Pb_{xs}$ inventories were not significant either between or within sampling periods i.e. there were no significant differences between stations closer and further from the Mackenzie River. There was furthermore, no evident pattern in $^{210}Pb_{xs}$ inventories with water column depth (stns 49, 101, 108, 750, 850 had depths 550-1100 m; all other stns 1-300 m). Sites within 10 km of the coast, at the tip of Cape Bathurst however, showed evidence of higher $^{210}Pb_{xs}$ inventories compared to those

further offshore (CA-6, 309). At these coastal sites, continental erosion may have supplied sediment that caused enhanced scavenging of ^{210}Pb.

^{137}Cs activities in sediments

Specific activities of ^{137}Cs were generally between 0.1-.7 dpm/g however the Amundsen Gulf site (stn 108) in June, 2004 had two depths where ^{137}Cs activities were 1.6-1.7 dpm/g (Table 1, Fig. 3- 7). Depths at which ^{137}Cs activities were 0, were reached at all stations except for the core taken at stn 718 in Oct 2002. ^{137}Cs penetration depths generally were centered ~ 5 cm but exceptions included CA-10 from October, 2003 and stn 200 from October, 2002 when ^{137}Cs penetrated to a depth ~13 cm (Fig. 3-7, Table 3). At stn 718, ^{137}Cs penetrated to > 20 cm in October, 2002 but extended only to 7 cm in October, 2003 (Table 3). Several cores (stns 803, CA-06, 101, and 108) showed maxima centered between 2-3 cm.

C, C/N ratios and δ^{13}C in sediments

Sedimentary organic carbon (SOC) values in surficial sediments ranged from 0.86 to 1.95 % measured at stations 49 (shelf/slope) and 718 (Mackenzie inner shelf) respectively (Table 2). Average SOC values from all depths and sampling times were 1.3 to1.5 % and thus showed comparative homogeneity over time despite uneven sampling coverage from one leg to the next. However, a large range in C/N ratios was observed (2.2 to 17.2) determined at inner shelf (stn 718) and shelf/slope (stn 49) sites, respectively. There were also spatial differences in $C/N_{0\text{-}1\ cm}$ values between inner (718, 724, n = 3) and outer (750, 850, 49, n=3) shelf stations (6.4 ± 1.4, 8.6 ± 1.1, respectively). C/N $ratios_{0\text{-}1\ cm}$ from Cape Bathurst in June, 2004 averaged 7.9 ± 0.9 (n = 5).

δ^{13}C values ranged from -24.0 to - 27.2 ‰ (all depths and stations included). The heavier values were determined in both the Amundsen Gulf and Cape Bathurst Polynya while the lightest value was found from the Mackenzie River (Table 2). In the Cape Bathurst Polynya, δ^{13}C values were confined to the range -24.0 - -25.2 ‰. There were no apparent patterns with depth in δ^{13}C values (Table 2). A spatial pattern was however evident along a June, 2004 transect beginning within Reindeer Channel (stn 724) of the Mackenzie River and ending along the shelf/slope break (stn 49). δ^{13}C in surficial sediments along this transect follow the order -27.2 ‰ to -26.5 ‰ to -24.6 ‰ (Table 2).

DISCUSSION

^{210}Pb sediment accumulation rates

An important goal of this study was to determine burial rates of organic carbon. This requires determination of the sediment accumulation rate. Such rates in the CASES area are exceedingly challenging to determine due to the presence of ice scour in inner shelf regions < 50 m, storms that can resuspend and redistribute large amounts of sediments, bioturbation, and the Mackenzie River plume whose direction and magnitude are subject to large interannual variability and mesoscale patchiness intrinsic to plume dynamics (Macdonald et al. 1998).

A convenient starting point for sorting out the effects of particle mixing and sediment accumulation is the general diagenetic equation applied to a radionuclide (Berner,1980):

$$\frac{\partial A}{\partial t} = D_B \frac{\partial^2 A}{\partial x^2} - S\frac{\partial A}{\partial x} - \lambda A \qquad (7)$$

where A is the $^{210}Pb_{xs}$ activity, t is the time, x is the depth in the sediment column, D_B is the particle mixing bioturbation coefficient, S is the sediment accumulation rate, and λ is the ^{210}Pb decay constant. In order to solve equation (7), it is helpful to estimate the relative importance of bioturbation and advection terms upon $\partial A/\partial t$. The Peclet number (defined by LS/D_B where L is the length scale of interest, S is the sedimentation rate, and D_B is the bioturbation coefficient), can be useful in determining which process may be controlling the shape of measured activity profiles. Using a length scale of 10 cm, a typical D_B value of 7 cm^2 y^{-1}(Lecroart et al. 2005) and a sedimentation rate of ~.1 cm yr^{-1} estimated from the study region (Macdonald et al. 1998), one obtains a Peclet # of ~ 0.1 with the interpretation that both sedimentation and bioturbation will influence activity profiles of ^{210}Pb. It should be noted however that our choice of D_B does not reflect any depth dependence in bioturbation rates that can span at least two orders of magnitude in the surface 0-10 cm (Guinasso and Shink, 1975). Discriminating between biodiffusion or advection controlled profiles is made more complicated by the fact that solutions of the diagenetic equation for either advection of diffusion yield exponential functions that have similar shapes. The presence of ice scour would further complicate interpretation of radionuclide activity profiles since the effects of this process upon sediments may either be horizontal ("pushing" sediments laterally) or vertical (an "up and down" motion of ice). However, with maximum water depths of ice scour of ~ 50 m (Hill et al. 1991), this process would only affect nearshore sites such as stn 718.

^{137}Cs profiles (Fig. 3-7) may be used to determine whether the $^{210}Pb_{xs}$ profiles were affected by bioturbation. In some sediment systems, ^{137}Cs displays a pronounced peak related to its maximum fallout in the period 1961-1963, prior to the Nuclear Test Ban Treaty. More commonly, however, shelf sediments display ^{137}Cs gradients with no clear maximum. Thus, the depth to which ^{137}Cs is present compared with $^{210}Pb_{xs}$ can provide clues as to which processes are dominating the profiles. This use of ^{137}Cs is limited however by its mobility in marine sediments. As well, portions of the Arctic also received ^{137}Cs from the 1986 Chernobyl accident, and there may be other inputs from nuclear fuel reprocessing facilities (Cochran et al. 1995). All ^{137}Cs sources post-date ~ 1953, however.

^{210}Pb and ^{137}Cs profiles from the shallow (30 m) near-river station 718 in October-2002 provide an end-member example of sediments that are mixed to a depth > 20 cm, yet the agent of mixing remains undetermined.

The best use of ^{137}Cs profiles is through their comparison with excess ^{210}Pb distributions in a core. If the ^{137}Cs and $^{210}Pb_{xs}$ are present to the same depth in a sediment column, mixing is likely important in controlling the profiles (or migration of ^{137}Cs is occurring). If, however, $^{210}Pb_{xs}$ is present

significantly deeper than ^{137}Cs, sediment accumulation is likely dominating: an example of the latter is stn CA-5 (Oct-03) and stn 101 (Oct-02). At stn 101, ^{137}Cs is present to 4-5 cm, while excess ^{210}Pb persists to 8-9 cm. At stn CA-6, ^{137}Cs disappears by 10-14 cm and excess ^{210}Pb is present at least until 20-24 cm in the core.

Additional information about the influence of particle mixing can be inferred from the $^{210}Pb_{xs}$ and $^{234}Th_{xs}$ profiles. Nozaki et al. (1977) found ^{210}Pb excesses in deep- sea sediments below depths at which one expects to find them based on sedimentation rates obtained from ^{14}C dating. This observation was explained by biomixing whereby infaunal burrows act to transport $^{210}Pb_{xs}$ from the surface to depths below that which can be explained by sedimentation alone. For our data, based on an upper limit on the sedimentation rate of 0.1 cm/yr, one would not expect $^{210}Pb_{xs}$ to be present below 10 cm and excess ^{234}Th should be confined to the upper 0.1 mm. Only two stations, CA-10 and CA-06 showed evidence of ^{210}Pb excesses below 10 cm while the rest had ^{210}Pb concentrations that were largely invariant. The presence of $^{234}Th_{xs}$ to at least several cm in most of the cores suggests they are mixed to at least that depth. The lack of excess ^{210}Pb at depths > 10 cm seen in most profiles, provides some evidence that mixing is confined to the upper few centimeters of these cores. Exceptions to this pattern include stations CA-10 and CA-6 both of which display a minimum in ^{210}Pb centered around 10 cm with increases below. This C-shape $^{210}Pb_{xs}$ profile is consistent with non-local mixing by burrowing infauna.

For purposes of this calculation, we assume that the second term in equation (7) is much larger than the first. Despite the presence of surficial mixing in most of the cores, an upper limit on sediment accumulation can be made from $^{210}Pb_{xs}$ data.

Assuming steady state diagenesis $\partial A/\partial t = 0$, neglecting the mixing term, and rearranging, equation (1) becomes:

$$\frac{\partial A}{\partial x} = -\frac{\lambda}{S} A, \qquad (8)$$

with the solution:

$$A = A_o \exp^{(-\lambda / S)} \qquad (9)$$

Thus, linear plots of ln A_{xs}/A_{xs0} versus depth (x) will have a slope of $-(\lambda/S)$, from which S may be calculated. These are shown in Figure 3-8.

The range in sedimentation accumulation rates for the CASES area was .04 -.39 cm/yr, with an average from all stations and times of .15 ± .08 cm/yr (Fig. 3-8) Within standard deviations from a given area, no apparent pattern in accumulation rates with distance from the Mackenzie River, water column depth, or with time, was found. Rather, sediment accumulation rates were remarkably uniform. The exception to this relative homogeneity was the Franklin Bay site (stn 200) that displayed an accumulation rate of .39 cm/yr (Fig. 3-8. This apparent lack of gradients in sediment accumulation rates in time or geographically is in contrast to the findings of O'Brien et al. (2006) who used sediment traps deployed at 200 m to observe higher mass fluxes in the west during spring freshet, while eastern areas had higher fluxes later in the

season. This finding was attributed to early-season southeasterly winds that confined the emerging Mackenzie River plume to western areas that switched to northeasterly winds late-season when loading from the Mackenzie waned (O'Brien et al. 2006). Because the time-scale for ^{210}Pb dating is ~100 years, the discrepancy between our results and those of O'Brien et al. (2006), suggests that while interannual variability in sedimentation rates may be large, on centennial time scales, sediment arising from the Mackenzie River is uniformly deposited across the Beaufort Shelf.

Although > 90 % of sedimenting material on the Beaufort Shelf originates from the Mackenzie River (Hill et al. 1991), myriad factors such as wind speed and direction, seasonality in sediment loading from the Mackenzie River, storms, ice coverage, tidal range, and bottom contouring will determine where local sediment depot centers reside. An example of the latter is the presence of the Mackenzie Trough (Fig. 3-1) directly seaward of the delta to depths of 100 m. Within this trough, the holocene sediment accumulation is between 20-30 m while eastward of the trough, Holocene thickness is < 20 m (Hill et al. 1991). Settling material may also be expected to follow isobaths. This is observed in our data along roughly the 200 m isobath in which stations 906, 803, CA-6, and 206 had accumulation rates that varied ~ .02 cm/yr (Fig. 3-8).

Mass balance of carbon between water column and sediments

For an idealized situation where advection and other non-vertical transport terms are small, POC export at the base of the euphotic zone can be compared to carbon fluxes into sediments and sediment community carbon respiration (Table 4). POC export values shown here are derived in chapter 4. Sediment burial of organic carbon is calculated from equation (4):

$$F_{soc} = S * \rho * SOC * f_{MAR}(f_{TERR}) \qquad (4)$$

where, S is the sedimentation rate (cm y^{-1}), ρ is the dry bulk density (g cm^{-3}), SOC is the organic carbon content of the sediment (g C g sediment $^{-1}$), f is the fraction of marine or terrestrial organic carbon (derived in Chapter 4 from $\delta^{13}C$ values in surficial sediments). The sediment community O_2 demands were measured by Paul Renaud (University of Connecticut) and converted into carbon respiration using a stoichiometric coefficient of 1.

The results in Table 4 indicate large but variable percentages of marine carbon fluxes reach sediments at a given location (% = POC_{MAR} Flux 50 m/ Sed Carbon flux = 46-99 %) compared to 73-99 % of POC_{TERR} fluxes. Surprisingly, lower percentages were found in the Cape Bathurst Polynya area where one might have expected fresher, more labile POC to be present, and lateral effects originating from the Mackenzie River to be minimized. Perhaps even more startling is the large percentages of POC_{TERR} fluxes from all regions that appear to be lost from the water column before reaching sediments. Many of the sites that registered these large losses were sites where floating trap ^{234}Th fluxes were within a factor of 2 of fluxes determined from in situ pumps, suggesting that horizontal effects can not solely explain losses of POC_{TERR} (Chapter 2). It is furthermore unlikely that lateral effects completely dominate the large carbon

flux attenuations since it is improbable that such effects would create a pattern in which similar percentages of marine or terrestrial carbon are advected at every location, with no discrimination closer or further from the Mackenzie River. On the other hand, the imprint of the Mackenzie River plume is plainly evident in the Cape Bathurst area, especially in July, where, POC_{TERR} values, although lower than those near the Mackenzie, are substantial, and most likely can not be explained by local phenomena. Hence, the issue of lateral effects ultimately becomes one of time and length scaling, and of understanding the direction and velocity of current fields; data which are not presently available.

Another consideration regarding lateral effects is the fact that the along-shelf spatial scale we sampled was ~ 800 km. This scale is long enough so that along-shelf local carbon sources and sinks should have been captured. Only station 200 registered significantly higher marine and terrestrial POC sediment fluxes (Table 4) compared to other stations, marking this area as a local carbon sink. That all other sites show small sediment carbon fluxes coupled to comparatively large water column POC fluxes suggests either that along-shelf coverage was insufficient (unlikely), or that this system is efficiently transporting material across the shelf. Equally as plausible as the advective arguments described above, is local water column oxidation of sinking organic material as the agent causing the carbon flux decreases. One general consideration in support of local remineralization is that the calculation of 10 % or less to marine carbon fluxes exiting the water column and reaching sediments is a well entrenched paradigm that has also been found in high latitudes (Dugdale and Goering, 1967, Tremblay et al. 2002).

The accuracy of the sediment carbon fluxes we calculated may also be evaluated by comparing them with sediment community carbon respiration obtained from ^{14}C incubations that yielded community oxygen demands that were converted stoichiometrically to carbon respiration (values courtesy of Paul Renaud at the University of Connecticut). A comparison of these carbon respiration values with our sediment carbon fluxes (marine + terrestrial) reveals that carbon respiration is higher by about a factor of 2 than C burial (Table 4). Additional support for the sediment fluxes we obtained comes from comparing the terrestrial sediment carbon fluxes (gradients in marine sediment carbon fluxes were too small to permit comparison) with the carbon respiration values. The station-to-station pattern in carbon respiration is 718>>906>803 ~ 709>406 that compares to 718>906>803>709>406 for sediment terrestrial carbon fluxes (Table 4). The close agreement of these trends suggests that terrestrial carbon is an important food source for bottom dwelling animals. Furthermore, the fact that marine sediment carbon fluxes are lower than terrestrial carbon ones and much lower than sediment carbon respiration rates implies that the rain rate of marine carbon is simply not enough to satisfy the nutritional requirements of benthic fauna. The observation that the site (406) farthest from the Mackenzie River also has the lowest sediment carbon respiration and sediment carbon flux is also consistent with infauna utilizing terrestrial carbon as a substrate that decreases with distance from the Mackenzie River.

TABLES

Table 3-1	Sediment radionuclide data															
Depth	**$\rho_{dry\ blk}$**	**H_2O**	**Porosity**	**Total**	**Supp**	**$^{234}Th_{xs}$**			**^{210}Pb**	**^{228}Ra**	**$^{210}Pb_{xs}$**			**^{137}Cs**		
in core	**(g dry/**	**(%)**	**(cm^3 water/**	**^{234}Th**	**^{234}Th**											
(cm)	**cm^3 wet)**		**cm^3 wet sed)**	**(dpm/g)**		**(dpm/g)**			**(dpm/g)**	**(dpm/g)**	**(dpm/g)**			**(dpm/g)**		
October, 2002																
STATION 65A(718), 10/1, 38m,LAT-70° 10.2 LON-133° 32.1																
0-1	0.47	63.7	0.82	3.63		†.61	±	0.44	2.87	nd	0.06	±	0.01	0.32	±	0.02
1-2	0.72	50.4	0.73	2.54		-0.48			2.77	nd	nd			0.37	±	0.03
2-3	0.78	47.4	0.70	2.85		-0.17			2.99	nd	0.18	±	0.03	0.39	±	0.03
3-4	0.59	57.0	0.78	2.62		-0.40			2.25	nd				0.27	±	0.02
4-5	0.67	52.7	0.75	3.08		†.06			2.82	nd	0.01	±	0.00	0.32	±	0.02
5-6	0.63	54.9	0.76	2.81		-			2.56	nd				0.34	±	0.02
6-7	0.92	41.3	0.65	3.00		-			2.49	nd				0.26	±	0.02
8-9	0.75	49.0	0.72	3.23		-			2.50	nd				0.33	±	0.02
10-12	0.80	46.8	0.70	3.45		-			3.01	nd	0.20	±	0.03	0.34	±	0.02
12-14	0.82	45.8	0.69	2.80		-			2.62	nd				0.31	±	0.02
14-16	0.73	49.8	0.72	3.02		-			3.02	nd	0.21	±	0.03	0.36	±	0.03
18-20	0.88	43.1	0.67	2.80		-			2.80	nd				0.34	±	0.02
				3.02												
STN 12(200), 10/12, 255m, LAT-69° 50.22 LON-126° 9.65																
0-2	0.50	60.2	0.81	2.50		-0.20			4.90	nd	1.80	±	0.25	0.66	±	0.05
2-3	0.56	54.1	0.79	3.11		†.41			4.36	nd	1.26	±	0.18	0.12	±	0.01
3-4	0.64	54.2	0.76	2.93		†.23			4.65	nd	1.55	±	0.22	0.26	±	0.02
4-5	0.64	53.5	0.76	2.81		†.11			4.56	nd	1.46	±	0.20	0.14	±	0.01
5-6	0.65	53.0	0.75	2.84		-			4.73	nd	1.63	±	0.23	0.18	±	0.01
6-7	0.66	51.3	0.75	2.62		-			3.84	nd	0.74	±	0.10	0.2	±	0.01
7-8	0.70	55.1	0.74	2.48		-			3.92	nd	0.82	±	0.11	0.2	±	0.01
8-9	0.62	56.1	0.76	2.72		-			3.24	nd	0.14	±	0.02	0.18	±	0.01
9-10	0.60	49.2	0.77	2.39		-			3.11	nd	0.01	±	0.01	0.18	±	0.01
11-13	0.74	47.0	0.72	2.78		-			3.23	nd	0.13	±	0.02	0.08	±	0.01
13-15	0.79	66.0	0.70	2.80		-			3.40	nd	0.30	±	0.04	0.01	±	0.01
15-17	0.43	46.6	0.84	3.13		-			2.96	nd	0.00			0		
17-19	0.80	50.2	0.70	2.51		-			2.88	nd	0.00			0		
				2.70												
STN 1, 9/27, 250m, LAT-71° 32.9 LON-131° 11.7																
0-1	0.44	65.5	0.83	2.85		†.13			7.01	nd	4.70	±	0.66	0.22	±	0.02
1-2	0.65	53.8	0.76	2.52		-0.20			6.79	nd	4.48	±	0.63	0.22	±	0.02
2-3	0.55	58.8	0.79	2.57		-0.15			5.79	nd	3.48	±	0.49	0.23	±	0.02
3-4	0.60	56.4	0.77	2.18		-0.54			5.85	nd	3.54	±	0.50	0.25	±	0.02
4-5	0.55	59.0	0.79	2.33		-0.39			4.53	nd	2.22	±	0.31	0.19	±	0.01

6-7	0.65	53.9	0.76	2.55		-			3.01	nd	0.70	±	0.10	0.09	±	0.01
7-8	0.62	55.1	0.77	2.45		-			2.91	nd	0.60	±	0.08	0		
8-9	0.68	52.1	0.74	2.97		-			3.20	nd	0.89	±	0.12	0		
9-10	0.82	45.8	0.69	3.17		-			2.56	nd	0.25	±	0.04	0		
10-12	0.83	45.1	0.69	2.41		-			2.39	nd	0.08	±	0.01	0		
14-16	1.00	38.4	0.62	3.03		-			2.20	nd	0.00			0		
18-20	1.11	34.4	0.58	2.49		-			2.36	nd	0.00			0		
				2.72												
STN 101, 10/10, 500 m, LAT-70° 43.46 LON-124° 10.95																
0-2	0.50	65.0	0.80	2.23		0.00			7.62	nd	4.22	±	0.59	0.21	±	0.01
2-3	0.49	62.6	0.77	1.96		-0.27			9.97	nd	6.57	±	0.92	0.35	±	0.02
3-4	0.59	56.8	0.82	2.43		†.20			10.00	nd	6.60	±	0.92	0.17	±	0.01
4-5	0.59	56.8	0.78	1.89		-0.32			4.88	nd	1.48	±	0.21	0.05	±	0.01
5-6	0.61	55.8	0.78	2.14		-			5.04	nd	1.64	±	0.23	0		
6-7	0.59	56.7	0.77	2.26		-			4.05	nd	0.65	±	0.09	0		
7-8	0.59	56.6	0.78	2.03		-			4.52	nd	1.12	±	0.16	0		
8-9	0.60	56.3	0.78	2.56		-			4.10	nd	0.70	±	0.10	0		
9-10	0.59	56.8	0.77	2.64		-			nd	nd	0.00			0		
10-12	0.61	55.7	0.78	1.90		-			3.50	nd	0.00			0		
14-16	0.62	55.4	0.75	1.99		-			3.30	nd	0.00			0		
				2.23												
STN 49, 9/28, 1200 m, LAT-71° 26.71 LON-133° 47.17																
1-2	0.68	52.5	0.75	2.50		†.33			6.53	nd	4.12	±	0.58	0.24	±	0.02
2-3	0.90	42.3	0.66	2.10		-0.07			4.05	nd	1.64	±	0.23	0.08	±	0.01
3-4	0.92	41.7	0.65	2.70		†.53			4.06	nd	1.65	±	0.23	0.16	±	0.01
4-5	0.97	39.5	0.63	2.47		†.30			2.30	nd	0.00			0.07	±	0.01
5-6	1.07	35.9	0.60	1.83		-			1.74	nd	0.00			0.05	±	0.01
6-7	0.96	40.0	0.64	2.28		-			2.33	nd	0.00			0		
7-8	0.94	40.7	0.65	2.49		-			2.63	nd	0.22	±	0.03	0		
8-9	0.95	40.4	0.64	2.18		-			2.76	nd	0.35	±	0.05	0		
10-12	1.10	34.8	0.59	1.49		-			2.30	nd	0.00			0		
12-14	1.01	37.9	0.62	2.15		-			2.37	nd	0.00			0		
14-16	0.65	53.5	0.75	2.53		-			2.39	nd	0.00			0		
18-20	1.04	36.7	0.61	2.41		-			2.47	nd	0.00			0		
				2.17												
October, 2003																
STN 718, 10/1, 30 m, LAT-70° 10.2 LON-133° 32.1																
0-1	0.95	40.2	0.64	3.01	2.53	0.37	±	0.23	4.03	1.41	2.62	±	0.37	0.24	±	0.02
1-2	1.04	36.8	0.61	2.17		-0.47	±	0.3	3.88	1.39	2.49	±	0.35	0.16	±	0.01
2-3	1.01	37.9	0.62	2.68		0.04	±	0.1	3.27	1.54	1.73	±	0.24	0.18	±	0.01
3-4	1.05	36.5	0.60	4.53		6.10	±	1.50	6.73	3.02	3.71	±	0.52	0.23	±	0.02
4-5	1.05	36.5	0.60	3.04		-			3.95	2.03	1.92	±	0.27	0.15	±	0.01
5-7	1.05	36.6	0.60	2.82		-			6.03	1.80	4.23	±	0.59	0.10	±	0.01
7-9	1.08	35.4	0.59	2.80		-			3.92	1.94	1.98	±	0.28	0.00	±	
11-13	1.24	30.1	0.53	2.37		-			2.49	1.71	0.78	±	0.11	0		

13-15	1.26	29.2	0.52	2.58		-			2.99	1.68	1.31	±0.18	0		
				2.64											
STN CA-10, 10/6, 250 m, LAT-69° 56.20 LON-138° 34.5															
0-2	0.57	58.3	0.79	4.57	2.50	2.20	±	0.83	18.0	2.66	15.3	±2.14	0.68	±	0.05
2-3	0.55	59.2	0.79	3.46		0.01	±	0.01	12.6	2.55	10.0	±1.41	0.57	±	0.04
3-4	0.67	52.5	0.75	3.40		-0.05	±	0.04	9.11	2.95	6.16	±0.86	0.49	±	0.03
4-5	0.66	53.0	0.75	3.49		0.04	±	0.03	7.63	3.00	4.63	±0.65	0.27	±	0.02
5-7	0.62	55.1	0.76	2.89		-			10.5	2.53	7.95	±1.11	0.11	±	0.01
7-9	0.67	52.9	0.75	3.41		-			6.43	2.93	3.50	±0.49	0.11	±	0.01
11-13	0.74	49.4	0.72	3.81		-			7.41	3.04	4.37	±0.61	0.11	±	0.01
15-17	0.72	50.1	0.73	3.68		-			9.69	2.98	6.71	±0.94	0.00		
				3.45											
STN CA-06, 10/11, 250 m, LAT-70° 37.808 LON-127° 15.168															
0-2	0.58	57.6	0.78	7.29	2.70	5.70	±	2.20	18.2	2.70	15.5	±2.17	0.32	±	0.02
2-3	0.60	56.3	0.77	4.16		0.35			14.9	2.55	12.3	±1.73	0.36	±	0.03
3-4	0.54	59.5	0.80	2.75		-1.06			12.0	2.86	9.14	±1.28	0.42	±	0.03
4-5	0.54	59.6	0.80	3.56		-0.25			11.5	2.95	8.55	±1.20	0.45	±	0.03
5-7	0.60	56.6	0.78	3.99		-			nd	3.04	0.00		0.19	±	0.01
7-9	0.63	54.7	0.76	3.51		-			6.59	2.76	3.83	±0.54	0.07	±	0.01
11-13	0.63	51.6	0.76	3.57		-			4.70	2.41	2.29	±0.32	0.00		
15-17	0.74	49.2	0.72	3.63		-			10.5	2.66	7.79	±1.09	0		
21-23	0.79	47.2	0.70	4.36		-			10.6	3.09	7.49	±1.05	0		
				3.81											
June, 2004															
STN 406, 6/15, 188 m, LAT-71° 18.647 LON-127° 41.648															
0-1	0.42	66.7	0.84	2.97	2.11	-1.10			4.36	2.49	1.87	±0.26	0.28	±	0.02
1-2	0.71	50.9	0.73	2.39		-1.68			4.70	2.45	2.25	±0.31	0.18	±	0.01
2-3	0.69	51.7	0.74	2.85		-1.22			6.40	2.43	3.97	±0.56	0.27	±	0.02
3-4	0.62	55.1	0.77	2.91		-1.16			3.79	2.09	1.70	±0.24	0.08	±	0.01
4-5	0.81	46.2	0.69	3.87		-0.19			3.25	2.43	0.82	±0.11	0.04	±	0.01
5-6	0.82	45.6	0.69	3.89		-			2.94	2.31	0.63	±0.09	0		
6-7	0.90	42.5	0.66	4.49		-			2.65	2.14	0.51	±0.07	0		
16-18	0.84	44.7	0.68	3.65		-			3.31	1.44	1.87	±0.26	0		
				4.07											
STN 108, 6/7, 533 m, LAT-70° 37.67 LON-123° 09.1															
0-1	0.95	40.3	0.64	3.07	2.21	3.86	±	1.20	8.16	2.71	5.45	±0.76	0.88	±	0.06
1-2	1.03	37.1	0.61	2.40		2.00	±	0.45	6.64	2.17	4.47	±0.63	1.64	±	0.11
2-3	0.90	42.3	0.66	2.95		3.52	±	1.23	9.34	2.43	6.91	±0.97	1.7	±	0.12
3-4	0.94	40.6	0.64	1.54		-0.14			5.86	2.88	2.98	±0.42	0.12	±	0.01
4-5	0.85	44.5	0.68	1.52		-0.16			4.19	2.34	1.85	±0.26	0		
6-8	1.04	36.8	0.61	1.53		-			3.31	1.79	1.52	±0.21	0		
8-10	1.00	38.3	0.62	1.46		-			2.99	1.68	1.31	±0.18	0		
14-16	1.44	24.0	0.46	0.70		-			1.69	1.11	0.58	±0.08	0		
18-20	1.60	19.8	0.40	2.06		-			1.88	1.28	0.60	±0.08	0		

				1.68												
STN 117, 6/9, 300 m, LAT-70° 54.822 LON-125° 34.436																
0-1	0.64	54.1	0.76	4.79	2.31	5.12	±	2.00	15.7	6.90	8.81	±	1.23	0.68	±	0.05
1-2	0.75	48.8	0.72	2.44		-0.29			4.66	0.92	3.74	±	0.52	0.12	±	0.01
2-3	0.64	54.3	0.76	2.71		-0.02	±		6.84	2.45	4.39	±	0.62	0.29	±	0.02
3-4	0.59	56.7	0.78	2.58		-0.15	±		11.4	8.10	3.33	±	0.47	0.17	±	0.01
4-5	0.48	63.1	0.82	2.70		-			10.6	6.11	4.46	±	0.62	0.2	±	0.01
6-8	0.73	50.0	0.73	2.63		-			5.20	2.53	2.67	±	0.37	0		
8-10	0.76	48.2	0.71	2.53		-			4.76	2.55	2.21	±	0.31	0		
18-20	0.66	53.5	0.75	3.04		-			3.99	2.81	1.18	±	0.16	0		
				2.73												
STN 303, 6/18, 255 m, LAT-70° 47.524 LON-127° 0.254																
0-1	0.52	60.6	0.80	4.24	2.43	3.58	±	1.50	14.2	2.12	12.1	±	1.70	0.46	±	0.03
1-2	0.58	57.5	0.78	3.04		-0.02			9.75	2.03	7.72	±	1.08	0.39	±	0.03
2-3	0.63	54.8	0.76	2.24		-0.82			5.84	nd	3.25	±	0.46	0.21	±	0.01
3-4	0.60	56.2	0.77	3.01		-0.05			7.37	3.05	4.32	±	0.60	0.28	±	0.02
4-5	0.55	59.0	0.79	2.07		-0.99			3.96	2.48	1.48	±	0.21	0.1	±	0.01
6-8	0.72	50.3	0.73	2.35		-			3.11	2.03	1.08	±	0.15	0		
8-10	0.63	54.6	0.76	3.00		-			3.81	2.20	1.61	±	0.22	0		
18-20	0.73	50.0	0.73	3.82		-			2.59	2.59	0.01	±		0		
				3.06												
STN 206, 6/3, 80 m, LAT-70°.322 LON-124°.845																
0-1	0.46	64.4	0.83	2.71		-0.56			6.82	2.29	4.53	±	0.63	0.25	±	0.02
1-2	0.73	49.8	0.72	2.74		-0.53			7.40	3.06	4.34	±	0.61	0.26	±	0.02
2-3	0.74	49.2	0.72	2.33		-0.94			7.77	2.82	4.95	±	0.69	0.30	±	0.02
3-4	0.80	46.4	0.70	2.78		-0.49			7.14	3.09	4.05	±	0.57	0.25	±	0.02
4-5	0.74	49.3	0.72	2.66		-0.61			6.34	3.48	2.86	±	0.40	0.17	±	0.01
6-8	0.79	46.9	0.70	2.74		-			3.82	2.51	1.31	±	0.18	0		
8-10	0.58	57.2	0.78	3.24		-			3.93	2.80	1.13	±	0.16	0		
16-18	0.70	50.0	1.25	3.70		-			2.72	2.42	0.30	±	0.04	0		
18-20	0.80	46.6	0.70	3.39		-			3.03	2.49	0.54	±	0.07	0		
				3.27												
July, 2004																
STN 718, 7/11, 30 m, LAT-70° 10.2 LON-133° 32.1																
0-2	0.57	57.7	0.78	3.67	2.51	4.40	±	1.67	4.51	2.44	2.07	±	0.29	0.35	±	0.02
2-3	0.52	60.4	0.80	3.23		0.27			5.62	2.76	2.86	±	0.40	0.53	±	0.04
3-4	0.71	50.6	0.73	2.90		0.06			5.09	2.68	2.41	±	0.34	0.47	±	0.03
4-5	0.65	53.7	0.75	2.95		-0.01			4.62	2.52	2.10	±	0.29	0.58	±	0.04
6-8	0.65	53.5	0.75	2.91		-			4.55	1.98	2.57	±	0.36	0.43	±	0.03
8-10	0.78	47.4	0.70	3.04		-			4.10	2.48	1.62	±	0.23	0.47	±	0.03
12-14	0.91	42.1	0.66	2.93		-			4.25	2.51	1.74	±	0.24	0.22	±	0.02
				2.96												
STN 850, 7/3, 1000 m, LAT-70° 34.0 LON-137° 35.454																

0-1	0.47	63.5	0.82	4.03	2.55	1.81	±	4.60	17.5	3.38	14.1	±	1.97	0.58	±	0.04
1-2	0.48	62.9	0.82	3.20		0.98	±	3.20	15.7	2.30	13.4	±	1.88	0.49	±	0.03
2-3	0.50	61.9	0.81	2.57		0.35			15.0	2.99	12.0	±	1.68	0.51	±	0.04
3-4	0.56	58.4	0.79	nd		nd			nd	nd	nd			nd		
4-5	0.66	53.2	0.75	2.26		0.04			8.14	2.56	5.58	±	0.78	0.22	±	0.02
6-7	0.62	55.3	0.77	nd		nd			nd	nd	nd			nd		
8-10	0.67	52.8	0.75	2.15		-			5.36	2.18	3.18	±	0.45	0.05	±	0.01
16-18	0.73	49.9	0.72	2.26		-			3.35	2.20	1.15	±	0.16	0		
				2.22												
STN 906, 7/3, 100 m, LAT-70° 1.2 LON-138° 35.8																
0-1	0.50	61.7	0.81	4.31		10.14	±	5.10	13.1	2.85	10.2	±	1.43	0.71	±	0.05
1-2	0.57	58.2	0.79	2.70	2.47	0.00			10.9	2.72	8.16	±	1.14	0.66	±	0.05
2-3	0.77	47.7	0.71	2.69		0.00			8.66	2.34	6.32	±	0.88	0.67	±	0.05
3-4	0.68	52.0	0.74	2.13		0.00			6.85	2.00	4.85	±	0.68	0.49	±	0.03
4-5	0.65	53.9	0.76	2.87		0.00			6.47	2.81	3.66	±	0.51	0.38	±	0.03
5-6	0.67	52.6	0.75	2.73		*			5.67	2.32	3.35	±	0.47	0.39	±	0.03
8-10	0.83	45.3	0.69	3.15		*			4.84	2.66	2.18	±	0.30	0.15	±	0.01
12-14	0.82	45.8	0.69	2.78		*			2.38	2.44	0.00	±		0.04	±	0.01
				2.89												
STN 406, 7/24, 188 m, LAT-71° 18.647 LON-127° 41.648																
0-1	0.57	58.0	0.79	2.47		0.00			12.3	2.80	9.53	±	1.33	0.45	±	0.03
1-2	0.51	61.3	0.81	2.62		0.00			9.52	2.89	6.63	±	0.93	0.37	±	0.03
2-3	0.70	51.2	0.74	nd		nd			nd	nd	nd			nd		
3-5	0.65	53.5	0.75	2.06		0.00			3.78	2.00	1.78	±	0.25	0.12	±	0.01
5-7	0.71	50.8	0.73	2.07		0.00			2.88	1.80	1.08	±	0.15	0.09	±	0.01
7-9	0.82	45.7	0.69	2.20		0.00			2.50	2.00	0.50	±	0.07	0		
				2.13												
STN 200, 7/17, 150 m, LAT-69° 55.0 LON-126° 36.0																
0-1	0.70	51.5	0.74	4.49	2.40	10.70	±	4.81	7.63	2.10	5.53	±	0.77	0.29	±	0.02
1-2	0.63	54.6	0.76	3.44		1.10	±	0.49	11.6	3.46	8.14	±	1.14	0.33	±	0.02
2-4	0.59	56.8	0.78	nd		nd			nd	nd	nd			nd		
6-8	0.58	57.2	0.78	2.45		0.00			7.16	2.53	4.63	±	0.65	0.3	±	0.02
8-10	0.79	47.2	0.70	2.88					5.96	2.92	3.04	±	0.43	0.4	±	0.03
				2.67												
STN 803, 7/8, 250 m, LAT-70° 38.5 LON-135° 53.5																
0-2	0.52	60.8	0.80	3.74	2.44	3.34	±	1.30	8.96	2.55	6.41	±	0.90	0.44	±	0.03
2-3	0.75	48.8	0.72	2.99		0.00	±		10.2	2.67	7.56	±	1.06	0.47	±	0.03
3-4	0.63	54.5	0.76	2.69		0.00	±		7.76	2.77	4.99	±	0.70	0.49	±	0.03
4-5	0.77	47.9	0.71	2.91		0.00	±		6.56	2.90	3.66	±	0.51	0.71	±	0.05
7-8	0.84	44.6	0.68	nd		nd			nd	nd	nd			nd		
8-10	0.86	43.8	0.67	2.96			±		4.51	2.53	1.98	±	0.28	0.39	±	0.03
12-14	0.80	46.6	0.70	nd		nd			nd	nd	nd			nd		
16-18	0.89	42.8	0.66	2.91			±		4.30	2.54	1.76	±	0.25	0.33	±	0.02
				2.94												

STN 709, 6/30, 80 m, LAT-70° 57.0 LON-133° 45.4																
0-1	1.07	35.9	0.60	2.20		0.00			6.05	1.80	4.25	±	0.59	0.21	±	0.01
1-2	1.10	34.9	0.59	3.10		8.20	±	4.50	3.10	1.80	1.30	±	0.18	1.38	±	0.10
2-3	1.23	30.5	0.54	2.10		0.00			1.90	1.38	0.52	±	0.07	0.12	±	0.01
3-4	1.13	33.5	0.57	nd		nd			nd	nd	nd			nd		
4-5	1.18	32.1	0.56	1.73					1.26	1.30				0.02	±	0.01
8-10	1.22	30.7	0.54	1.80					1.88	1.33	0.55	±	0.08	0		
12-14	1.48	22.9	0.44	nd		nd			nd	nd	nd			nd		
16-18	1.46	23.6	0.45	2.44					1.32	1.25	0.07	±	0.01	0		
				2.12												
STN 750, 7/14, 900 m																
0-2	0.63	52.6	0.76	3.38	2.35	6.33	±	2.15	17.9	3.47	14.4	±	2.02	0.57	±	0.04
2-4	0.67	48.6	0.75	2.54		*			7.95	2.64	5.31	±	0.74	0.39	±	0.03
4-6	0.76	49.5	0.71	2.76		*			5.98	2.82	3.16	±	0.44	0.36	±	0.03
8-10	0.73	49.7	0.72	2.73		*			4.13	2.59	1.54	±	0.22	0.12	±	0.01
				2.44												
STN 309, 7/19, 300 m,LAT- 71° 7.5 LON-125° 50.0																
0-2	0.48	63.3	0.82	3.25	2.38	*			15.5	4.00	####	±	1.61	0.5	±	0.04
2-4	0.58	57.4	0.78	3.33		*			13.6	4.87	8.71	±	1.22	0.59	±	0.04
4-6	0.62	55.1	0.76	3.21		*			12.9	4.08	8.83	±	1.24	0.47	±	0.03
6-8	0.58	57.2	0.78	2.58		*			11.3	3.73	7.55	±	1.06	0.13	±	0.01
8-10	0.63	54.5	0.76	2.09		*			11.0	1.47	9.55	±	1.34	0.41	±	0.03
				2.34												
* = not measured																
† = not decay corrected																
nd = no data																

Table 3- 2. Sediment C, N and $\delta^{13}C$ data

STN	Sampling Month-Year	Depth cm	C %	N %	C/N	$\delta^{13}C$ ‰
49	Oct-02	0-1	1.04	0.11	9.5	-25.2
49	Oct-02	1-2	0.86	0.05	17.2	-25.4
49	Oct-02	4-5	nd	nd	nd	-25.5
49	Oct-02	18-20	nd	nd	nd	-25.0
200	Oct-02	0-1	1.63	0.19	8.6	-25.7
200	Oct-02	1-2	1.49	0.19	7.8	nd
200	Oct-02	8-9	nd	nd	nd	-26.0
200	Oct-02	13-15	nd	nd	nd	-26.0
200	Oct-02	18-20	nd	nd	nd	-25.6
101	Oct-02	0-1	1.3	0.10	13.0	-24.0
101	Oct-02	1-2	1.00	0.09	11.1	-24.1
718	Oct-02	0-1	1.10	0.25	4.4	-25.6
718	Oct-02	1-2	1.00	0.45	2.2	-26.1
718	Oct-02	6-7	nd	nd	nd	-26.1
CA-6	Oct-03	0-1	1.49	0.20	7.5	-25.0
CA-6	Oct-03	0-1	1.41	0.30	4.7	-25.3
718	Oct-03	0-1	nd	nd	nd	-25.6
718	Oct-03	5-7	nd	nd	nd	-26.0
117	June-04	0-1	1.42	0.15	9.5	-28.3
309	June-04	0-1	1.35	0.19	7.1	-24.7
406	June-04	0-1	1.51	0.20	7.6	-25.1
303	June-04	0-1	1.62	0.22	7.4	-25.2
303	June-04	1-2	nd	nd	nd	-24.0
303	June-04	4-5	nd	nd	nd	-24.3
303	June-04	14-16	nd	nd	nd	-24.4
206	June-04	0-1	1.39	0.45	3.1	-25.7
108	June-04	0-1	1.55	0.22	7.0	-25.2
108	June-04	1-2	nd	nd	nd	-25.2
108	June-04	5-6	nd	nd	nd	-24.0
718	Jly-04	0-1	1.95	0.26	7.5	-26.5
850	Jly-04	0-1	1.49	0.16	9.3	-24.9
850	Jly-04	3-4	nd	nd	nd	-24.9
750	Jly-04	0-2	1.07	0.15	7.1	-24.6
724	Jly-04	0-1	1.29	0.18	7.2	-27.2
MACK	Jly-04	0-1	nd	nd	nd	-27.2
MACK	Jly-04	2-4	nd	nd	nd	-27.3

nd=no data

Table 3-3

CASES sediment penetration depths for $^{234}Th_{xs}$, $^{210}Pb_{xs}$, ^{137}Cs

STN-yr	$^{234}Th_{xs}$	$^{210}Pb_{xs}$	^{137}Cs
	cm	cm	cm
718-02	nd	15	20
12-02	nd	14	14
1-02	nd	11	7
101-02	nd	9	5
49-02	nd	9	6
718-03	3	15	7
CA-10-03	3	17	13
CA-6-03	3	23	9
406-04	0	18	5
108-04	3	20	4
117-04	1	20	5
303-04	1	10	5
206-04	0	18	5
718-04	2	14	14
850-04	3	18	10
906-04	1	10	10
406-04	0	9	7
200-04	2	10	10
803-04	2	18	18
709-04	2	10	5
750-04	2	10	10
309-04	nd	10	10

Table 3-4 **Fluxes of SOC and POC**

Stn	Sed * C demand mmol C/m^2/d	Sed rate x 10^3 cm/d	Sed %C gC/gsed	Sed C Flux$_{MAR}$ mmolC/m^2/d	Sed C Flux$_{TERR}$ mmolC/m^2/d	POC Flux$_{MAR\ 50m}$ mmolC/m^2/d	POC Flux$_{TERR\ 50m}$ mmolC/m^2/d
				JUNE, 2004			
117	nd	0.66	1.42	0.5	4.5	4.2	28
206	nd	0.44	1.39	0.7	1.64	1.3	13
303	nd	0.19	1.62	0.5	0.8	3.3	9
108	nd	0.38	1.55	1.9	2.8	5.1	12
				JULY, 2004			
406	2.0	0.14	1.50	0.4	0.8	12.6	71
906	5.3	0.36	1.50	0.3	2.6	8.8	108
709	3.2	0.16	1.50	0.4	1.5	29	160
803	3.5	0.36	1.50	0.6	2.5	<1	163
718	6.5	0.36	1.95	0.3	3.0	30	110
200	nd	1.1	1.63	3.1	7.3	11	59

* Values courtesy of Paul Renaud

FIGURES

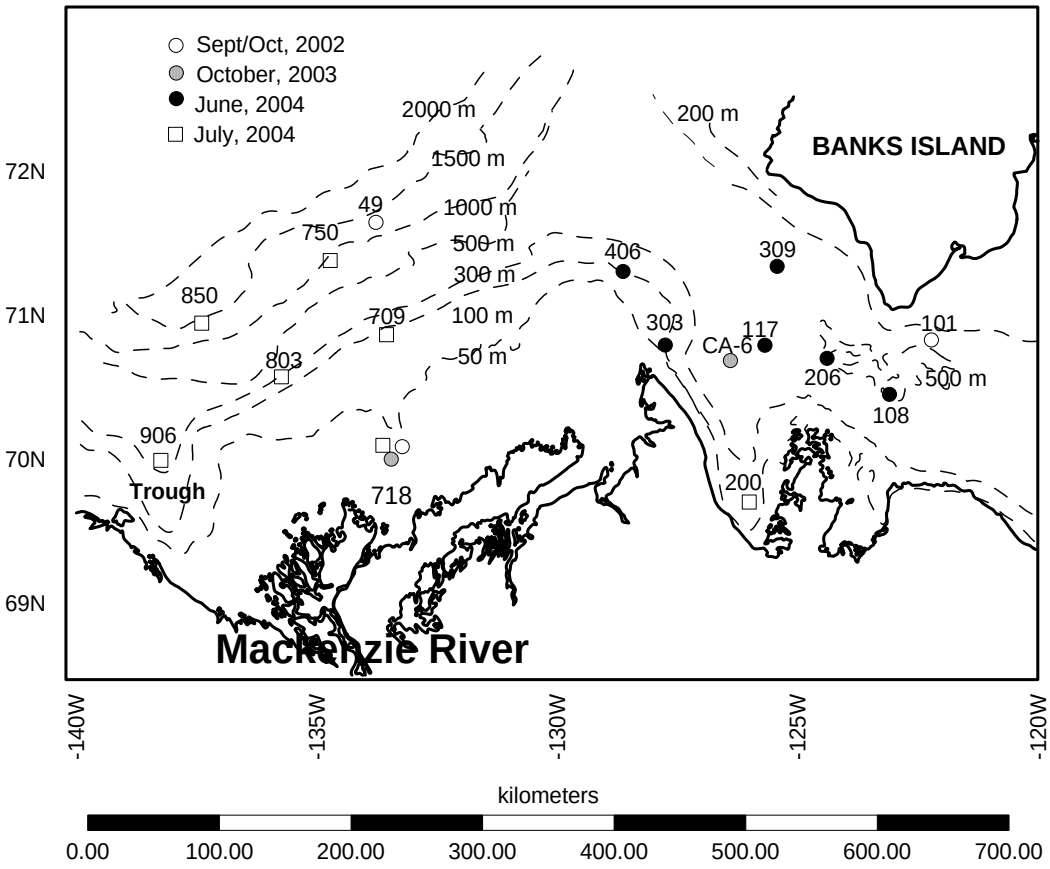

Figure 3-1. Sites where sediments were sampled

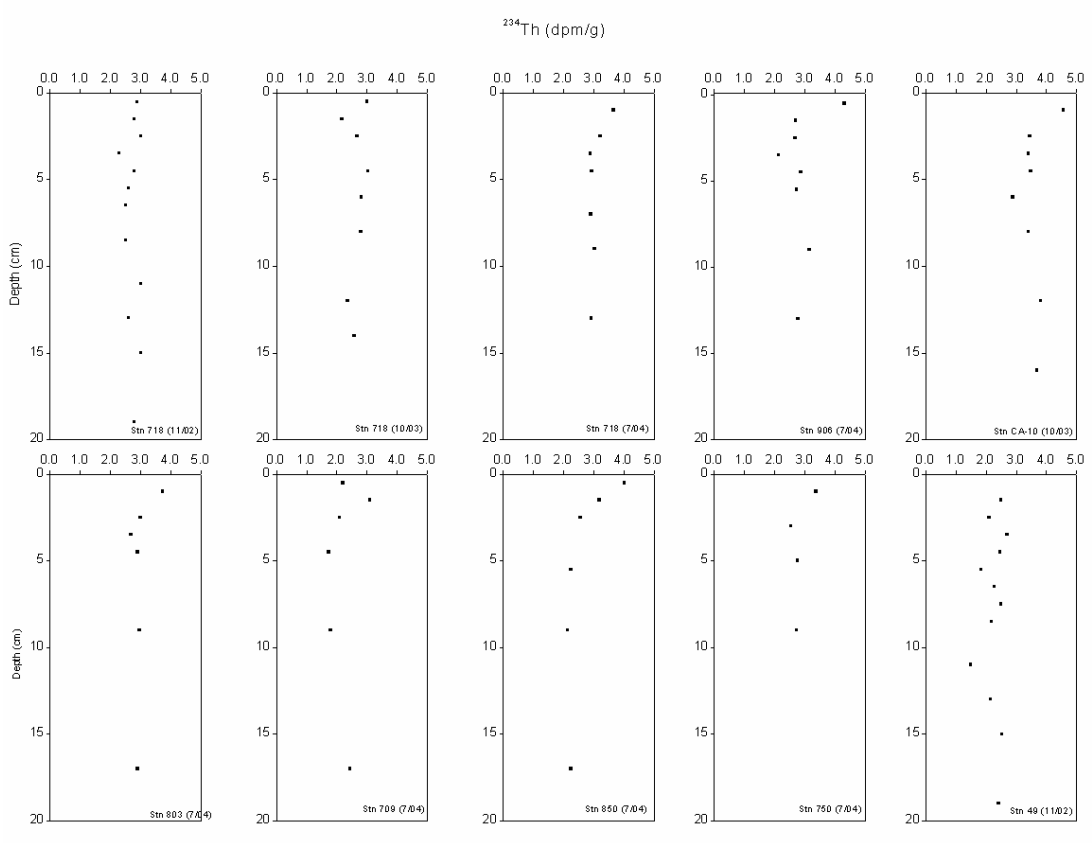

Figure 3-2a. ^{234}Th (dpm/g) profiles in sediments from western locations.

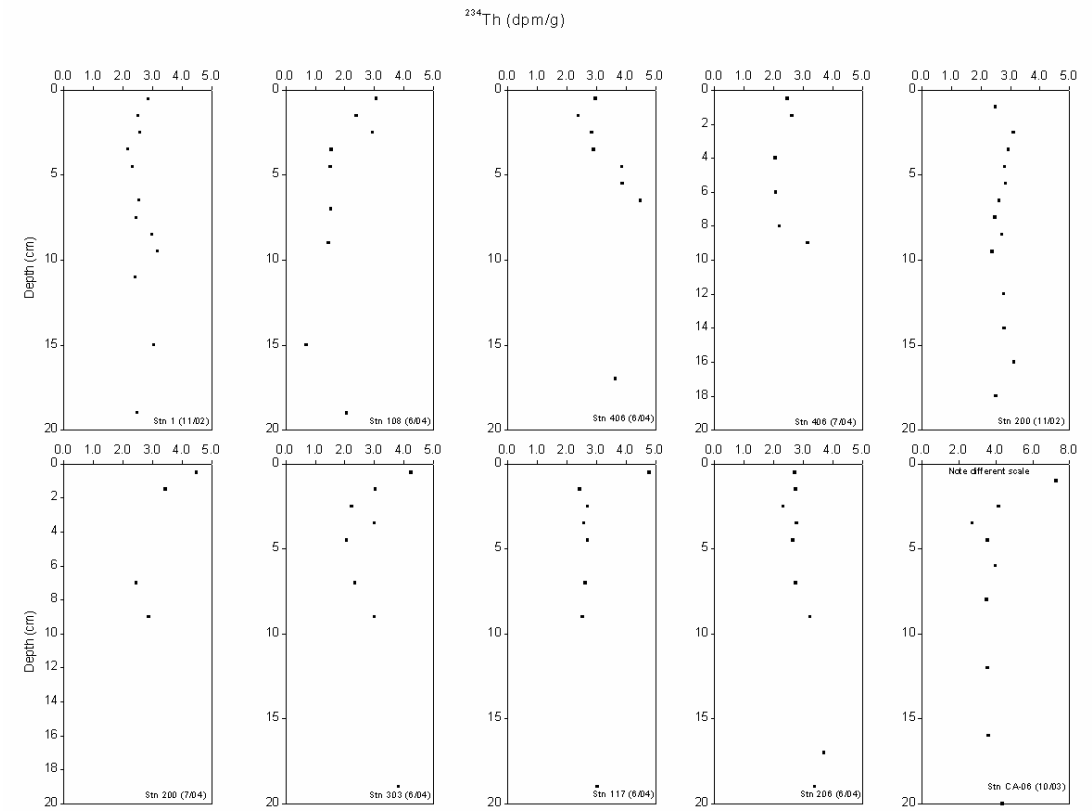

Figure 3-2b. ^{234}Th (dpm/g) profiles in sediments from western locations.

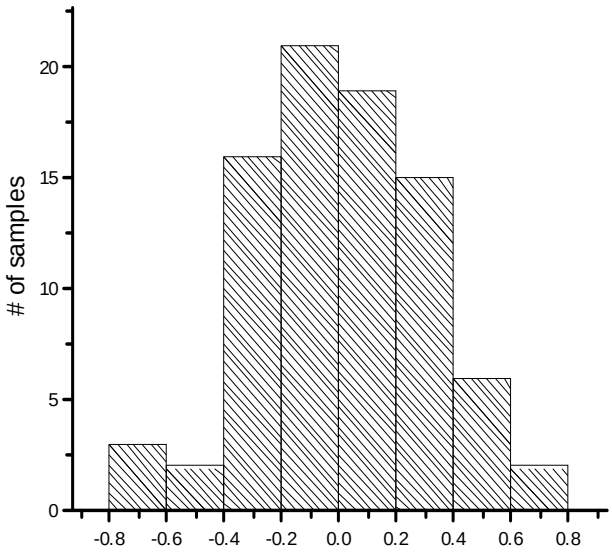

Figure 3-3. $^{234}Th_{measured}$ - $^{234}Th_{avg}$ for depths > 5cm.

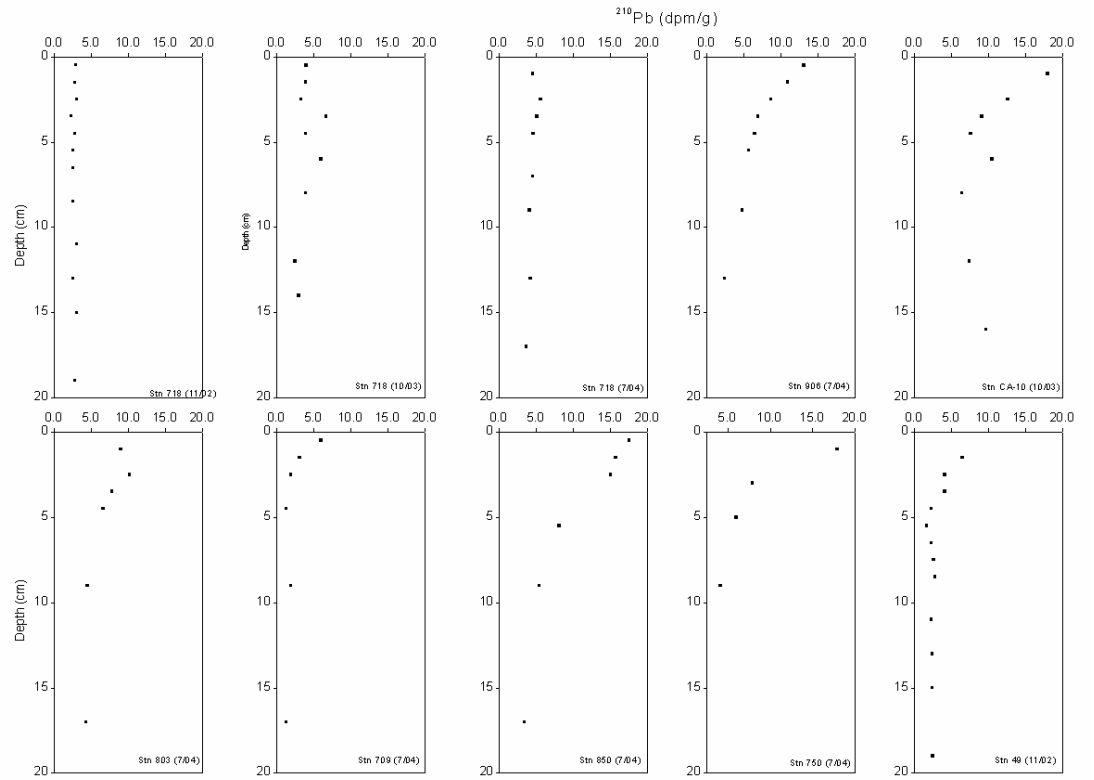

Figure 3-4a. ^{210}Pb profiles in sediments from western locations.

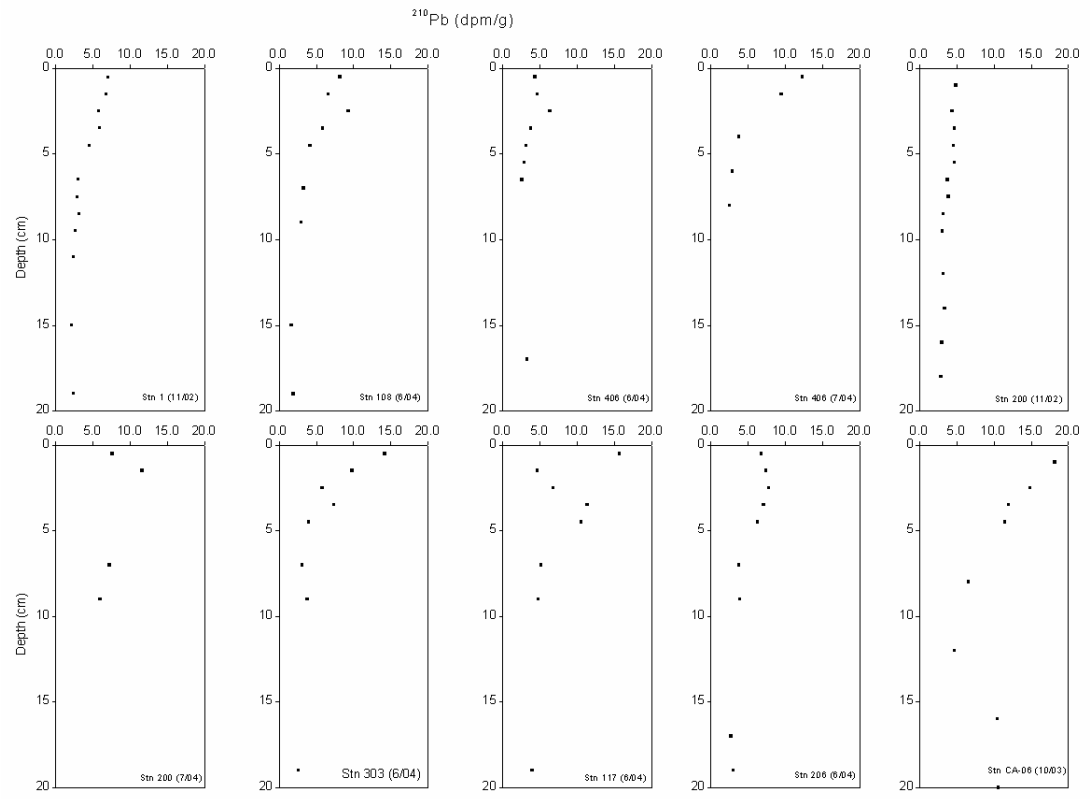

Figure 3-4b. ^{210}Pb profiles in sediments from eastern locations.

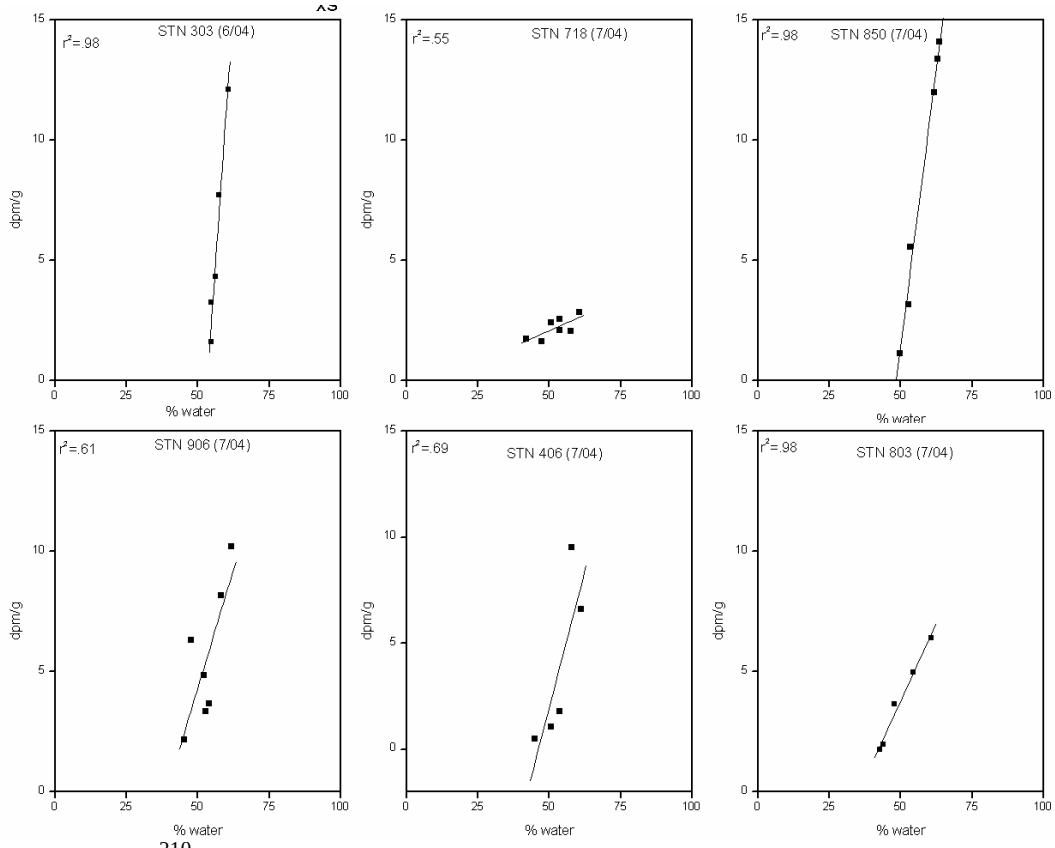

Figure 3-5. ^{210}Pbxs vs % water for selected sites.

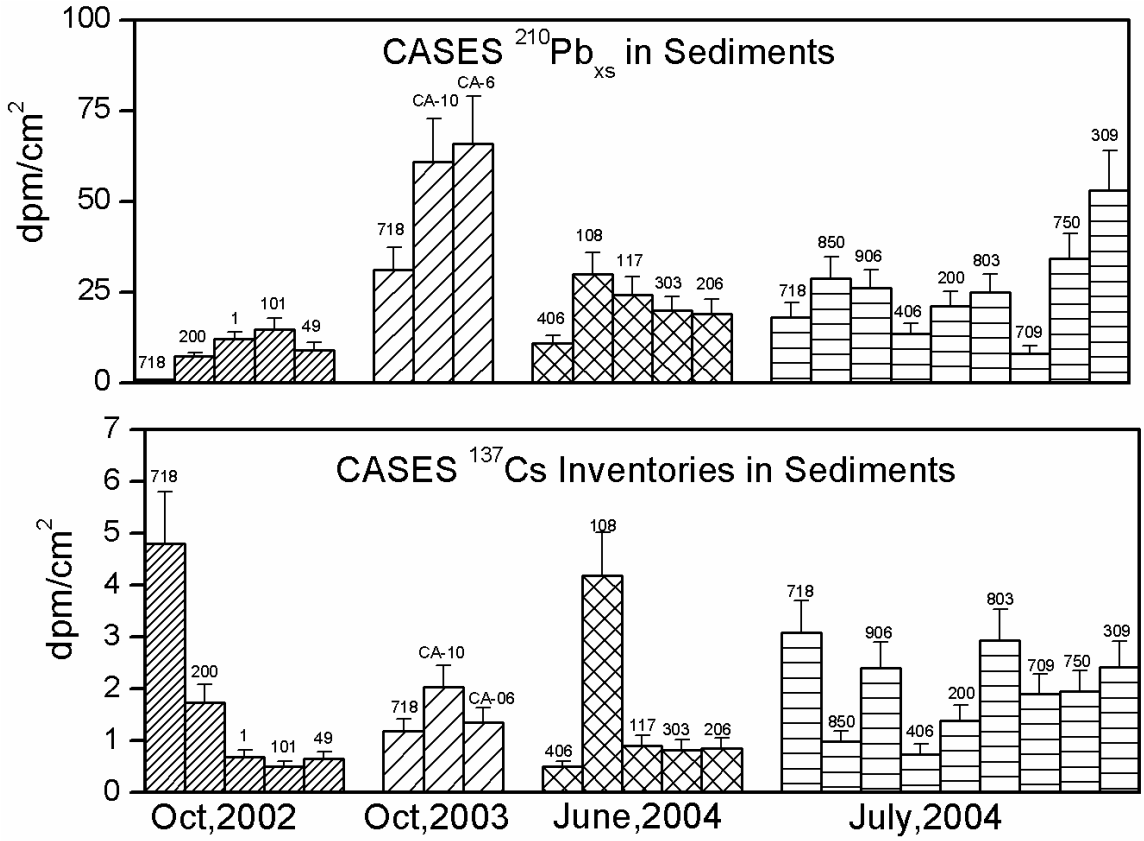

Figure 3-6. $^{210}Pb_{xs}$ and ^{137}Cs inventories in sediments.

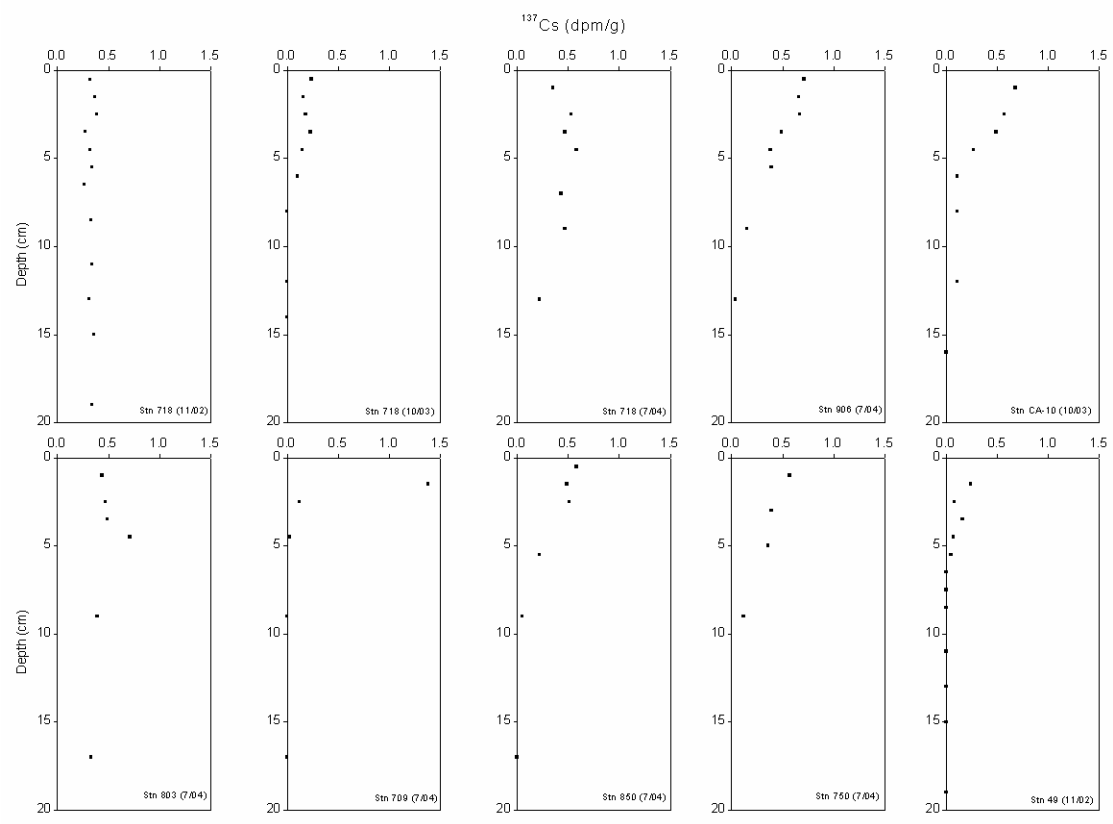

Figure 3-7a. ^{137}Cs profiles in sediments from western locations.

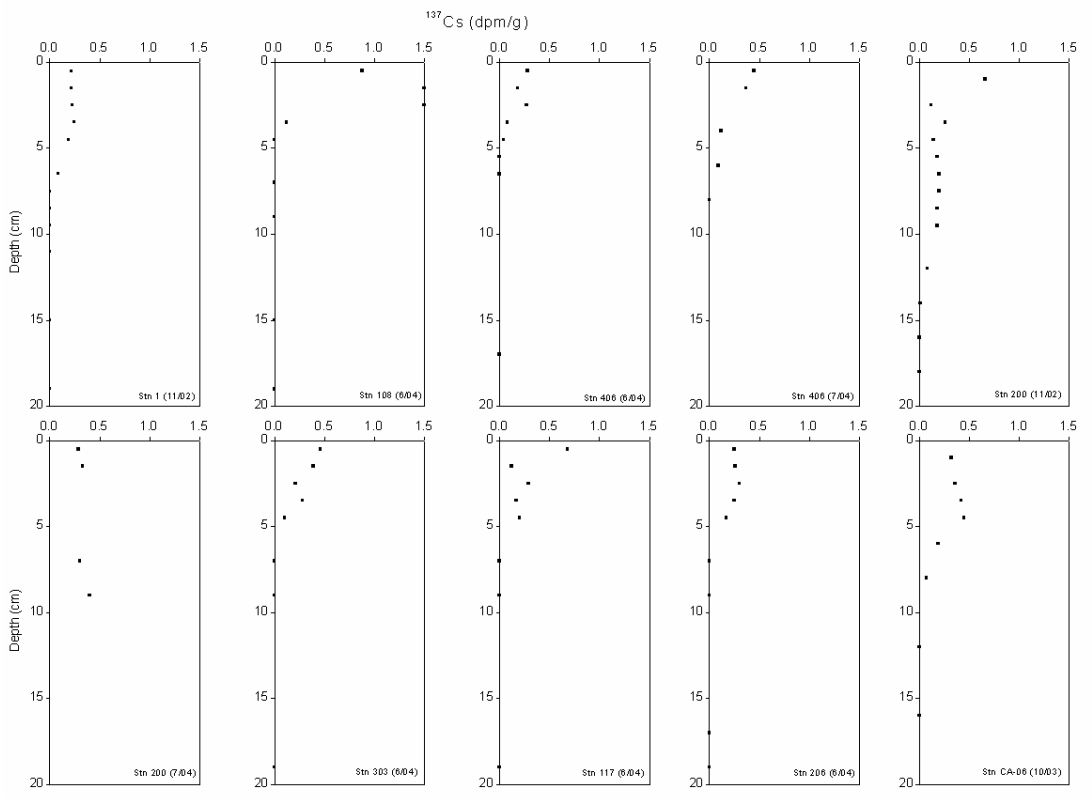

Figure 3-7b. ^{137}Cs profiles in sediments from eastern locations.

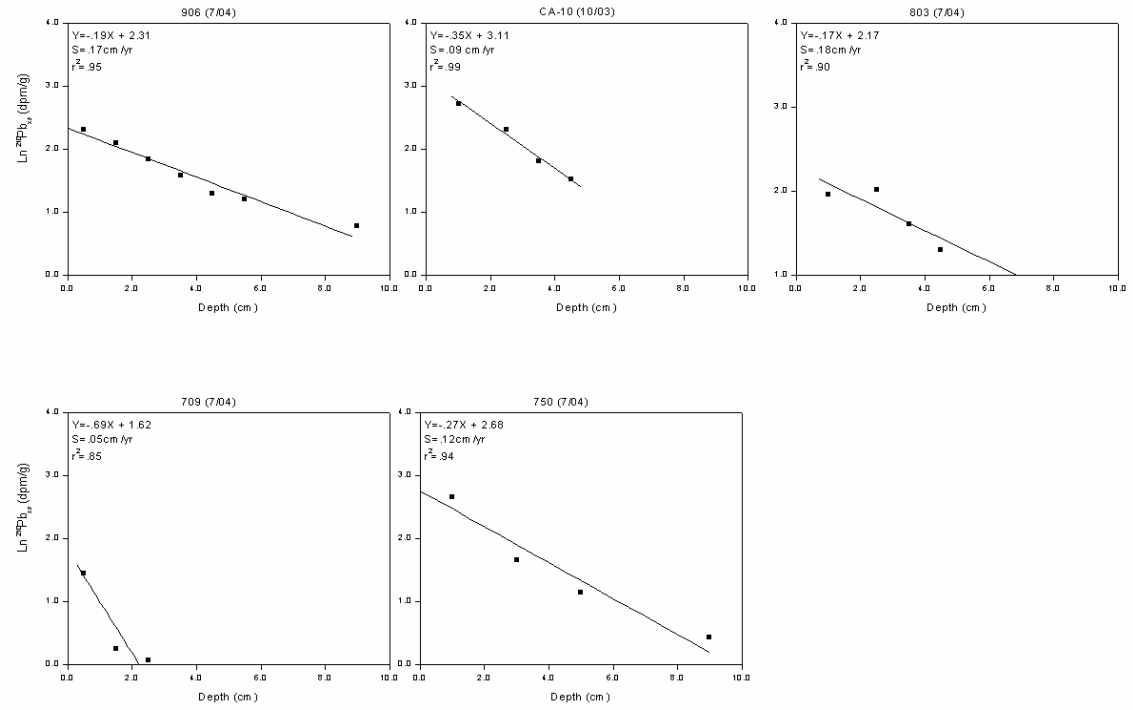

Figure 3-8a. Sedimentation rates in western areas derived from $^{210}Pb_{xs}$ in sediments.

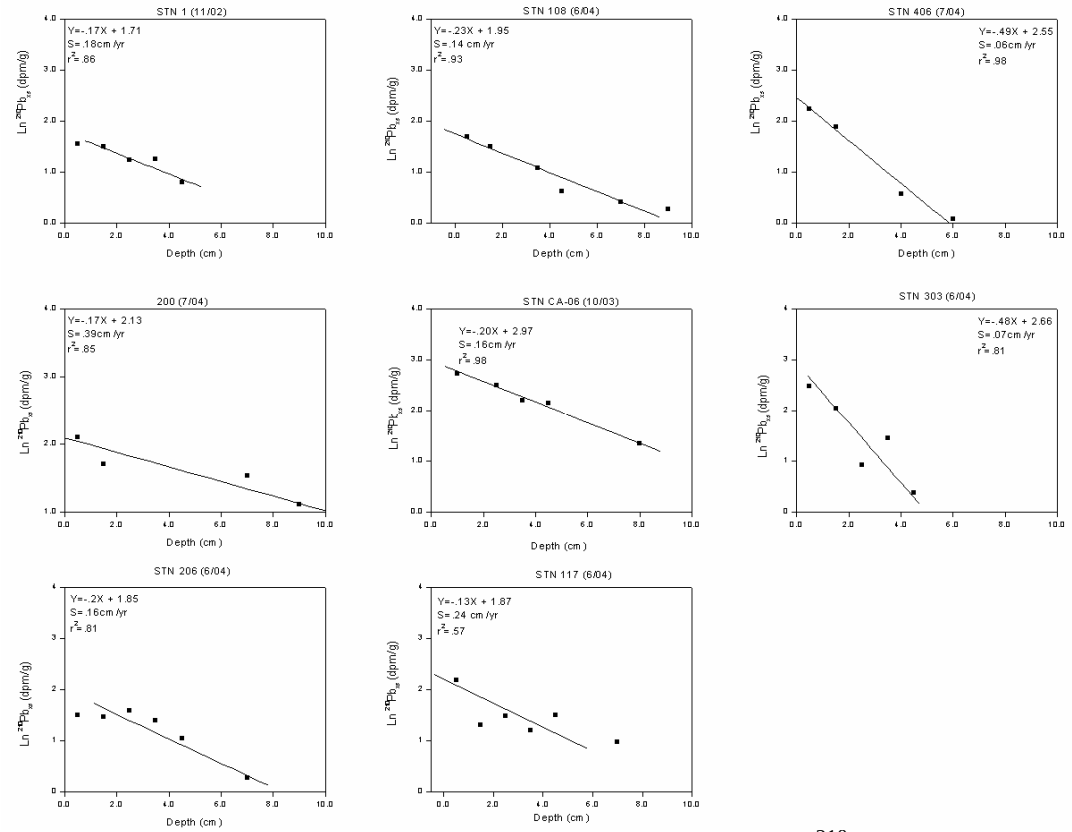

Figure 3-8b. Sedimentation rates in eastern areas derived from $^{210}Pb_{xs}$ in sediments.

REFERENCES

Baskaran, M., Naidu, A.S., 1995. ^{210}Pb-derived chronology and the fluxes of ^{210}Pb and ^{137}Cs isotopes into continental shelf sediments, East Chukchi Sea, Alaskan Arctic. *Geochimica et Cosmochimica Acta 59. 4435-4448.*

Benninger, L.K., Aller, R.C., Cochran, J.K., Turekian, K.K., 1979. Effects of biological sediment mixing on the ^{210}Pb chronology and trace metal distribution in a Long Island Sound sediment core. *Earth and Planetary Science Letters* 43. 241-259

Carpenter, R., Bennet, J.T., Peterson, M.L., 1981. ^{210}Pb activities and fluxes to sediments of the Washington continental slope and shelf. *Geochimica et Cosmochimica Acta* 45. 1155-1172.

Carmack, E.C., Macdonald, R.W., 2002. Oceanography of the Canadian Shelf of the Beaufort Sea: a setting for marine life. *Arctic* 55, 29-45.

Cochran, J.K., Hirschberg, D.J., Livingston, H.D., Buesseler,K.O., Key, R.M., 1995. Natural and anthropogenic radionuclide distributions in the Nansen Basin, Arctic Ocean: Scavenging rates and circulation timescales. *Deep-Sea Research II* 42. 1495-1517.

DeMaster, D.J., Cochran, J.K., 1982. Particle mixing rates in deep-sea sediments determined from excess ^{210}Pb and ^{32}Si profiles. *Earth and Planetary Science Letters* 61. 257-271.
Guinasso, N.L., Schink, D.R., 1975. Quantitative estimates of biological mixing rates in abyssal sediments. *Journal of Geophysical Research* 80. 3032.

Hill, P.R., Blasco, S.M., Harper, J.R, Fissel, D.B., 1991. Sedimentation on the Canadian Beaufort Shelf. *Continental Shelf Research 11. 821-842.*

Krishnaswami, S., Benninger, L.K., Aller, R.C., Von Damm, K.L., 1980. Atmospherically-derived radionuclides as tracers of sediment mixing and accumulation in near-shore marine and lake sediments:evidence from ^{7}Be, ^{210}Pb, ^{239,240}Pu. *Earth and Planetary Science Letters 47. 307-318.*

Lecroart, P., Schmidt, S., Jouanneau J.M., Weber, O., 2005. Be-7 and Th-234 as tracers of sediment mixing on seasonal time scale at the water-sediment interface of the Thau Lagoon. Radioprotection*, Vol. 40, n° Suppl. 1, pages S661-S667*
DOI: 10.1051/radiopro:2005s1-097

Macdonald, R., Solomon, S.M., Cranston, R.E., Welch, H.E., Yunker, M.B., Gobeil, C., 1998. A sediment and organic carbon budget for the Canadian Beaufort Shelf. *Marine Geology*. 144: 255-273.

Nozaki, Y., Cochran, J.K., Turekian, K.K., Keller, G., 1977. Radiocarbon and 210Pb distributions in submersible-taken deep-sea cores from project FAMOUS. *Earth and Planetary Science Letters* 34. 167.

O'Brien, M.C., R. W. Macdonald, H. Melling, and K. Iseki (2006) Particle fluxes and geochemistry on the Canadian Beaufort Shelf: implications for sediment transport and deposition. *Continental Shelf Research* 26: 41-81

Roberts, K.A., Cochran, J.K., Barnes, C., 1996. 210Pb and 239,240Pu in the Northeast Water Polynya, Greenland:particle dynamics and sediment mixing rates. *Journal of Marine Systems* 10. 401-413.

Turekian, K.K., Cochran, J.K., 1978. Determination of marine chronologies using natural radionuclides. In: Chemical Oceanography, vol 7. J.P and R,Chester, Eds. Acadmeic Press, New York.

Chapter 4. Cycling and fluxes of particulate organic carbon on the Mackenzie Shelf

INTRODUCTION

One outstanding issue in Arctic ecosystems is the degree to which organic matter is recycled in the euphotic zone and twilight zones. The Arctic has been shown to have high concentrations of DOC in both deep and surface waters compared to other oceans (Wheeler et al. 1997). One explanation for this has been that low temperatures adversely affect bacterial activity (Pomeroy et al. 1991). On the other hand, Huston et al. (2002) found high bacterial activities on aggregates recovered from floating sediment traps from the North Water Polynya. Also in the North Water, a comparison between POC fluxes < 100 m with POC fluxes > 200 m showed 5-10 fold attenuations in the 500 m deep basin providing further evidence that flux attenuations due to bacterial decomposition at higher latitudes may be similar to those from lower ones (Hargrave et al. 2002, Amiel et al. 2002, Suess et al. 1980). Moored traps however, deployed 50 m above bottom in the North Water, registered higher mass fluxes compared to the >200 m ones; an unusual finding that was explained by lateral effects and particle rebound (Hargrave et al. 2002).

This chapter focuses on carbon cycling on the Mackenzie Shelf (that includes the Cape Bathurst Polynya). Unlike the North Water Polynya, measuring the fluxes of autochthonous POC is complicated by the large inputs of terrestrial organic carbon from the Mackenzie River. The approach taken here is to use stable carbon isotopes to distinguish between marine terrestrial POC. This data is combined with ^{234}Th fluxes (Chapter 2) to resolve marine and terrestrial carbon fluxes. Separation of marine from terrestrial POC is accomplished using δ^{13}C values on > 70 μm particles collected from in situ pumps (details are provided in Chapter 2).

Thus, my objectives are to:

- Extend the application of ^{234}Th-derived POC fluxes to include a river-dominated shelf setting that includes both marine and terrestrial components.
- Compare POC export from the euphotic zone with POC fluxes deposited at the sediment-water interfaces and buried.

METHODS

Sampling

Water samples were collected during June and July, 2004 aboard the C.C.G.S Amundsen (Fig. 4-1). For purposes of comparison, we partition the study region into two areas: eastern (Cape Bathurst Polynya and Amundsen Gulf: Stns 406, 303, 200, 117, 124, 309, 206,108) and western (Mackenzie

inner and outer shelf: Stns 906, 803, 709, 718). These two areas were sampled in June and July, 2004 respectively. This choice of partitioning is more general than the more finely resolved regions defined in Chapter 2 data since the Th data presented in Chapter 2 were collected from four legs while this Chapter highlights data from only two legs. Details on collection of samples from the water column are given in Chapter 2.

Thorium

Details for sampling and analysis for ^{234}Th are given in Chapter 2. In this section, ^{234}Th fluxes obtained from ^{234}Th profiles are used to calculate POC fluxes (see equation 1).

POC analyses

In situ pumps were used to filter particles in 1-70 and > 70 μm size fractions (see Chapter 2 for details). Subsamples from these size fractions were taken with a 1 cm diameter punch. These were exposed overnight to concentrated HCl fumes to dissolve any calcium carbonate. The subsamples were run on a Carlos Erba CHN Analyzer for carbon and nitrogen, scaled to the total area of the filters, and divided by the volume passed through the pumps to obtain POC concentrations in units of μM. Twenty replicate subsamples, ten each to estimate precision, from the 1-70 μm and > 70 μm size fractions were analyzed. The >70 μm samples had precisions of ± 10 % for C and ± 25 % for N. The 1-70 μm samples had precisions of ± 7 and 10 % for C and N respectively. The larger errors associated with the > 70 μm set are most likely attributed to the combination of lesser sample size and inhomogeneous distribution of POC on the filter.

δ^{13}C *analyses*

A six-loop glass trap was fitted to the outflow of a Carlos-Erba CHN Analyzer to trap CO_2 gas generated from the combustion of carbon in the 1-70 and >70 μm filter samples. The CO_2 in the trap was then sealed and manually transported to a gas collection line. Once on the line, the gas from the trap was transferred to a manometer to evaluate the size of the sample, and to insure that no leaks were present during collection from the CHN analyzer. This latter objective was achieved by plotting the area of the carbon peak generated from the CHN versus the manometer reading (Fig. 4-2). If leaks had occurred during collection from the CHN, this would result in values that fall below the 1:1 line. That such a good correlation was obtained (r^2= .95; Fig. 4-2) suggests that the CO_2 collected from the CHN was transferred efficiently to the manometer. Samples were then transferred to a sample bottle and run on a Finnegan Delta Plus Mass Spectrometer to obtain δ^{13}C values. A reference standard (8539:NBS22.Oil) calibrated against VPDB was obtained from the National Institute Standards and Technology, and analysis yielded an accuracy of ± 0.1 ‰. Also, an internal δ^{13}C standard was created using ground peach leaves. Three replicates from this internal standard had a precision of ± 0.3 per mil.

Sediments

Details concerning the calculation of dry bulk density, sediment accumulation rates, sediment community O_2 demand, sediment organic carbon (SOC), and sediment $\delta^{13}C$ values are given in Chapter 3. Briefly, dry bulk density was calculated from water content (see Chapter 3 for formula). Sediment accumulation rates were obtained from ^{210}Pb inventories from dried sediments that were gamma counted on a planar intrinsic Germanium detector. Carbon content (μmol C/ g dry sed) was obtained by treating a few milligrams of sediment with fuming HCl in a dessicator (to remove inorganic carbon) and then run on a CHN analyzer. The CO_2 gas emitted from the CHN was collected and run on a Finnegan Delta Plus Mass Spec to obtain $\delta^{13}C$ values in 1 and 2 cm layers of sediment. Details on estimation of sediment community oxygen demand are given in Renaud et al. (In Press).

RESULTS

1-70 μm POC distributions from June and July, 2004

POC profiles from the 1-70 μm filterable fraction generally displayed high values at the surface with decreases to 100 m (Stn's 906, 108, 117, 124, 406, 200, 206; Fig. 4- 3). One profile from the 1-70 μm fraction showed a maximum at 50 m (station 406, July) while the profile obtained from station 803 was invariant with depth. Still another profile (station 117) showed increases towards bottom. Average concentrations from all the stations 0-50 m were 66 ± 40 μM and no clear geographic variation was discernable.

>70 μm POC distributions from June and July, 2004

Decreases with depth were less apparent for this size fraction compared to the 1-70 μm data although attenuations were evident in a few of the profiles (Fig. 4-4). In some profiles, a maximum at ~ 50 m was observed (Stn's 200, 406, 303; Fig. 4-4). Average POC concentrations in the 0-50 m depth interval between western and eastern areas were 6.5 ± 2.5, 2.4 ± 2.4 μM, respectively.

$\delta^{13}C$ profiles in 1-70 and > 70 μm size fractions

The range in $\delta^{13}C$ for all the samples was –24.3 to –28.5 ‰ (Fig. 4-5). The 1-70 and > 70 μm size fractions had averages from all depths of –26.7 ± 1.0 ‰. Despite this, two stations from the Cape Bathurst Polynya region (303, 309) had $\delta^{13}C$ values in the > 70 μm size fraction that were consistently heavier than the 1-70 μm one. Stations from Cape Bathurst and Amundsen Gulf areas often had $\delta^{13}C$ values at 100 m that were heavier than those at 50 m.

Sampling at stations 117, 718, 906, 206, and 200 extended to within 50 m of the bottom. The deepest, station 117, had $\delta^{13}C$ values in the 1-70 μm, and > 70 μm size fractions that became heavier to ~ 200 m, and then lighter towards bottom. Spatial gradients between east (stns 108, 206, 117,124, 303, 309, 406) and west (stns 718, 709, 906, 803) were not evident in the1-70 μm $\delta^{13}C$ values (-27.4 ± 0.9 ‰, -27.3 ± 0.5 ‰, from all depths, east and west respectively) but were discernable in the > 70 μm size fraction (-26.3 ± 0.5 ‰, -27.1 ± 0.4 ‰, east and west respectively), but the values are essentially the same within errors.

DISCUSSION

Application of ^{234}Th, $\delta^{13}C$, and POC:Th ratios to obtain Marine and terrestrial POC fluxes

To estimate POC fluxes, we begin by using Th deficits in the upper 100 m (Chapter 2). ^{234}Th fluxes calculated using a one dimension model assume invariance in Th profiles over time (steady state) and neglect diffusive and lateral effects. To evaluate lateral effects, Chapter 2 presented data on pump and floating trap Th fluxes, as well as comparison of sediment Th_{xs} inventories with water column Th deficits. These results were interpreted as a crude estimate of lateral effects that were estimated to contribute ~ a factor of 2 to ^{234}Th fluxes estimated without including them. Moreover, steady state ^{234}Th fluxes showed values that were within a factor of 2 of non-steady state ones at stations where this could be evaluated. These results suggest that the assumption of steady state and lateral effects contribute not more than a factor of ~ 4 to ^{234}Th flux estimates derived from the simple box model.

POC fluxes are classically derived from ^{234}Th fluxes as (see Buesseler et al. 1992):

$$F_{POC} = (POC/Th)P_{Th} \quad (1)$$

Where F_{POC} is the flux of POC (mmol C m^{-2} d^{-1}), POC/Th is the ratio of POC:Th (μmolC dpm^{-1}) from the >70 μm size fraction at 100m, and P_{Th} is the ^{234}Th flux at 100 m (dpm m^{-2} d^{-1}). However, the Mackenzie Shelf has terrestrial as well as marine carbon sources and equation (1) must be modified.

To account for both terrestrial and marine carbon sources, $\delta^{13}C$ values from the > 70 μm size fraction were used to discriminate between marine and terrestrial carbon sources. Equation (1) was modified to:

$$F_{POC} = (POC/Th)P_{Th} * f_{Mar} (or \quad f_{Terr}) \quad (2)$$

where f_{mar} and f_{terr} are the fraction of marine and terrestrial carbon respectively.

Calculation of $f_{mar, terr}$ values

The fraction of marine or terrestrial carbon in the > 70 μm samples are derived from a two end-member, linear mixing model (Hedges et al. 1988). The conceptual basis for this model is that, although C^{13}/C^{12} ratios do not mix linearly, differences in $\delta^{13}C$ between marine and terrestrial POC are small and can thus be represented by a straight line obtained by linear interpolation between two measured end members (see et al. 2000). This mixing equation is:

$$f_{Terr} = \frac{\delta^{13}C_{TOC} - \delta^{13}C_{MAR}}{\delta^{13}C_{TERR} - \delta^{13}C_{MAR}} \quad (3)$$

where f_{terr} is the mass fraction of terrestrial carbon (thus, f_{mar} =1-f_{terr}), $\delta^{13}C_{TERR}$, $_{MAR}$ are marine and terrestrial end-members, and $\delta^{13}C_{TOC}$ are measured $\delta^{13}C$ values obtained from the >70 μm size fraction. The utility of the model is governed by the precision to which end-members are constrained and the degree to which they remain constant over the sampling period (et al. 2000). Literature values for these end-members are -18.0 to-22.0 ‰ and -28.0 to -24.0 ‰, for $\delta^{13}C_{MAR}$ and $\delta^{13}C_{TERR}$ respectively (Goericke and Frye, 1994 and

references therein). The terrestrial value assumes the presence of only C3 plants. This is justified in the present situation because the Mackenzie River watershed is not characterized by grasses that follow the C4 metabolic pathway due to temperature inhibition (et al. 2000).

Sampling up river also afforded the opportunity to measure $\delta^{13}C_{TERR.}$ Samples from up- river surficial sediments yielded a value of -27.2 ± 0.1 ‰. However, some filter samples had even lighter values (e.g. stn 803, 25, 50 m; Fig. 4-5) suggesting lighter values could be found that also have a river provenance. For purposes of calculation, we chose a value of -28.0 ‰ for $\delta^{13}C$ of terrestrial carbon (see sensitivity analysis described below).

$\delta^{13}C_{MAR}$ is more difficult to constrain due to the fact that the marine end-member is not clearly observed in the samples collected. Gõni et al. (2000) correlated $\delta^{13}C_{TOC}$ versus various biomarkers (at sites that extended only to the 30 m isobath) and these yielded $\delta^{13}C_{MAR}$ estimates that had a large range (-19.0 to -24.5 ‰). Through various simplifications, a value of -21.4 ‰ for $\delta^{13}C_{MAR}$ was settled upon by Gõni et al. (2000). From our data, $\delta^{13}C$ values from surficial sediments at sites along a 1000 m isobath (and ~ 200 km from the Mackenzie River mouth) from a northern transect (stns 850, 750) and from the far eastern Amundsen Gulf (stn 108) yielded a value of -24.9 ± 0.2 ‰. In the following flux estimations we use the value of -21.4 ‰ obtained by Gõni et al. (2000). We argue that although sampling did not occur far enough out on the shelf to reach a purely marine isotopic signature, there is no evidence from the literature for an unusual $\delta^{13}C$ of marine particulate organic carbon at high latitudes compared to lower ones. Thus, the "true" $\delta^{13}C$ signature of marine organic carbon likely lies within the range -19.0 to -22.0 ‰. The implication regarding this choice of $\delta^{13}C_{MAR}$, is that, as one proceeds far enough out into the Arctic Ocean, a completely marine $\delta^{13}C$ imprint is likely present. The sensitivity of equation (3) to changing the $\delta^{13}C$ marine and terrestrial end-members is such that for each $\delta^{13}C$ change of 0.5 ‰, f changes by 10 %. This can be compared to the uncertainty of individual $\delta^{13}C$ values of ~ ± 0.3 ‰ (Fig. 4-5).

The range of f_{MAR} determined from all samples is 0.01-.6 indicating that no more than 60 % of the POC in the > 70 μm fraction is of marine provenance throughout the entire study region (Fig. 4-6). It is furthermore clear that higher f-mar values are found in eastern regions that are further away from the terrestrial carbon source. This is reasonable in that the Mackenzie River strongly influences western samples.

Profiles of the fraction of marine POC in the > 70 μm fraction divide into those that exhibit C-shapes with depth (stns 108, and 406 June, most pronouncedly) and those that are invariant and low (stns 709, 906, 803). This dichotomy is again a reflection of distance from the terrestrial carbon source, as well as proximity to the bottom. Profiles in June from Cape Bathurst and Amundsen Gulf had f_{MAR} values in the 50 to 100 m depth range that showed increases with depth, while no trend was observed in stations near the Mackenzie.

(POC:Th)$_{MAR}$ ratios

Values of (POC:Th)$_{MAR}$ are calculated by multiplying the POC:Th ratios determined from the > 70 μm size fraction by f_{MAR} (Fig. 4-7). Typically, the range in (POC:Th)$_{MAR}$ from other environments in the 0-100 m depth range lies between 0-100 μmol/dpm (Amiel et al. unpublished, 2002, Buesseler et al. 1992, Cochran et al. 2000). Average 0-100 m values of (POC:Th)$_{MAR}$ throughout the CASES region were 46.0 μmol/dpm. Consistent with other data sets, profiles generally showed relatively high values near the surface with decreases below ~ 30 m. In contrast, stn 803 (situated near the river), had little or no marine signature to its POC:Th ratios (Fig. 4-7). In the Cape Bathurst Polynya, at stn 303 where the CTD fluorometer recorded maximum values, (POC:Th)$_{MAR}$ ratios were the highest of any station at 25 and 50 m (97, 77 μmol C dpm^{-1}, respectively).

Based on these observations, it is our contention that the ratio of two primary measurements (POC and Th collected from the same sampling method) multiplied by the δ^{13}C-derived weighting factor (f), yields results that are within the range of other data sets, possess expected gradients in POC:Th$_{MAR}$ that attenuate away from the river, and show trends with depth similar to those found in other environments. In other words, estimation of (POC:Th)$_{MAR}$ values results in horizontal and vertical patterns that are quite reasonable.

POC Fluxes

Equation (2) was applied to obtain marine and terrestrial POC fluxes from June and July, 2004 (Fig. 4-8). Depths of 50 and 100 m were chosen as reference depths primarily for purposes of comparison with other data sets. Frequently, the base of the euphotic zone is used to estimate POC export from ^{234}Th profiles however these were often in the 20-30 m range due to turbidity generated from the Mackenzie River plume (Yves Gratton, personal communication). This depth range is too small to make good use of the data (resolution of the profiles would be comprised of only 2-3 points instead of 5-7), and thus 50 m was chosen to estimate POC export. Since two of the three terms (POC:Th, f) in the flux equation might increase or decrease between a shallower euphotic zone and 50 m, it is not evident how the choice of 50 m used to obtain carbon export fluxes compares to carbon export at the base of the euphotic zone. In any event, we assume the difference is small and would not affect relative differences between stations although under or over-estimation of the "true" export-at-the-base-of-the-euphotic-zone remains a possibility.

Fluxes of POC_{MAR} from Cape Bathurst and Amundsen Gulf (all in June, 2004) averaged 3.7 ± 1.4 and 10.5 ± 13 mmol C m^{-2} d^{-1} at 50 and 100 m respectively (errors are standard deviations of fluxes from individual stations). In July, 2004 POC_{MAR} fluxes were 11.5 ± 1.1 and 4.3 ± 1.8 mmol C m^{-2} d^{-1} at 50 and 100 m respectively, from the Cape Bathurst Polynya (Fig. 4-8). Fluxes of POC_{TERR} from Cape Bathurst and Amundsen Gulf in June, 2004 were 29 ± 22 and 22 ± 14 mmol C m^{-2} d^{-1} at 50 and 100 m, respectively. In July from Cape Bathurst, POC_{TERR} fluxes were 50 ± 21 and 22 ± 3 mmol C m^{-2} d^{-1} at 50

and 100 m, respectively. On the Mackenzie Shelf, POC_{MAR} fluxes averaged 12.5 ± 12 and 10.4 ± 9 mmol C m^{-2} d^{-1} at 50 and 100 m, respectively. POC_{TERR} fluxes on the Mackenzie Shelf were 144 ± 25 and 132 ± 12 at 50 and 100 m respectively (stations 803, 709, 906 from July). Station 200, situated between Cape Bathurst and the Mackenzie Shelf registered a similarly large POC_{TERR} flux as the Mackenzie Shelf at 50 m (180 mmol C m^{-2} $d^{-}1$) but was closer to the Cape Bathurst value at 100 m (32 mmol C m^{-2} d^{-1}).

Neglecting the contribution of other POC_{TERR} sources (continental denudation, aolian transport) that are most likely much smaller than the Mackenzie River, POC_{TERR} fluxes are roughly correlated with the Mackenzie River plume and in June in the Cape Bathurst Polynya are ~ 20 % of those from the Mackenzie Shelf. This percentage increases to ~ 33 % in July. Seasonality is also apparent in 50 m fluxes of POC_{MAR} from Cape Bathurst that increase roughly 2-fold between June and July. Surprisingly, POC_{MAR} fluxes on the Mackenzie Shelf are comparable to those from Cape Bathurst in July.

Overall our data show that POC_{TERR} is substantially larger than POC_{MAR} by factors ~2-5 (Exceptions are stations 108 and 303, Fig. 4-8). Furthermore, the ratio of POC_{MAR}:POC_{TERR} fluxes decreases from 73 ± 43 in June to 24 ± 9 in July indicating larger contributions of POC_{TERR} to overall POC fluxes between June and July. This view of significantly larger terrestrial POC fluxes than marine ones is in contradistinction to the data presented by O'Brien et al. (2006). Using data collected from sediment traps deployed over the year 1987-88, these authors used the POC/Al ratio to distinguish between POC_{TERR} and POC_{MAR} to obtain fluxes for each type of carbon they found (at sites comparable to ours) that in all cases, fluxes of POC_{MAR} were significantly larger than POC_{TERR}, and averaged about 70 % of the total POC flux over an annual cycle (O'Brien et al. 2006). Conspicuously, the late 1980's preceded the warming trend of the 1990's that continues until the present. Indeed the picture of ice retreat, and opening of the flaw lead, though begun in early June 1987, was radically different than for our sampling periods. Between June 8-23, 1987, a massive flaw lead opened that ended from the Mackenzie River to the Amundsen (O'Brien et al. 2006). In contrast, in 2004, a much smaller, localized flaw lead developed near Cape Bathurst (700 km from the Mackenzie River) as a result of easterly winds. O'Brien et al. (2006) also recorded a massive pulse of terrigenous material in the trap deployed in the Mackenzie Trough (~ station 906) that lasted for 40 days and was directly related to the Mackenzie River flow. Despite the large terrestrial source near the Mackenzie Trough, O'Brien et al. (2006) obtained higher POC_{MAR} fluxes at this site, even during the terrestrial pulse of early summer; a result that is quite unexpected given this sites close proximity to the river plume.

In a budget by O'Brien et al. (2006), only ~ 9 % of sediment from the Mackenzie is deposited in eastern regions, consistent with their findings of low POC_{TERR} contributions to overall POC fluxes.

A simple mass balance of POC based on the present study is discussed further in Chapter 5.

Table 4-1. June and July, 2004-POC, PON, POC:Th

STN	m	POC* 1-70 um µMol	PON** 1-70 um µMol	C/N 1-70 um µMol	Th 1-70 um dpm/l	C/Th 1-70 um µMolC/dpm	N/Th 1-70 um µMolC/dpm	POC >70 um µMol	PON >70 um µMol	C/N >70 um	C/Th µMolC/dpm
206	5	38.6	4.7	8.2	0.8	48.2	5.9	1.5	0.1	17.3	144.1
	15	31.3	5.0	6.3	0.8	37.8	6.0	1.1	0.0	25.9	152.8
	50	20.0	4.0	5.0	1.0	20.0	4.0	1.3	0.0	117.8	127.0
	80	10.0	2.0	5.0	1.1	9.5	1.9	1.0	0.0	100.0	100.0
	10	58.0	8.6	6.7	0.2	263.6	39.1	3.0	0.6	5.4	989.6
108	25	24.8	5.4	4.6	0.5	49.6	10.8	0.8	0.0	20.4	70.9
	50	18.4	3.6	5.1	0.9	21.4	4.2	1.0	0.0	28.3	79.8
	75	9.2	2.0	4.6	1.1	8.4	1.8	1.0	nd	nd	55.6
	100	5.0	1.0	5.0	0.9	5.7	1.1	1.0	0.1	0.0	66.7
	200	0.2	0.1	2.0	0.2	1.0	0.5	0.2	nd	nd	66.7
117	5	67.4	2.0	33.7	0.3	246.1	7.3	1.4	0.2	8.1	234.3
	30	40.0	8.0	5.0	0.4	104.7	20.9	0.7	0.1	8.9	83.0
	60	16.0	3.1	5.2	0.9	17.9	3.5	0.5	0.0	78.0	90.9
	100	10.0	2.4	4.2	0.8	12.0	2.9	0.6	0.0	20.9	29.7
	200	9.8	1.1	8.9	1.0	9.7	1.1	0.1	nd	nd	3.7
	300	48.2	4.0	12.0	0.6	84.6	7.1	0.2	0.0	178.9	28.5
124	5	152.0	22.3	6.8	0.5	314.7	46.2	10.5	0.7	15.5	752.4
	10	94.0	18.7	5.0	0.3	313.3	62.3	1.5	0.1	14.5	247.9
	50	32.5	8.3	3.9	0.8	40.1	10.2	2.7	0.0	77.6	456.3
	100	10.0	3.0	3.3	0.9	11.2	3.4	1.2	0.2	6.1	203.2
406	3	122.0	10.5	11.6	0.4	324.5	28.0	3.4	0.3	11.0	378.7
	20	104.0	18.0	5.8	0.3	371.4	64.3	1.4	0.1	19.0	282.6
	50	62.8	8.1	7.8	0.7	84.9	10.9	1.0	0.1	15.2	137.7
	100	20.5	2.5	8.2	0.9	22.8	2.8	0.4	0.2	2.5	38.3
303	5	125.0	17.5	7.1	0.3	416.7	58.3	4.1	0.6	6.6	205.5
	10	nd	nd	nd	0.4	nd	nd	4.7	0.5	10.1	236.0
	30	110.0	19.4	5.7	0.5	215.7	38.0	26.1	3.7	7.1	280.5
	50	42.0	8.6	4.9	1.0	41.2	8.4	0.6	0.0	27.3	36.5
	100	15.9	2.7	5.9	1.0	16.1	2.7	0.1	0.0	132.1	12.6
709	5	57.1	6.3	9.1	0.2	300.5	33.2	4.5	0.5	9.7	150.6
	15	nd	nd	nd	0.2	nd	nd	3.6	0.4	8.8	149.1
	50	11.3	1.6	7.1	0.1	86.9	12.3	3.0	0.4	8.1	100.0
	70	61.9	7.7	8.0	0.7	83.6	10.4	3.4	0.4	8.0	67.6
906	5	130.0	12.2	10.7	0.1	1083.3	101.7	10.8	1.2	9.0	271.0
	25	80.0	7.6	10.5	0.2	400.0	38.2	8.6	0.6	14.4	122.7
	50	86.0	6.8	12.6	0.4	226.3	17.9	7.9	0.6	14.1	98.8
	100	65.4	7.8	8.4	0.8	82.8	9.9	7.1	0.6	11.8	102.3
	5	30.0	5.0	6.0	0.2	125.0	20.8	2.1	0.2	10.5	300.0
912	18	40.0	7.0	5.7	0.3	116.6	20.4	3.1	0.2	15.5	387.2
	25	60.0	8.0	7.5	0.2	262.0	34.9	2.9	0.3	8.5	360.6
803	5	22.7	2.5	9.1	0.1	379.0	41.7	nd	nd	nd	nd
	20	nd	nd	9.5	0.1	426.7	45.0	5.9	0.6	9.8	347.1
	50	25.6	2.7	7.6	0.1	353.6	46.3	7.7	0.6	12.8	163.2

	100	28.3	3.7	7.6	0.7	41.0	5.4	2.2	0.6	3.9	49.1
718	5	118.0	12.0	9.8	0.1	842.9	85.7	71.0	4.1	17.3	606.8
	15	27.6	3.0	9.2	0.2	172.2	18.8	51.0	4.4	11.6	424.8
	25	110.0	3.7	29.7	0.2	733.3	24.7	51.4	6.2	8.3	467.1
200	5	149.0	15.5	9.6	0.4	346.5	36.0	1.0	0.2	5.0	50.0
	25	61.3	8.5	7.2	0.4	142.6	19.8	2.0	0.5	4.3	39.5
	50	50.0	6.0	8.3	0.4	116.3	14.0	6.1	1.6	3.8	304.0
	100	23.2	3.4	6.8	0.9	25.8	3.8	1.8	0.5	3.5	44.5
309	5	72.7	9.0	8.1	1.1	68.6	8.4	1.0	nd	nd	100.0
	50	59.1	16.0	3.7	0.5	116.0	31.4	2.0	nd	nd	200.0
	100	7.9	1.8	4.4	0.6	12.3	2.8	1.0	nd	nd	100.0
406	5	42.0	2.5	16.8	0.6	68.9	4.1	1.0	0.1	10.0	100.0
	50	76.2	9.5	8.0	0.6	133.7	16.7	4.2	0.6	6.9	208.2
	75	19.0	2.7	7.0	0.6	34.5	4.9	1.3	0.9	1.4	65.0
	100	1.6	0.2	8.0	0.7	2.3	0.3	0.5	0.1	5.0	25.0

* Analytical precision =7%

** Analytical precision = 10%

FIGURES

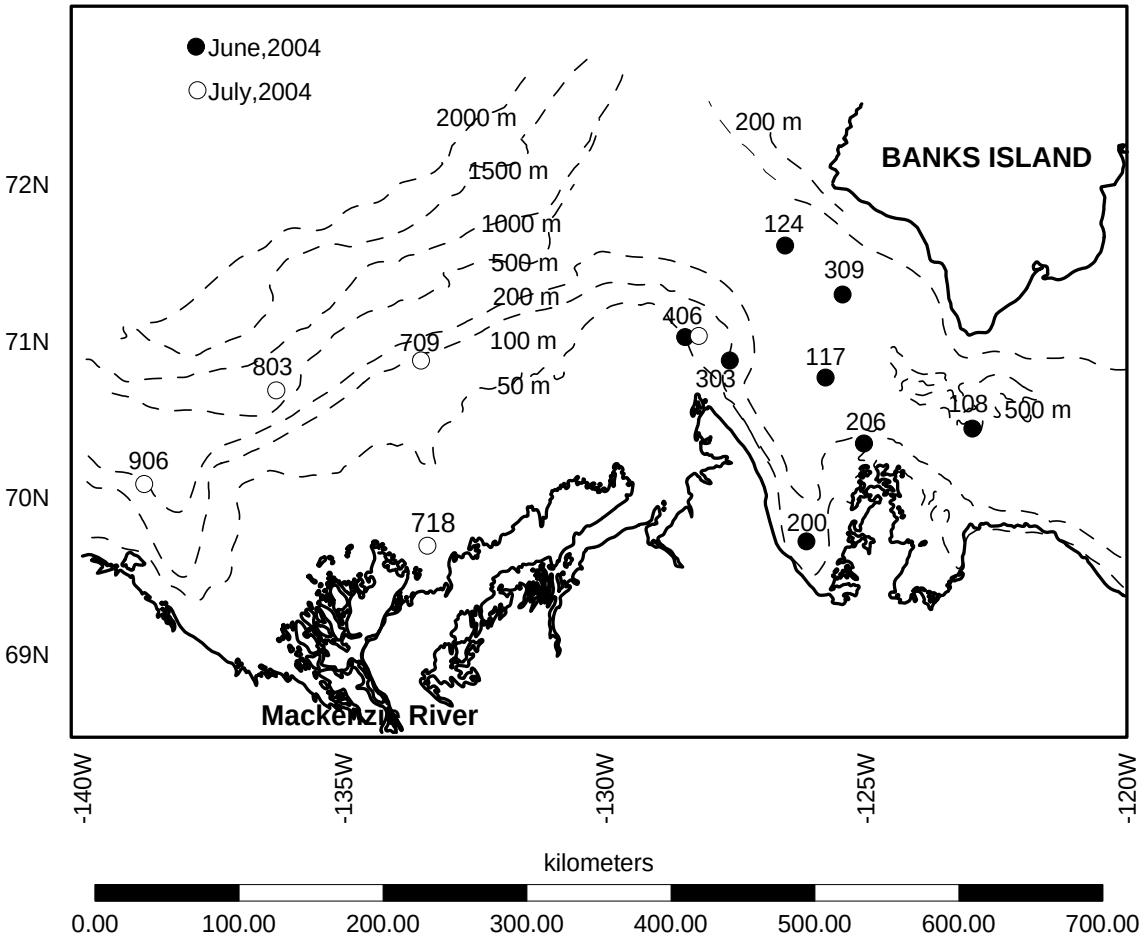

Figure 4-1. Stations where POC fluxes were obtained

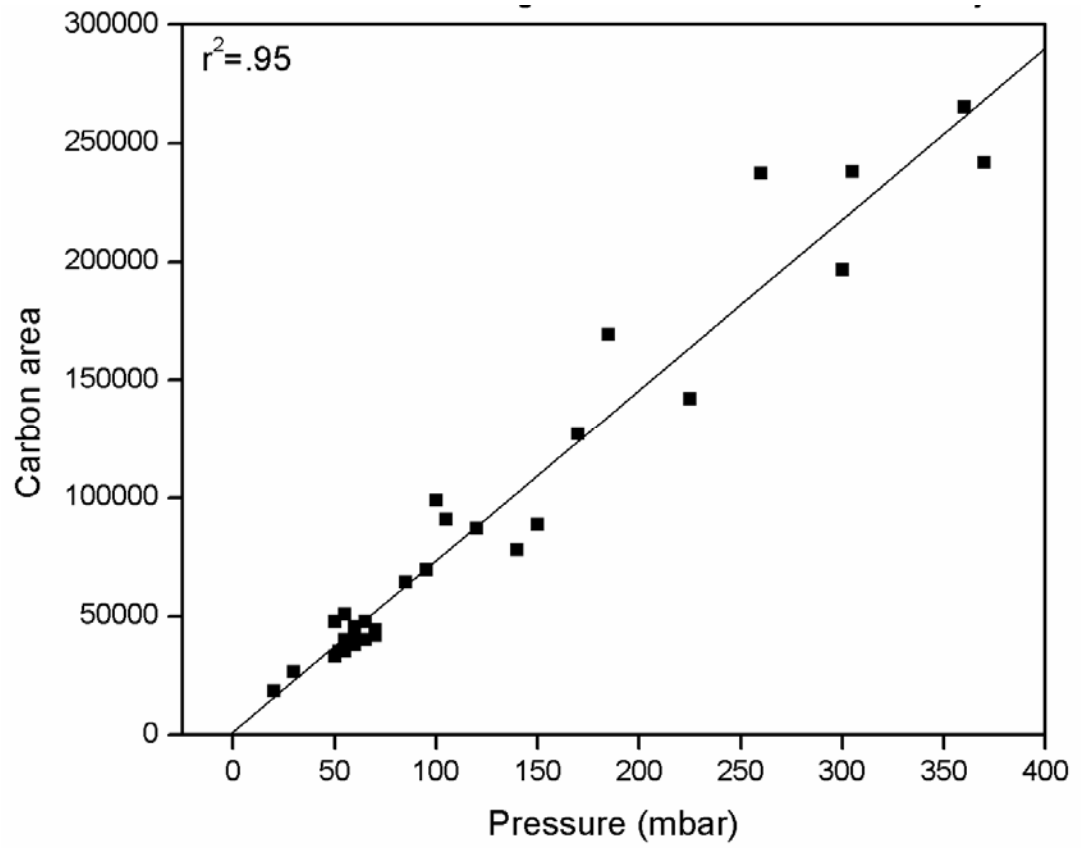

Figure 4-2. Area of carbon from CHN analyzer vs. manometer readings (mbar)

POC (um)

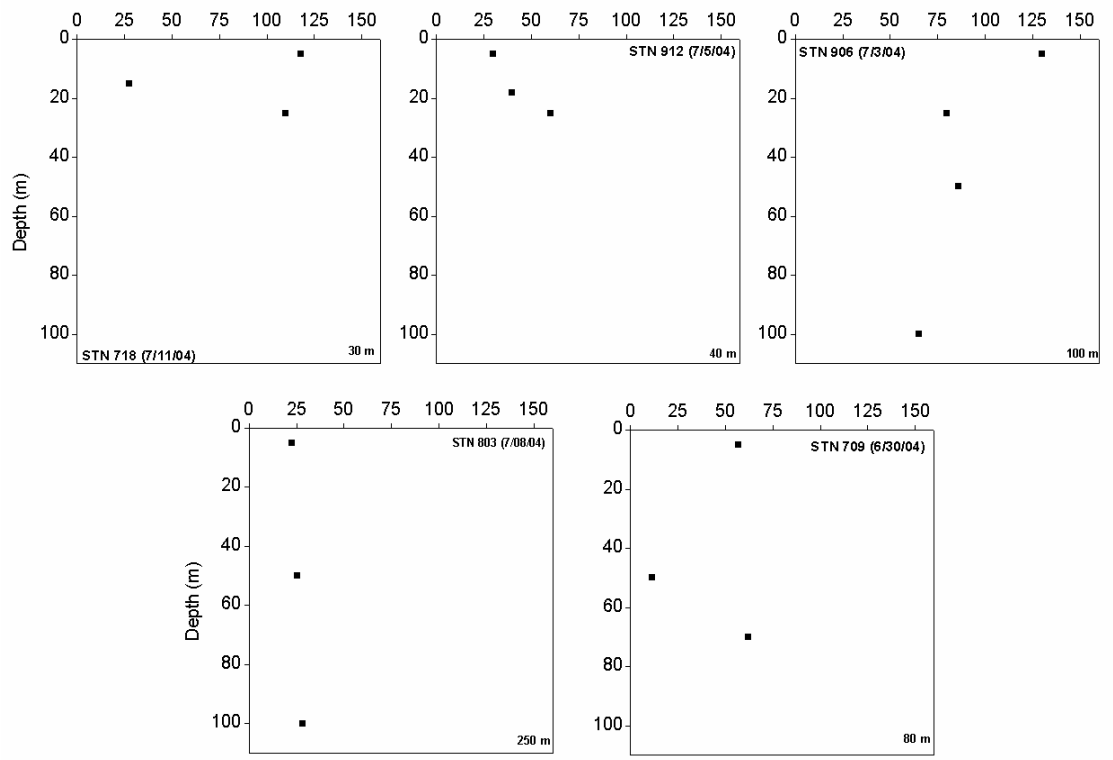

Figure 4-3a. 1-70 um POC profiles from western areas.

POC (um)

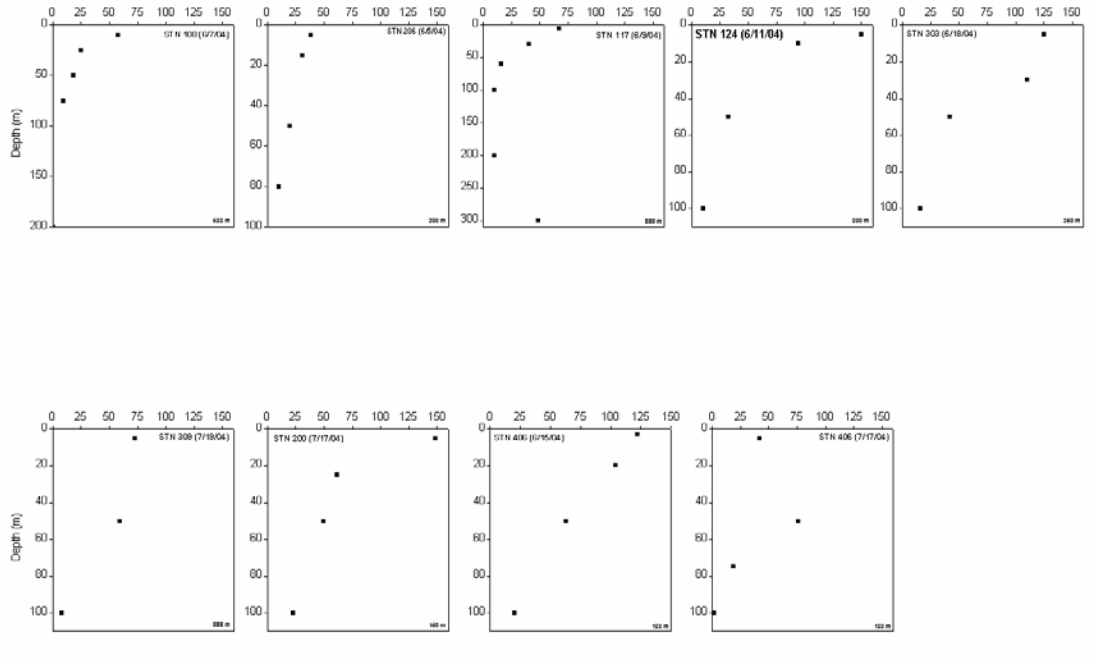

Figure 4-3b. 1-70 um POC profiles from eastern areas.

POC (um)

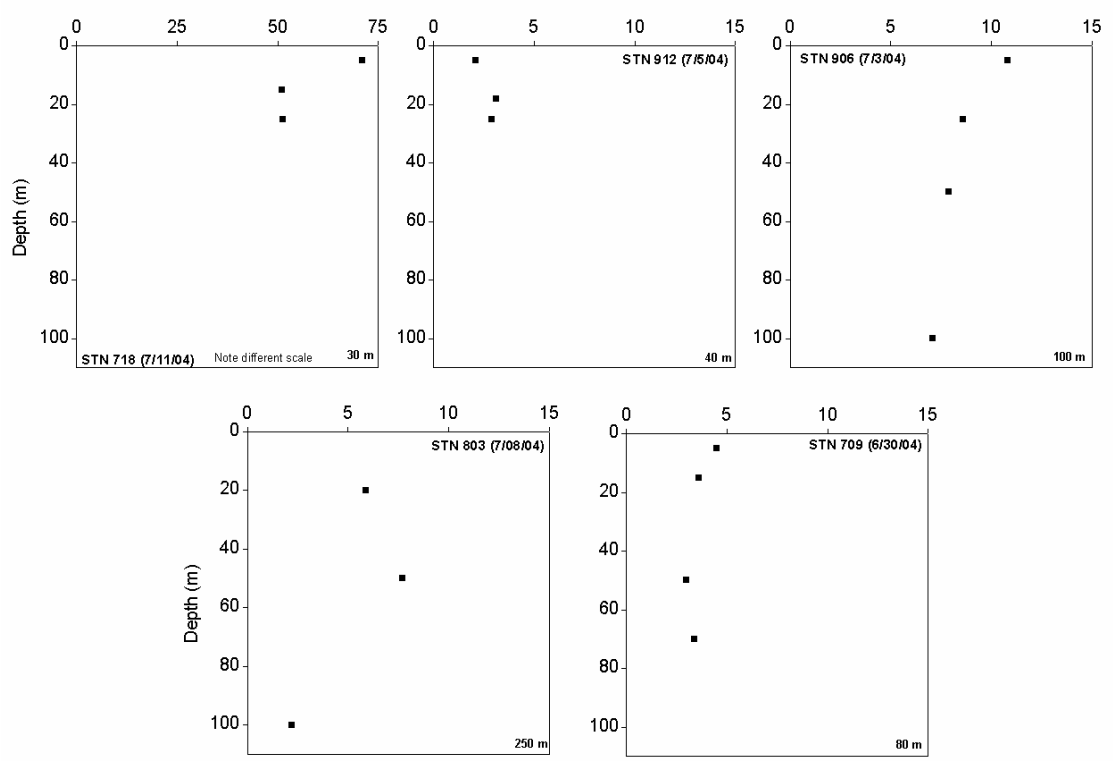

Figure 4-4a. > 70 um POC profiles from western areas.

POC (um)

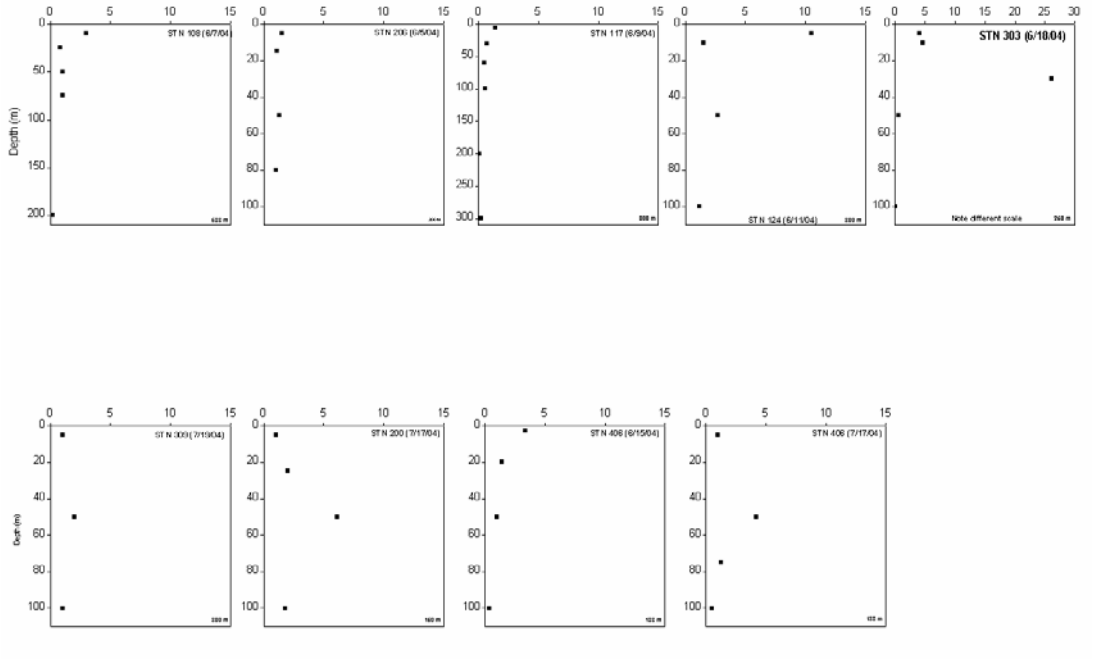

Figure 4-4b. > 70 um POC profiles from western areas.

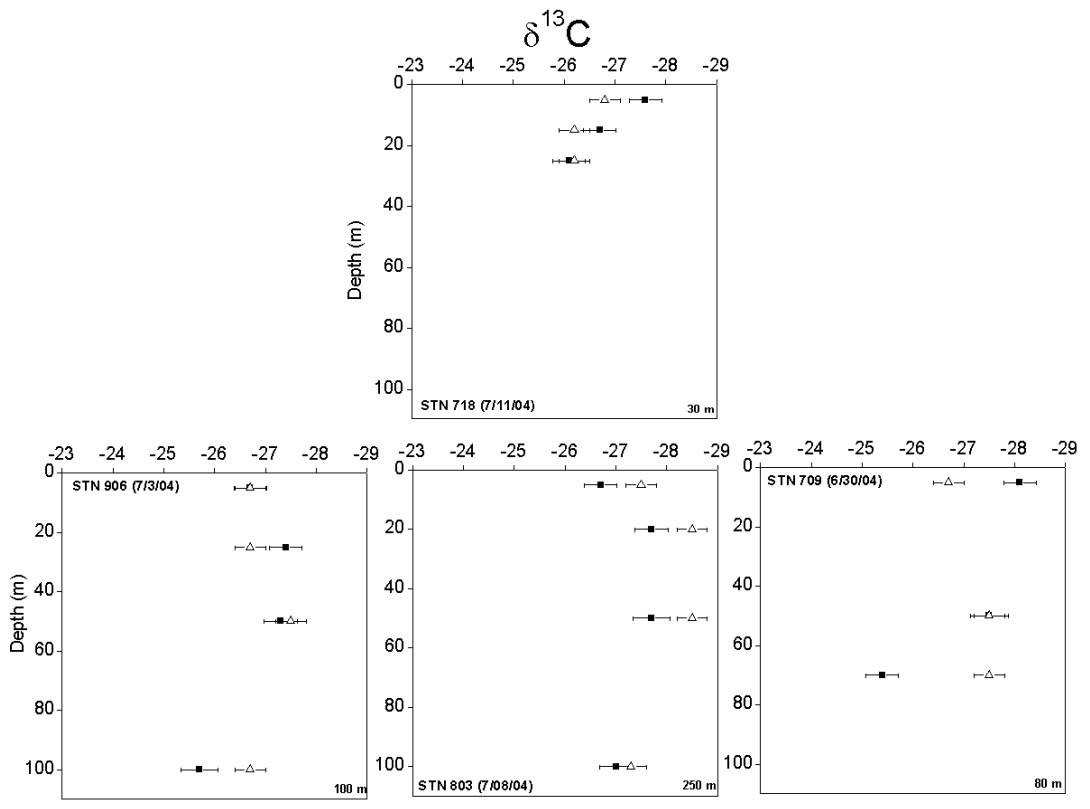

Figure 4-5a. $\delta^{13}C$‰ profiles from western regions.

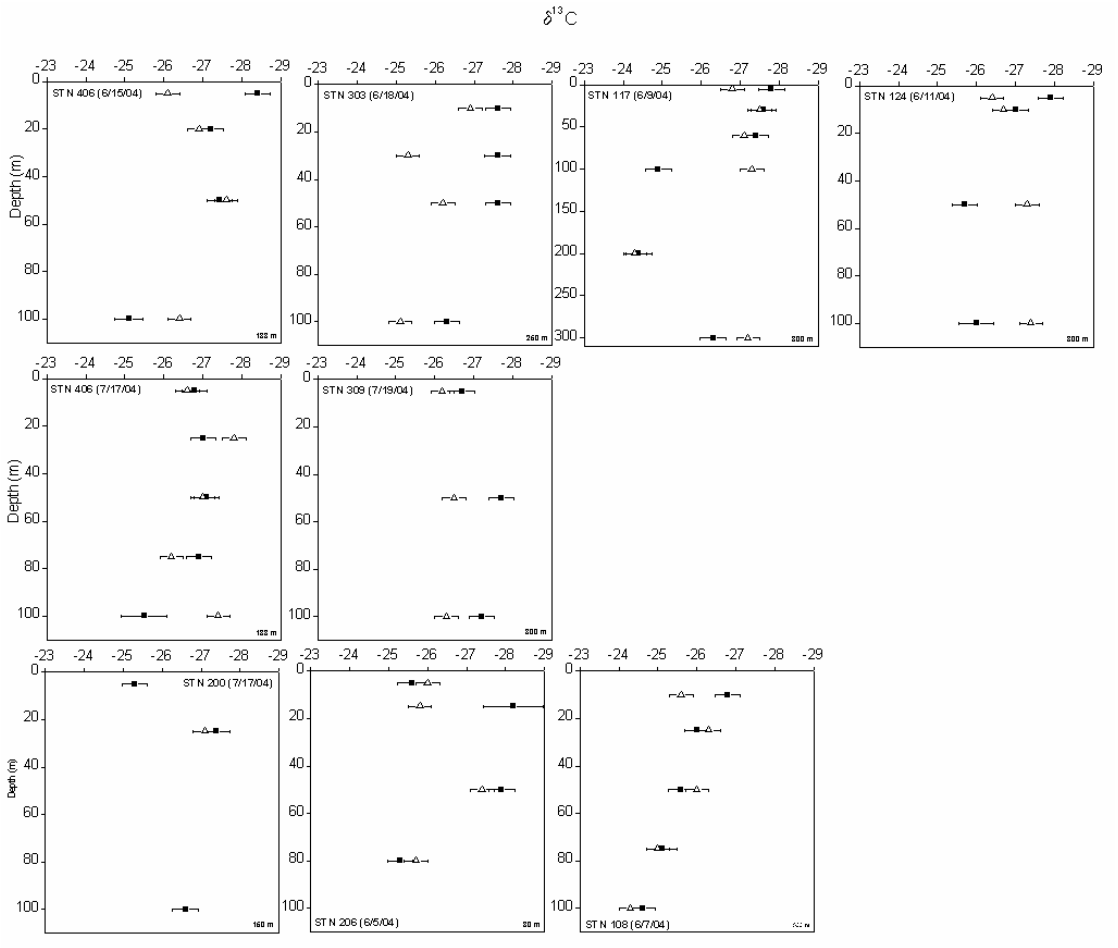

Figure 4-5b. $\delta^{13}C$‰ profiles from western locations.

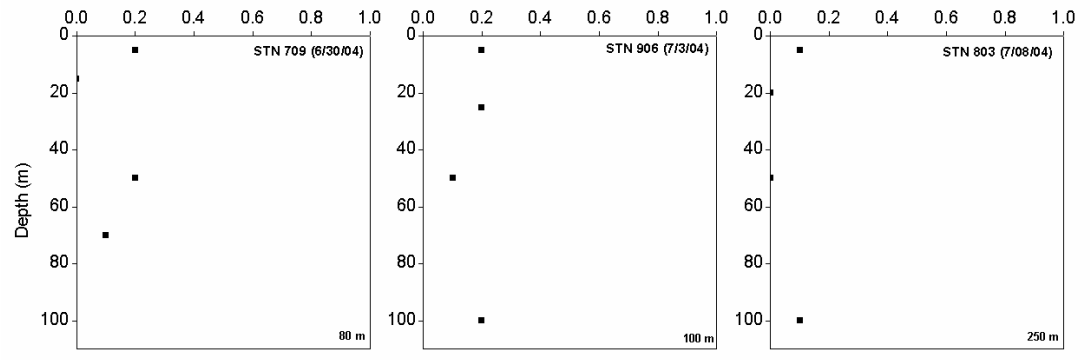

Figure 4-6a. >70 um f_{MAR} profiles from western regions.

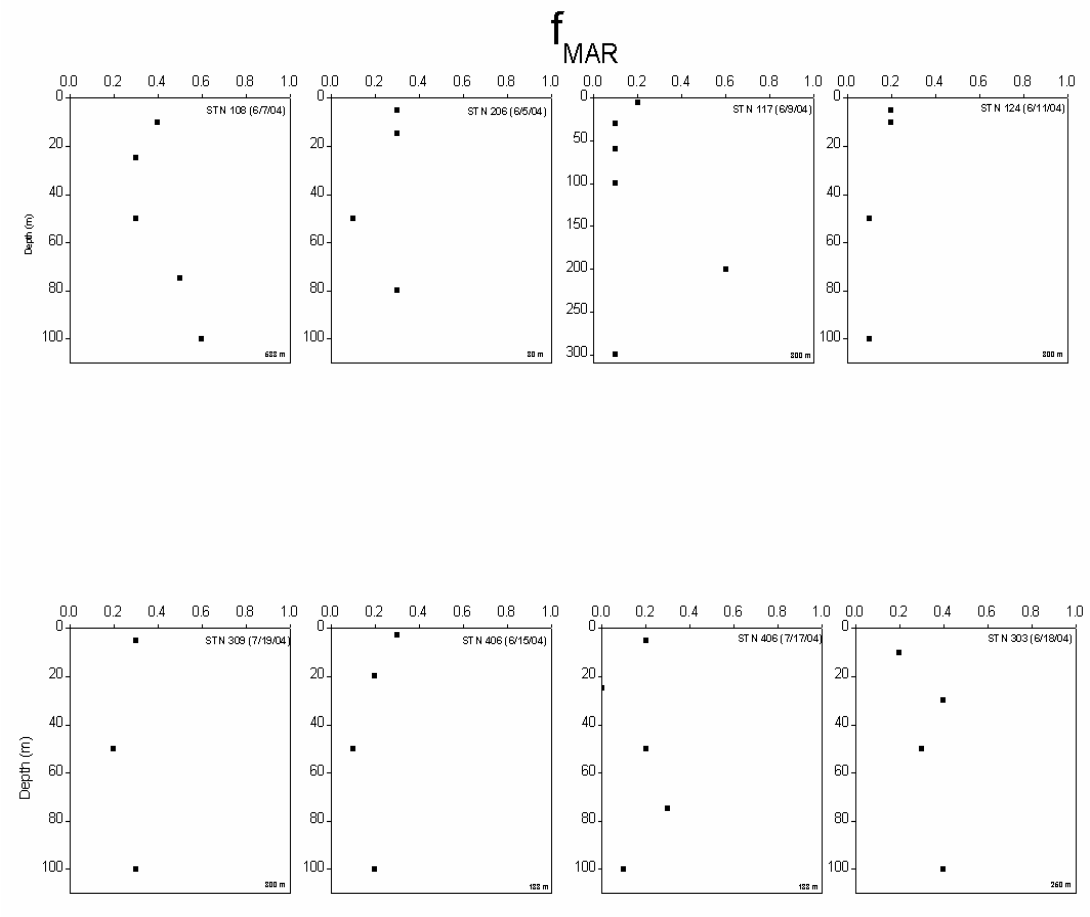

Figure 4-6b. >70 um f_{MAR} profiles from eastern regions.

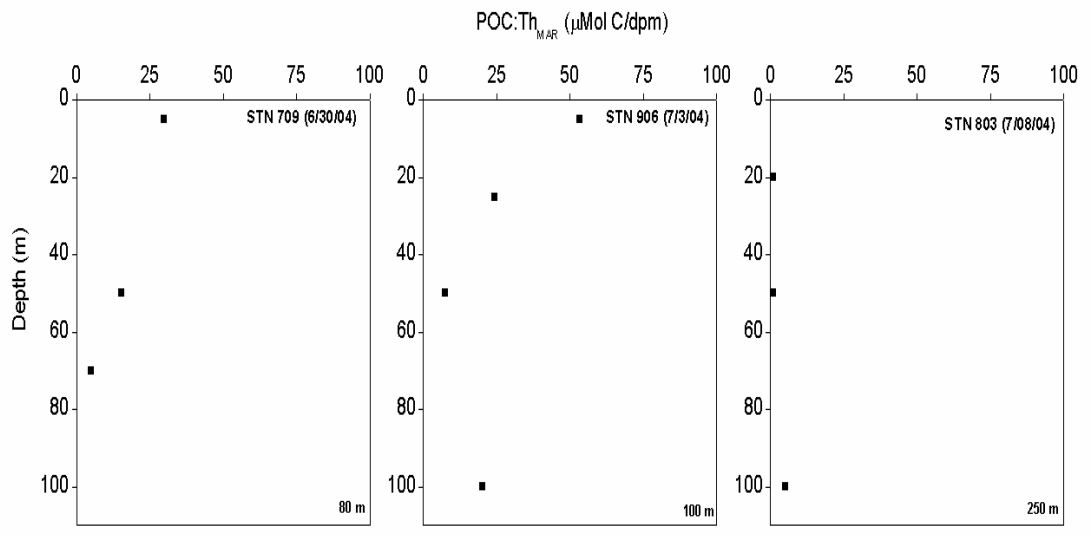

Figure 7a. >70 um POC:Th ratios from western regions.

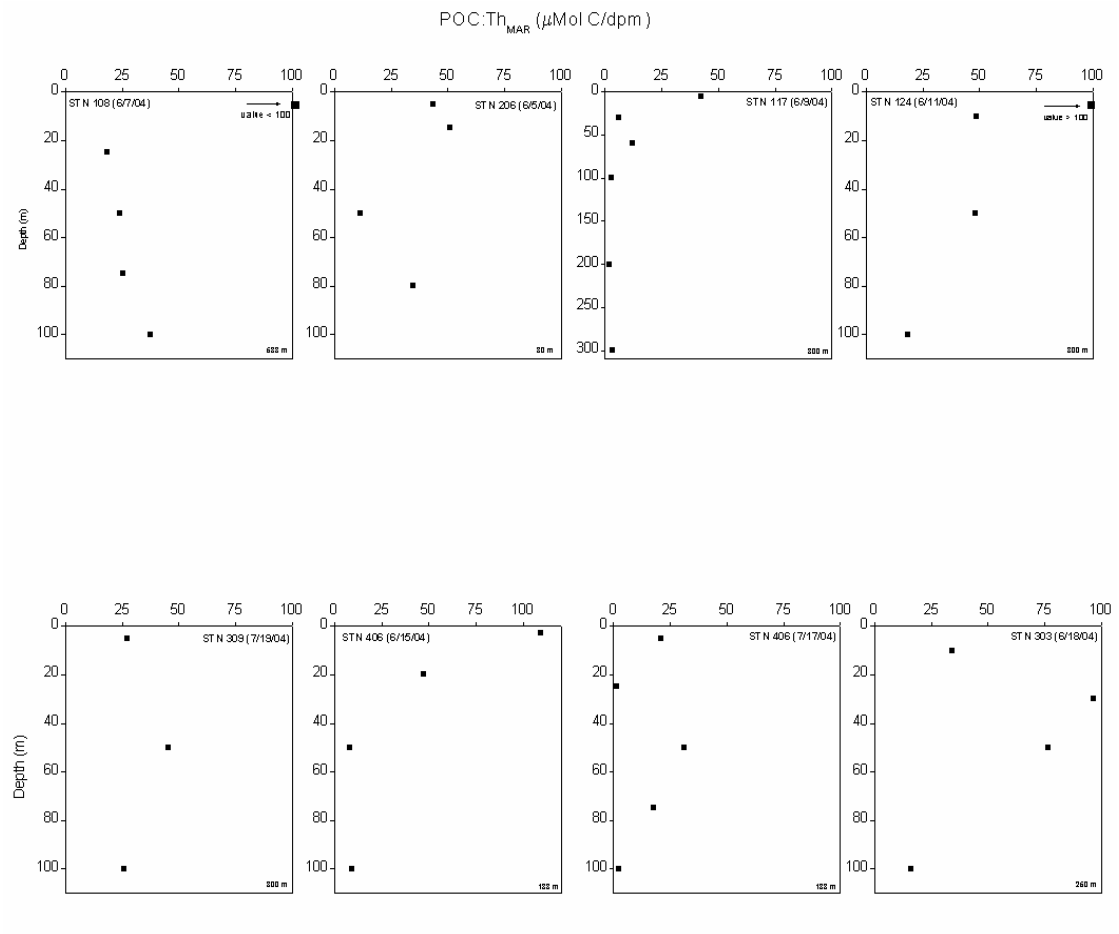

Figure 7b. >70 um POC:Th ratios from eastern regions.

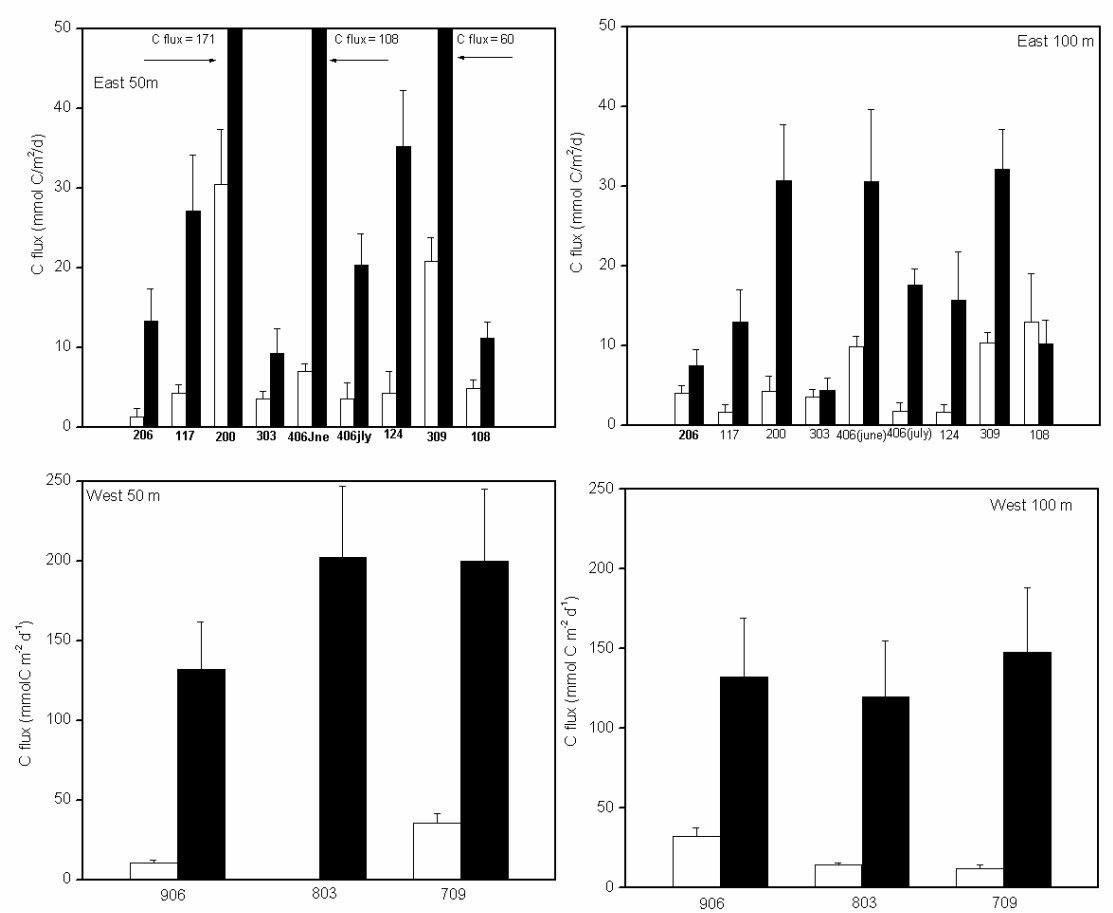

Figure 8. POC fluxes at 50 and 100 m from western and eastern regions. Note different scale between eastern and western areas.

REFERENCES

Amiel, D., Cochran, J.K., Hirschberg, D.J., 2002. $^{234}Th/^{238}U$ disequilibrium as an indicator of the seasonal export flux of particulate organic carbon in the North Water. *Deep-Sea Research II*, 49:5191-5210.

Buesseler, K.O., Bacon, M., Cochran, J.K., Livingston, H., 1992. Carbon and nitrogen export during the JGOFS North Atlantic Bloom Experiment estimated from $^{234}Th:^{238}U$ disequilibria. *Deep-Sea Research*, 39:1115-1137.

Cochran, J.K., Buesseler, K.O., Bacon, M.P., Wang, H.W., Hirschberg, D.J., Ball, L., Andrews, J., Crossin, G., Fleer, A., 2000. Short-lived thorium isotopes (^{234}Th, ^{228}Th) as indicators of POC export and particle cycling in the Ross Sea, Southern Ocean. *Deep-Sea Research II*, 45:3451-3490.

Dugdale, R.C., Goering, J.J., 1967. Uptake of regenerated forms of nitrogen in primary productivity. *Limnology and Oceanography*, 12:196-206.

Goericke, R., Frye, B., 1994. Variations of marine plankton $\delta^{13}C$ with latitude, temperature, and dissolved CO_2 in the world ocean. *Global Biogeochemical Cycles*, 8:85-90.

Gõni, M.A., Yunker, M.B., Macdonald, R., Eglington, T., 2000. Distribution of organic biomarkers in arctic sediments from the Mackenzie River and Beaufort Shelf. *Marine Chemistry*, 71:23-51.

Hargrave, B.T., Walsh, I.D., Murray, D.W., 2002. Seasonal and spatial patterns in mass and organic matter sedimentation in the North Water. *Deep-Sea Reseacrh II*, 49: 5227-5244.

Hedges, J.I., Clark, W.A., Cowie, G.L., 1988. Organic matter sources to the water column and surficial sediments of a marine bay. *Limnology and Oceanography*. 33:1116-1136.

Huston, A.L., Deming, J. Relationships between microbial extracellular enzymatic activity and suspended and sinking organic matter: seasonal transformations in the North Water. *Deep-Sea Research II*, 49:5211-5226.

Macdonald, R., Solomon, S.M., Cranston, R.E., Welch, H.E., Yunker, M.B., Gobeil, C., 1998. A sediment and organic carbon budget for the Canadian Beaufort Shelf. *Marine Geology*. 144: 255-273.

O'Brien, M.C., R. W. Macdonald, H. Melling, and K. Iseki (2006) Particle fluxes and geochemistry on the Canadian Beaufort Shelf: implications for sediment transport and deposition. *Continental Shelf Research* 26: 41-81

Pomeroy, L.R., Wiebe, W.J., Deibel, D., Thompson, R.J., Rowe, G.T., Pakulski, J.D., 1991. Bacterial responses to temperature and substrate concentration during the Newfoundland spring bloom. *Marine Ecology Progress Series*, 75:143-159.

Suess, E., 1980. Particulate organic carbon flux in the oceans-surface productivity and oxygen utilization. *Nature*, 228: 260-263.

Tremblay, J-E., Gratton, Y., Fauchot, J., Price, N., 2002. Climatic and oceanic forcing of new, net and diatom production in the North Water. Deep Sea Research II, 49:4927-4946.

Wheeler, P.A., Watkins, J.M., Hansing, R.L., 1997. Nutrients, organic carbon, and organic nitrogen in the upper water column of the Arctic Ocean, implications for the sources of dissolved organic carbon. *Deep-Sea Research II*, 44: 1571-1592.

Chapter 5: Summary and Conclusions

^{234}Th Distributions

This work has shown that ^{234}Th distributions and deficits can be used to track the fate of particles in a system possessing two end-members; freshwater and marine. ^{234}Th deficits that quantify the rate of scavenging onto sinking particles displayed expected decreases with increasing distance from the Mackenzie River (Fig. 2-6). The total range in 0-50 m ^{234}Th deficits was ~ 0-100 x 10^3 dpm m^{-2}. A comparison of 0-50 m Th deficits from Cape Bathurst and the Mackenzie Shelf indicates that deficits vary by a factor of ~4 from the Mackenzie shelf (58 ± 21 dpm m^{-2}) to the Cape Bathurst Polynya (15 ± 11 dpm m^{-2}) for stations in water depths of 100-400 m). At greater water column depths (200-700 m) along the Mackenzie slope, Moran and Smith (2000) obtained a ^{234}Th deficit of 13.2 ± 4 x 10^3 dpm m^{-2} in the upper 50 m, and this agrees well with our mean deficit in the Cape Bathurst Polynya. In the Northeast Water Polynya, Cochran et al. (1995) obtained a ^{234}Th deficit of 22 ± 7 x 10^3 dpm m^{-2} for 0-50 m during July and August, 1992 at stations in water depths between 300-500 m. Along a 50-200 m transect in the Chukchi Shelf, Moran et al. (2005) obtained a value of 36.0 ± 10 x 10^3 dpm m^{-2}. These comparisons show that the results obtained in this work generally agree with deficits from other, similar Arctic systems.

The results of the present study also document increases with depth in 1-70 μm ^{234}Th activities. Such increases were found throughout the study region with the exception of the Amundsen Gulf where particle loading was the least of any region sampled (Fig. 2-3). Satellite images of the Mackenzie River plume suggest that the increases in 1-70 μm ^{234}Th activities may be related to the expansion of the river plume with time, although further work is needed to document this linkage. Alternatively, the 1-70 μm ^{234}Th activity increases may reflect resuspension of sediments from the bottom and subsequent scavenging of Th onto them. In this case, the particulate Th activity profiles can shed light on the role played by high winds that occur on the shallow inner shelf in resuspending sediment that is subsequently transported, perhaps as far as the continental slope (Hill et al. 1991). The comparatively shallow stations (206, 406 and 709, all < 200 m) are likely sites where resuspension of bottom sediments affected the Th profiles (Figs. 2-5b, 2-5d and 2-5e).

Biological processes also clearly play a role in particulate Th distributions. At stn 303, sampled in June 2004, a phytoplankton bloom was occurring and 1-70 μm ^{234}Th activities were greater than dissolved Th activities between 50-100 m (Fig. 2-5e). Because the water column depth is 240 m at this site, it is unlikely that the increases were due to particle resuspension. Instead,

the substantial increases in 1-70 μm ^{234}Th activities with depth suggest strong scavenging of Th onto biogenic particles.

Another result of this work is that ^{234}Th water column profiles sampled in newly ice-free regions commonly showed excesses 0-20 m (Ch 2, Fig 5e, CA-14,15,16). This may indicate a response of ^{234}Th systematics to the advance and retreat of Arctic pack ice in which excess Th is released from sea-ice algae during melting. This idea is supported from the results of the ^{234}Th measured in an ice-core (Fig. 2-6) that showed substantial excess Th to be present in the ice algae attached and incorporated into the bottom of the ice floe.

Lateral effects on ^{234}Th

The Mackenzie Shelf is a challenging system to attempt to model. The daily oscillations of pack-ice, seasonal variation in Mackenzie River flow, large interannual variability in primary production, and rapidly changing winds reveal a wide spectrum of physical and biological processes that operate on a multitude of time scales. Due to insufficient sampling coverage, a one-dimensional model that ignores lateral effects and assumes steady state (SS) was used to transform Th distributions into fluxes. To test the validity of this approach, ^{234}Th fluxes calculated from floating sediment traps were compared with those obtained from the water column. Sediment traps reflect hydrodynamic biases due to currents, eddies, and other lateral influences, and the degree of agreement between Th fluxes estimated from water column deficits and measured directly in traps provides an indication of the importance of trapping bias and other factors that affect water column Th distributions. The present study showed that trap and water column-deficit-derived Th fluxes agreed to within factor of two for upper water column (0-50 m) and agreement was less good at deeper depths (Fig.2-11). Another insight into the importance of lateral effects came from a comparison between water-column and surficial sediment inventories of ^{234}Th (Fig. 2-12). Within the limitations of the sediment data, agreement was within a factor of two and the conclusion was that a vertical model was sufficient (at least to a first approximation) to estimate sinking fluxes of ^{234}Th.

The assumption of steady state could not be rigorously tested because few stations were sampled repeatedly within a relatively short time period during the course of the study. One station (stn 406) however was sampled twice over an interval of five weeks. Application of a simple non-steady state (NSS) model to obtain the ^{234}Th flux at this station showed that the NSS Th flux agreed to within a factor of 2 with the SS flux.

POC fluxes

An important objective of this work was to develop a method for estimating marine POC fluxes in a system with significant injections of terrestrial POC. During the June and July 2004 cruises, δ^{13}C was measured on > 70 μm sized particles obtained from in situ pumps (assumed to comprise sinking POC). A linear mixing model of Hedges et al. (1988) that required estimation of freshwater and marine end-member values for δ^{13}C was then applied. End-member carbon isotope compositions were determined from

literature values sampled within the study area (Goñi et al. 2000) and from our own sample collection ($\delta^{13}C_{MAR}$ = -21.4‰, $\delta^{13}C_{TERR}$ = -28.0‰). The results suggest that marine POC comprised ~ 10 % of total POC on the Mackenzie shelf and up to 60 % in the Amundsen Gulf.

Terrestrial and marine POC fluxes were derived from the measured ^{234}Th deficits (0-50 and 0-100 m), the bulk POC/Th ratio on filterable particles >70 μm and the fraction of marine or terrestrial POC estimated from the $\delta^{13}C$ data. Marine POC_{MAR} fluxes at 50 m from all sites during June and July, 2004 ranged from ~ 0.0 to 35 mmol C m^{-2} d^{-1}. Marine POC fluxes at 50 m were highest closest to the Mackenzie River (16 ± 18 mmol C m^{-2} d^{-1}), and lowest with increasing distances from the Mackenzie River (5 ± 2 mmol C m^{-2} d^{-1}). Variation in POC fluxes from June to July, 2004 was not readily apparent in the Cape Bathurst Polynya, although station 309 had a POC_{MAR} flux at 50 m of 21mmol C
m^{-2} d^{-1} in July, 2004 that was significantly higher than any POC_{MAR} flux from June, 2004. On the other hand, station 406, occupied in both June and July, 2004, had POC_{MAR} fluxes that decreased from June to July, 2004 (Fig. 4-8).

Although primary production rates in the CASES study were not available at the time of writing of this thesis, Chl-a concentrations at station 303 suggested a bloom of low to moderate intensity in June 2004 (Chl-a ~ 20 μg/l). This is consistent with the preliminary results of J.-E.Tremblay (personal communication), who noted low concentrations of nitrate in the waters around Cape Bathurst. Though many rivers have high nitrate concentrations, the Mackenzie River may not, due to its drainage basin consisting primarily of frozen tundra. If primary production rates were indeed low in the CASES region during this study, then low sinking fluxes of POC might be expected in the Cape Bathurst Polynya. However, because algal blooms are light limited, they can occur within a few days after ice retreat. This implies that, although the June, 2004 sampling occurred within a few days of ice retreat, the low POC fluxes estimated from ^{234}Th may not be explained simply as a result of lack of a bloom at that time.

The POC fluxes estimated by the ^{234}Th-deficit method in the CASES region may be compared with other Arctic systems in which a similar approach was taken. For example, Lepore et al. (2007, submitted) used the ^{234}Th method to obtain POC fluxes of 20 mmol C m^{-2} d^{-1} in summer 2004 at 50 m on the Chukchi Shelf. Cochran et al. (1992) and Amiel et al. (2002) determined values of ~30 mmol C m^{-2} d^{-1} for both the Northeast Water and North Water polynyas while Moran et al. (2002) obtained 5 mmol C m^{-2} d^{-1} at the outer Mackenzie shelf/inner slope.

To the author, the surprising result of this study was not that POC_{MAR} fluxes were so low in Cape Bathurst during June, 2004 but that they can be high at sites residing within the swath of the Mackenzie River plume. Furthermore, a comparison of site 709 (36 mmol C m^{-2} d^{-1}) with 803 that had no POC_{MAR} flux, shows the high degree of patchiness in fluxes within the Mackenzie river plume. This is in contrast to the expectations of hypothesis 1 (Chapter 1). Indeed a satellite image taken from the Mackenzie river on June 29, 2004 (Fig. 2-8)

clearly shows that the surface flow from the Mackenzie river plume moves northwards across the shelf at that time. The image also suggests low river flow because the plume does not appear to have a large areal extent. This view of a relatively quiescent river during the time of our June, 2004 sampling is reinforced by the salinity contour plot (Fig. 1-7) that also shows a northwards movement of the Mackenzie river plume. These two pieces of evidence suggest that Cape Bathurst would have been shielded from the influence of the Mackenzie, and according to hypothesis 1, should therefore have had high POC_{MAR} fluxes. Instead, POC_{MAR} fluxes were only 5 mmol C m^{-2} d^{-1} in Cape Bathurst during June, 2004 and were in fact higher closer to the river during July, 2004.

One limitation of hypothesis 1 is that it assumes (as did most of the scientists on board) that the Cape Bathurst Polynya would not be nutrient limited early in the growing season. High nitrate concentrations have been measured in the Bering Straight and Chuckchi Shelf so it was reasonable to assume that there was abundant nitrate in the CASES region as well. However, preliminary results of J.-E. Tremblay (personal communication) indicate that the waters of Cape Bathurst had very little nitrate (<3 μM) during the June, 2004 cruise. This nutrient deficit raises important issues about the sources of nitrate to the Cape Bathurst polynya. Most rivers carry an abundant supply of nitrate to the adjacent waters. Was the low POC_{MAR} fluxes measured in this study attributed to low river flow and hence a small supply of nitrate? Could the higher POC_{MAR} fluxes obtained in this study near the Mackenzie reflect a closer proximity to a riverine nitrate source? Clearly, further work is needed to establish the role of riverine supply of nutrients in fueling primary production and export on the Mackenzie shelf. Given the importance of river dominated shelves in the Arctic (including those of the Lena, Ob and Yenisey Rivers), this issue merits further study.

Carbon balance

The water column carbon fluxes from June/July 2004 can be combined with data on carbon fluxes in the sediments to construct a simple carbon balance in the CASES area for summer, 2004 (Fig. 5-1). Sediment oxygen demand was measured on ship-based incubations of sediment cores (Renaud et al., 2006). These data may be converted to carbon remineralization rates using a 1:1 stoichiometry. As well, distributions of excess ^{210}Pb in the upper ~20 cm of the sediment column yield estimates of recent sediment accumulation rates (Fig 3-8). The ^{210}Pb distributions are likely affected by particle mixing and thus accumulation rates are upper limits. The ^{210}Pb and $\delta^{13}C$ data may be converted to upper limits on accumulation rates of marine and terrestrial sedimentary organic carbon (SOC)at the sediment-water interface

Marine POC fluxes are about 15 % of terrestrial fluxes in July on the Mackenzie outer shelf, and there is no significant difference in either marine or terrestrial fluxes between 50 and 100 m (Fig. 5-1). On the outer shelf, marine POC fluxes at 100 m are ~ 3 times greater than remineralization and burial of POC in underlying sediments (Fig. 5-1). Hence, a large amount of carbon

exported from the upper water column on the outer shelf appears not to be incorporated or processed in bottom sediments. Moreover, if the C oxidized in the sediments is considered to be dominantly marine, remineralization plus burial accounts for ~ 20-30 % of the sinking flux of marine POC at 100 m,

In contrast to the Mackenzie outer shelf, marine POC fluxes at 50 m and 100 m in the Cape Bathurst Polynya, comprise a greater fraction of the total flux, equivalent to ~25 % of the terrestrial flux. In June, there was little or no attenuation of the marine POC flux between 50 and 100 m at Cape Bathurst and remineralization and burial of marine SOC in sediments of the polynya yields a total of ~2.4 mmol C m^{-2} d^{-1} with ~4 mmol C m^{-2} d^{-1} fluxing in from the water column (Fig. 1). Marine POC fluxes in July are greater than in June, resulting in a greater disparity between the sinking flux of marine POC and regeneration and burial in the sediments.

Moran et al. (2005) and Lepore et al. (2007, submitted) observed a similar offset between the flux of POC at 50 m and benthic carbon burial and remineralization on the Chukchi Shelf. They noted that the offset may be partly one of time scale. The water column fluxes refer to a relatively short period of time (e.g. the summer season) while benthic C remineralization may continue throughout the year, mediated by microbial processes. As well, benthic carbon remineralization rates calculated from sediment oxygen demand are lower limits because they do not include remineralization by anaerobic processes.

In addition to comparisons of POC export from the photic zone with benthic carbon fluxes, attenuation of POC fluxes in a water column of ~500 m has been observed in other Arctic polynyas (e.g. the North Water; Tremblay et al., 2006 and references therein). Several possibilities may explain this attenuation. POC may be exported off the shelf to adjacent slope waters. Indeed, Moran et al. (2005) and Lepore et al. (2007) suggested that the discrepancy they observed between the flux of POC at 50 m and benthic C burial and remineralization on the Chukchi Shelf could be accounted for by off-shelf export.

Alternatively, the attenuation may reflect effective remineralization of sinking POC in the twilight zone. Indeed, Huston et al. (2002) measured high rates of enzymatic activity in filterable particles from the North Water Polynya, despite the low temperatures and the possibility of temperature inhibition of microbial activity.

A final possibility involves transfers of carbon through the various trophic levels of the system and incorporation into biomass. Such POC transfers and fluxes are difficult to quantify (Tremblay et al. 2006). In the water column, cycling of carbon through trophic transfers is likely to play a larger role in regulating the flux of POC exported from the photic zone (the “e-ratio” Buesseler et al. 1998) than in attenuation of fluxes between 50 m and the bottom. For POC that reaches the bottom, carbon storage in benthic biomass is possible (Grebmeier and McRoy, 1989). Clearly, further studies are required to resolve the fate of the twilight zone carbon pool in high latitude polynyas. Taken at face value, however, the results of the present study do not support the

expectations of hyspothesis 2 (Chapter 1) that a balance exists between POC exported from the photic zone and deposited in the underlying sediments.

FIGURES

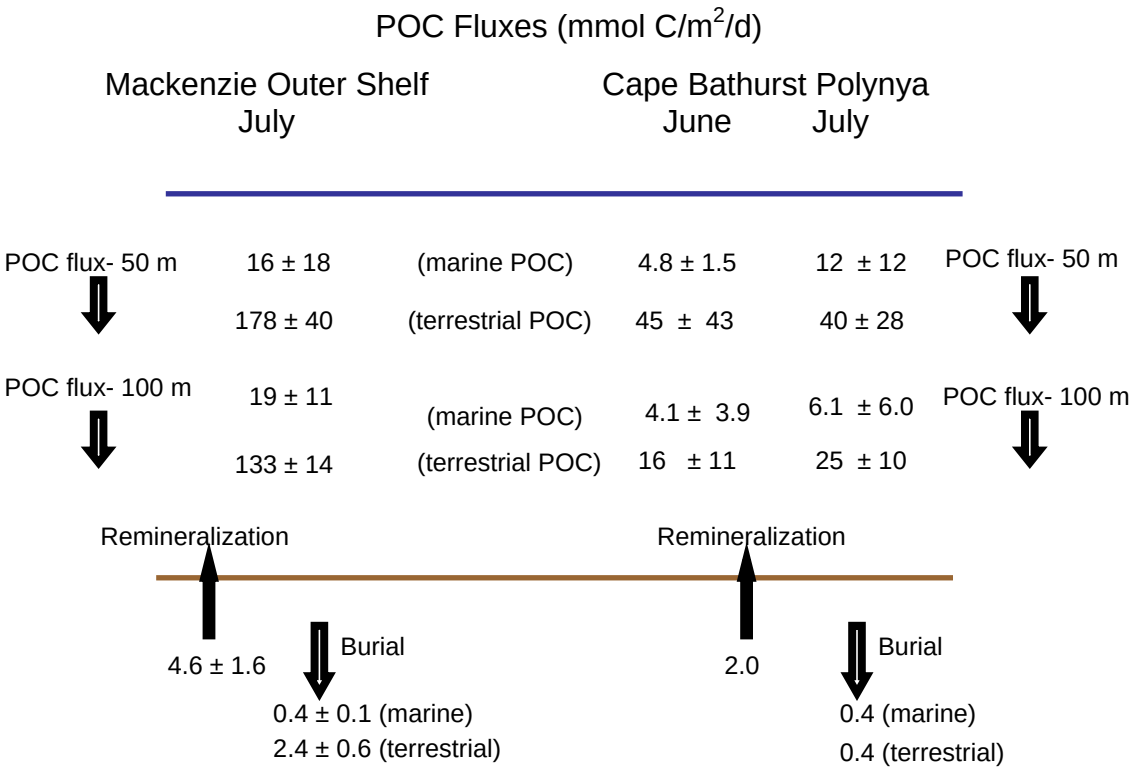

Figure 5-1. Mass balance of carbon between water column and sediments from the Mackenzie Outer Shelf and the Cape Bathurst polynya.

REFERENCES

Buesseler, K., L. Ball, J. Andrews, C. Benitez-Nelson, R. Belastock, F. Chai, and Y. Chao (1998) Upper ocean export of particulate organic carbon in the Arabian Sea derived from thorium-234. *Deep-Sea Research II* 45: 2461-2487.

Cochran, J. K., C. Barnes, D. Achman, D, J. Hirschberg (1995) Thorium-234/Uranium-238 disequilibrium as an indicator of scavenging rates and particulate organic carbon fluxes in the Northeast Water Polynya, Greenland. *Journal of Geophysical Research 100*: 4399-4410.

Huston, A., and J. Deming (2002) Relationships between microbial and extracellular enzymatic activity and suspended and sinking particulate organic matter: seasonal transformations in the North Water. *Deep-Sea Research II*. 49 5211-5225.

Grebmeier, J. M., and C. P. McRoy (1989), Pelagic-benthic coupling on the shelf of the northern Bering Sea and Chukchi Seas. III. Benthic food supply and carbon cycling, *Marine Ecology Progress Series*, *53*, 79-91.

Lepore, K., S. B. Moran, J. M. Grebmeier, L. W. Cooper, C. Lalande, W. Maslowski, V. Hill, N. R. Bates, D. A. Hansell, J. T. Mathis, and R. P. Kelly (2007). Seasonal and Interannual Changes in POC Export and Deposition in the Chukchi Sea. J. *Geophys. Res*., submitted

Moran, S. B. and J. N. Smith (2000) ^{234}Th as a tracer of scavenging and particle export in the Beaufort Sea. *Continental Shelf Research* 20: 153-167.

Moran, S. B., R. P. Kelly, K. Hagstrom, J. N. Smith, J. M. Grebmeier, L. W. Cooper, G.F. Cota, J. J. Walshe, N. R. Bates, D. A. Hansell, W. Maslowski, R. P. Nelson and S. Mulsowi (2005) Seasonal changes in POC export flux in the Chukchi Sea and implications for water column-benthic coupling in Arctic shelves. *Deep-Sea Res. II 52*, 3427-3451.

Hedges, J.I., W. A. Clark, and G. L. Cowie (1988) Organic matter sources to the water column and surficial sediments of a marine bay. *Limnology and Oceanography*. 33:1116-1136.

Hill, P.R., S. M. Blasco, J. R. Harper, and D. B. Fissel (1991) Sedimentation on the Canadian Beaufort Shelf. *Continental Shelf Research* 11:821-842.

Tremblay, J.-É., H. Hattori, C. Michel, M. Ringuette, Z.-P. Mei, C. Lovejoy, L. Fortier, K. A. Hobson, D. Amiel and K. Cochran (2006). Trophic structure and pathways of biogenic carbon flow in the eastern North Water Polynya. *Prog. Oceanogr*. 71, 402-425.

APPENDIX A

Water column
^{234}Th data

STN	Depth m	SAL PSU	U^{238} dpm/l	>70µm ^{234}Th dpm/l	1-70µm ^{234}Th dpm/l	^{234}Th-Dissolved dpm/l	Total ^{234}Th dpm/l
October, 2003-^{234}Th from Niskin bottles							
718	3	21.2	1.30	nd	nd	nd	0.32 ± 0.02
	25	24.5	1.50	nd	nd	nd	0.33 ± 0.02
	27	29.5	1.81	nd	nd	nd	0.41 ± 0.02
ca12	5	26.4	1.62	nd	nd	nd	1.91 ± 0.10
	15	28.0	1.72	nd	nd	nd	1.14 ± 0.06
	25	30.0	1.85	nd	nd	nd	1.46 ± 0.07
	50	31.5	1.94	nd	nd	nd	1.87 ± 0.09
	100	31.8	1.96	nd	nd	nd	1.82 ± 0.09
	200	32.0	1.97	nd	nd	nd	2.21 ± 0.11
ca10	5	25.5	1.56	nd	nd	nd	1.2 ± 0.06
	15	25.5	1.56	nd	nd	nd	2.28 ± 0.11
	25	30.0	1.85	nd	nd	nd	2.16 ± 0.11
	50	32.0	1.97	nd	nd	nd	2.17 ± 0.11
	100	32.5	2.00	nd	nd	nd	2.18 ± 0.11
	200	33.0	2.03	nd	nd	nd	2.58 ± 0.13
	227	33.0	2.03	nd	nd	nd	2.42 ± 0.12
ca6	5	25.0	1.53	nd	nd	nd	0.93 ± 0.05
	15	28.0	1.72	nd	nd	nd	2.2 ± 0.11
	25	32.0	1.97	nd	nd	nd	1.5 ± 0.08
	50	32.0	1.97	nd	nd	nd	1.86 ± 0.09
	75	32.5	2.00	nd	nd	nd	2.1 ± 0.11
ca13	5	28.5	1.75	nd	nd	nd	2.21 ± 0.11
	10	28.0	1.72	nd	nd	nd	2.18 ± 0.11
	25	27.0	1.66	nd	nd	nd	2.5 ± 0.13
	50	31.0	1.91	nd	nd	nd	1.99 ± 0.10
	100	32.0	1.97	nd	nd	nd	1.8 ± 0.09
	200	33.2	2.05	nd	nd	nd	2.93 ± 0.15
ca14	5	27.2	1.67	nd	nd	nd	1.66 ± 0.08
	10	27.2	1.67	nd	nd	nd	1.94 ± 0.10
	15	27.2	1.67	nd	nd	nd	1.76 ± 0.09
	25	27.2	1.67	nd	nd	nd	2.00 ± 0.10
	50	32.0	1.97	nd	nd	nd	2.39 ± 0.12
	100	33.0	2.03	nd	nd	nd	2.32 ± 0.12
	200	33.2	2.05	nd	nd	nd	2.22 ± 0.12
ca15	15	27.0	1.66	nd	nd	nd	1.73 ± 0.09
	20	27.0	1.66	nd	nd	nd	1.96 ± 0.10
	50	31.0	1.91	nd	nd	nd	2.22 ± 0.11
ca5	5	29.0	1.78	nd	nd	nd	1.75 ± 0.09
	15	28.0	1.72	nd	nd	nd	2.36 ± 0.12
	25	28.0	1.72	nd	nd	nd	2.63 ± 0.13
	50	33.0	2.03	nd	nd	nd	2.48 ± 0.12
	100	33.1	2.04	nd	nd	nd	2.27 ± 0.11

	200	33.2	2.05	nd			nd			nd			2.22		0.11
October, 2003-^{234}Th obtained from pumps														±	
718	3	21.2	1.30	0.016	±	0.0006	0.18	±	0.005	0.38	0.08	0.38	±	0.08	
	12	24.5	1.50	0.016	±	0.0006	0.14	±	0.004	0.38	0.08	0.38	±	0.08	
	27	29.5	1.81	0.011	±	0.0004	0.05	±	0.002	0.45	0.10	0.45	±	0.10	
ca12	5	26.4	1.62	0.012	±	0.0005	0.05	±	0.002	1.08	0.24	1.08	±	0.24	
	15	28.0	1.72	0.005	±	0.0002	0.12	±	0.004	1.2	0.26	1.20	±	0.26	
	25	30.0	1.85	0.023	±	0.0009	0.23	±	0.007	1.42	0.31	1.42	±	0.31	
	50	31.5	1.94	0.008	±	0.0003	0.49	±	0.015	1.36	0.30	1.36	±	0.30	
	100	31.8	1.96	0.024	±	0.0009	0.40	±	0.012	1.38	0.30	1.38	±	0.30	
	200	32.0	1.97	0.014	±	0.0005	0.76	±	0.023	0.96	0.21	0.96	±	0.21	
ca10	5	25.5	1.56	0.02	±	0.0009	0.58	±	0.017	1.45	0.32	1.45	±	0.32	
	15	25.5	1.56	0.02	±	0.0009	0.20	±	0.006	0.61	0.13	0.61	±	0.13	
	25	30	1.85	0.01	±	0.0004	0.38	±	0.011	0.45	0.10	0.45	±	0.10	
	50	32	1.97	0.01	±	0.0003	0.18	±	0.005	1.24	0.27	1.24	±	0.27	
	100	32.5	2.00	0.01	±	0.0006	0.28	±	0.008	0.36	0.08	0.36	±	0.08	
ca6	5	25	1.53	0.04	±	0.0014	0.44	±	0.013	1	0.22	1.00	±	0.22	
	15	28	1.72	0.01	±	0.0004	0.14	±	0.004	1.04	0.23	1.04	±	0.23	
	25	32	1.97	0.02	±	0.0008	0.56	±	0.017	0.45	0.10	0.45	±	0.10	
	50	32	1.97	0.00	±	0.0001	0.81	±	0.024	0.39	0.09	0.39	±	0.09	
	75	32.5	2.00	0.01	±	0.0004	0.59	±	0.018	0.72	0.16	0.72	±	0.16	
June, 2004															
206	5	31.54	1.94	0.010	±	0.0004	0.78	±	0.023	0.89	0.13	0.89	±	0.13	
	15	31.80	1.96	0.007	±	0.0003	0.83	±	0.025	1.14	0.06	1.14	±	0.06	
	25	31.87	1.96	0.007	±	0.0003	0.87	±	0.026	1.26	0.09	1.26	±	0.09	
	50	32.49	2.00	0.010	±	0.0004	0.97	±	0.029	1.11	0.14	1.11	±	0.14	
	80	32.90	2.03	0.008	±	0.0003	1.05	±	0.031	0.98	0.05	0.98	±	0.06	
108	10	30.30	1.86	0.003	±	0.0001	0.22	±	0.007	1.6	0.12	1.60	±	0.12	
	15	30.59	1.88	0.004	±	0.0001	0.36	±	0.011	1.41	0.07	1.41	±	0.07	
	25	31.00	1.91	0.011	±	0.0004	0.50	±	0.015	1.11	0.17	1.11	±	0.17	
	50	32.35	1.99	0.012	±	0.0005	0.86	±	0.026	1.07	0.11	1.07	±	0.11	
	75	32.69	2.01	0.018	±	0.0007	1.09	±	0.033	0.83	0.09	0.83	±	0.10	
	100	32.97	2.03	0.015	±	0.0006	0.88	±	0.026	0.97	0.04	0.97	±	0.05	
	200	34.35	2.12	0.003	±	0.0001	0.21	±	0.020	1.46	0.11	1.46	±	0.11	
117	5	30.53	1.88	0.006	±	0.0002	0.27	±	0.008	1.74	0.09	1.74	±	0.09	
	15	30.54	1.88	0.012	±	0.0005	0.33	±	0.010	1.26	0.06	1.26	±	0.06	
	30	30.90	1.90	0.008	±	0.0003	0.38	±	0.011	1.14	0.07	1.14	±	0.07	
	60	32.49	2.00	0.006	±	0.0003	0.90	±	0.027	1.09	0.05	1.09	±	0.06	
	100	32.87	2.02	0.020	±	0.0008	0.83	±	0.025	0.94	0.38	0.94	±	0.38	
	200	34.31	2.11	0.015	±	0.0005	1.01	±	0.030	1.10	0.05	1.10	±	0.06	
	300	34.73	2.14	0.008	±	0.0005	0.57	±	0.017	1.25	0.06	1.25	±	0.06	
124	5	30.59	1.88	0.014	±	0.0006	0.48	±	0.014	1.58	0.09	1.58	±	0.09	
	10	30.58	1.88	0.006	±	0.0003	0.30	±	0.009	1.29	0.09	1.29	±	0.09	
	20	30.60	1.88	0.018	±	0.0007	0.50	±	0.015	1.3	0.09	1.30	±	0.09	
	50	32.00	1.97	0.006	±	0.0002	0.81	±	0.024	1.3	0.18	1.30	±	0.18	
	100	32.69	2.01	0.006	±	0.0002	0.90	±	0.027	1.36	0.03	1.36	±	0.04	
406	3	30.42	1.87	0.009	±	0.0004	0.38	±	0.011	1.42	0.09	1.42	±	0.09	
	15	30.76	1.89	0.006	±	0.0003	0.33	±	0.010	1.1	0.1	1.10	±	0.10	
	20	30.85	1.90	0.005	±	0.0002	0.28	±	0.008	1.08	0.1	1.08	±	0.10	
	50	32.08	1.98	0.007	±	0.0003	0.74	±	0.022	0.86	0.1	0.86	±	0.10	
	100	32.71	2.01	0.010	±	0.0004	0.90	±	0.027	0.795	0.1	0.80	±	0.10	
	150	33.55	2.07	0.014	±	0.0005	1.01	±	0.030	0.73	0.06	0.73	±	0.07	
303	10	30.88	1.90	0.024	±	0.0010	0.37	±	0.011	1.34	0.10	1.34	±	0.10	
	20	30.85	1.90	0.020	±	0.0008	0.44	±	0.013	1.09	0.1	1.09	±	0.10	
	30	31.10	1.91	0.093	±	0.0037	0.51	±	0.015	1.05	0.13	1.05	±	0.13	
	50	31.44	1.94	0.017	±	0.0007	1.02	±	0.031	0.90	0.13	0.90	±	0.13	

	75	32.36	1.99	0.015	±	0.0006	1.01	±	0.030	0.74	0.05	0.74	±	0.06
	100	32.62	2.01	0.010	±	0.0004	0.99	±	0.030	0.74	0.1	0.74	±	0.10
July, 2004														
709	5	27.49	1.69	0.029	±	0.0012	0.19	±	0.006	0.64	0.1	0.64	±	0.10
	15	30.26	1.86	0.024	±	0.0010	0.16	±	0.005	0.55	0.10	0.55	±	0.10
	50	31.83	1.96	0.03	±	0.0012	0.13	±	0.004	0.21	0.1	0.21	±	0.10
	70	32.44	2.00	0.048	±	0.0019	0.74	±	0.022	1.58	0.21	1.58	±	0.21
906	5	22.00	1.35	0.04	±	0.0016	0.12	±	0.004	0.31	0.1	0.31	±	0.10
	15	30.11	1.85	0.03	±	0.0011	0.16	±	0.005	0.63	0.1	0.63	±	0.10
	25	30.28	1.86	0.07	±	0.0028	0.20	±	0.006	0.94	0.1	0.94	±	0.10
	50	32.12	1.98	0.08	±	0.0033	0.38	±	0.012	1.03	0.15	1.03	±	0.15
	75	32.60	2.01	0.031	±	0.0012	0.38	±	0.011	1.23	0.15	1.23	±	0.15
	100	32.75	2.02	0.069	±	0.0028	0.79	±	0.024	1.43	0.21	1.43	±	0.21
912	5	25.71	1.58	0.029	±	0.0012	0.24	±	0.007	1.06	0.37	1.06	±	0.37
	18	32.23	1.98	0.008	±	0.0003	0.34	±	0.010	0.84	0.11	0.84	±	0.11
	25	32.41	2.00	0.008	±	0.0003	0.23	±	0.007	1.26	0.35	1.26	±	0.35
803	5	23.87	1.46	0.03	±	0.0012	0.06	±	0.002	1.07	0.1	1.07	±	0.10
	10	29.21	1.80	0.056	±	0.0022	0.06	±	0.002	1.00	0.1	1.07	±	0.10
	20	30.37	1.87	0.017	±	0.0007	0.06	±	0.002	0.97	0.06	0.97	±	0.06
	50	31.72	1.95	0.047	±	0.0019	0.08	±	0.002	1.2	0.09	1.20	±	0.09
	75	32.55	2.00	0.052	±	0.0021	0.29	±	0.009	0.10	0.1	0.10	±	0.10
	100	32.76	2.02	0.045	±	0.0018	0.69	±	0.021	0.14	0.09	0.14	±	0.09
718	5	25.97	1.59	0.117	±	0.0047	0.14	±	0.004	1.03	0.35	1.03	±	0.35
	15	31.11	1.91	0.120	±	0.0048	0.16	±	0.005	0.14	0.14	0.14	±	0.14
	25	31.54	1.94	0.115	±	0.0046	0.15	±	0.005	0.75	0.09	0.75	±	0.09
200	5	29.34	1.80	0.02	±	0.0008	0.39	±	0.012	0.28	0.11	0.28	±	0.11
	15	29.97	1.84	0.09	±	0.0036	0.44	±	0.013	1.45	0.19	1.45	±	0.19
	25	30.60	1.88	0.02	±	0.0008	0.43	±	0.013	1.24	0.1	1.24	±	0.10
	50	31.83	1.96	0.01	±	0.0005	0.40	±	0.012	1.30	0.1	1.30	±	0.10
	75	32.43	2.00	0.02	±	0.0010	0.74	±	0.022	1.36	0.1	1.36	±	0.10
	100	32.68	2.01	0.04	±	0.0016	0.90	±	0.027	1.16	0.1	1.16	±	0.10
309	5	29.40	1.81	0.02	±	0.0008	1.06	±	0.032	0.56	0.04	0.56	±	0.05
	15	30.22	1.86	0.02	±	0.0008	0.91	±	0.027	1.44	0.06	1.44	±	0.07
	25	30.89	1.90	0.02	±	0.0008	0.75	±	0.022	0.36	0.1	0.36	±	0.10
	50	32.18	1.98	0.02	±	0.0008	0.51	±	0.015	1.05	0.15	1.05	±	0.15
	75	32.59	2.01	0.02	±	0.0008	0.61	±	0.018	0.46	0.1	0.46	±	0.10
	100	32.82	2.02	0.02	±	0.0008	0.64	±	0.019	0.58	0.05	0.58	±	0.05
406	5	28.17	1.73	0.01	±	0.0003	0.61	±	0.018	0.85	0.1	0.85	±	0.10
	15	29.68	1.82	0.003	±	0.0001	0.11	±	0.003	1.00	0.1	1.00	±	0.10
	25	30.41	1.87	0.01	±	0.0005	0.22	±	0.007	1.62	0.1	1.62	±	0.10
	50	31.54	1.94	0.02	±	0.0008	0.57	±	0.017	1.27	0.1	1.27	±	0.10
	75	32.33	1.99	0.02	±	0.0010	0.55	±	0.016	1.13	0.1	1.13	±	0.10
	100	32.65	2.01	0.02	±	0.0009	0.69	±	0.021	0.78	0.1	0.78	±	0.10